



Graduate Theses, Dissertations, and Problem Reports

2006

Relationship between damper resistance and damper insertion depth

Ranjit Jangam
West Virginia University

Follow this and additional works at: <https://researchrepository.wvu.edu/etd>

Recommended Citation

Jangam, Ranjit, "Relationship between damper resistance and damper insertion depth" (2006). *Graduate Theses, Dissertations, and Problem Reports*. 4235.
<https://researchrepository.wvu.edu/etd/4235>

This Thesis is protected by copyright and/or related rights. It has been brought to you by the The Research Repository @ WVU with permission from the rights-holder(s). You are free to use this Thesis in any way that is permitted by the copyright and related rights legislation that applies to your use. For other uses you must obtain permission from the rights-holder(s) directly, unless additional rights are indicated by a Creative Commons license in the record and/ or on the work itself. This Thesis has been accepted for inclusion in WVU Graduate Theses, Dissertations, and Problem Reports collection by an authorized administrator of The Research Repository @ WVU. For more information, please contact researchrepository@mail.wvu.edu.

Relationship between Damper Resistance and Damper Insertion Depth

Ranjit Jangam

**Thesis Submitted to the
College of Engineering and Mineral Resources at
West Virginia University
in partial fulfillment of the requirements
for the degree of**

Master of Science

in

Industrial Engineering

Steven Guffey Ph.D., Chair

Robert Creese Ph.D.

Kenneth Means Ph.D.

Department of Industrial Engineering

Morgantown, West Virginia

2006

**Keywords: Slide-Gate Dampers, Relation between Damper Resistance and Damper
Insertion Depth, Damper Edge, Duct Diameter, Airflow Levels, Velocity Pressure,
Static Pressure, Total Pressure**

Abstract

Relationship between Damper Resistance and Damper Insertion Depth

Ranjit Jangam

Experiments were performed to determine a predictive model for sliding gate damper resistance (X_{damper}). Independent variables included eight ratios of insertion depth (I) to duct diameter (D), two different values of D, four different levels of air velocity, two damper orientations, and two damper edges (Concave/Straight). Analysis of Log (X_{damper}) values showed a highly linear relationship with I/D and high statistical significance ($p<0.05$) for all independent variables and for most two-way interactions. Nearly the entire regression model ($R^2 = 0.985$) was explained by I/D, so all but I/D and Edge were dropped from the final model: $Y_{Log(X_{damper})} = -1.434 + 0.089 * (Edge) + 4.30 * \left(\frac{I}{D}\right)$ ($R^2 = 0.978$). The resulting predictive model: $X_{damper} = 0.037 * 10^{\left(0.089 * (Edge) + 4.3 * \frac{I}{D}\right)}$. However error for untransformed X_{damper} increased sharply with increasing (I/D) and percent errors were as high as 125% across all values of (I/D). Hence the predictive models are useful for only initial rough adjustment and should be followed by final trial and error adjustment to goal air flow.

Acknowledgements

The author wishes to thank the following for their support: Nordfab for donating the ductwork, the graduate committee members for their advice and input and James Dalton for machining the concave edge of the damper to a straight edge.

Table of Contents

Abstract	ii
Acknowledgements	iii
List of Figures	vii
List of Tables	ix
Abbreviations	x
Chapter 1 Background	1
1.1 Purpose of Study	2
1.2 Characteristics of Slide-Gate Dampers	3
1.3 Derivation of X_{damper} from Bernoulli's Equation	6
1.4 Problems Due to Use of Dampers	9
Chapter 2 Literature Review	11
2.1 Velocity Profile	11
2.2 Published Damper Resistance Values	12
Chapter 3 Apparatus	18
3.1 Test Duct System	18
3.2 Dampers Tested	19
3.3 Pitot Tube and Traverse Device	20
3.4 Pressure Sensor	23
3.5 Devices to Measure Environmental Conditions	24
Chapter 4 Methods	25
4.1 Study Design	25
4.2 Calculations	26
4.2.1 Density Factor Calculation	26
4.2.2 Average Velocity Calculation	27
4.2.3 Average Velocity Pressure Calculation	28
4.2.4 Total Pressure (ΔTP) Calculation	28
4.2.5 Damper Resistance (X_{damper}) Calculation	28
4.2.6 Reynolds Number Calculations	30

4.2.7 Pipe Factor Calculations.....	30
4.3 Test Procedure	31
4.3.1 Calibration.....	31
4.3.2 Leak Tests	31
4.3.3 Preparation for Data Collection.....	32
4.3.4 Running the Experiment.....	32
4.3.5 Running a Test	33
4.3.6 Replications.....	33
Chapter 5 Results	34
5.1 Manometer Calibration.....	34
5.2 Characteristics of Velocity Measurements	35
5.2.1 Reynolds Number.....	35
5.2.2 Velocity Profile	35
5.2.3 Pipe Factor.....	36
5.3 Results of Replicated Data	37
5.4 Results of Relationship between X_{damper} and Relative Insertion Depth (I/D) – For All Data.....	39
5.5 Effect of (I/D) and remaining Independent Variables on Log(X_{damper})	41
5.5.1 Effect of (I/D) and Damper Edges (Edge) on Log (X_{damper})	42
5.5.2 Effect of (I/D) and Air Flow Levels (VP_{CLopen}) on Log (X_{damper})	43
5.5.3 Effect of (I/D) and Damper Orientation (Orient) on Log (X_{damper})	44
5.5.4 Effect of (I/D) and Duct Diameter (D) on Log (X_{damper}).....	45
Chapter 6 Discussion	46
6.1 Normality of Residuals for Log-transformed Data.....	46
6.2 Identifying Outlying Observations	47
6.3 Analysis of Variance	47
6.4 Regression Analysis	49
6.4 Reduced Regression Analysis Based on R^2	50
6.5 Non Log-Transformed Predictive Models.....	54
6.5.1 Predictive Models for X_{damper}	54
6.5.2 Complete Regression Model	55

6.5.3 Reduced Regression Model.....	57
Chapter 7 Conclusions	61
Bibliography	62
Appendix I: HVAC Regulation Dampers	64
Appendix II: Calibration of Digital Manometer	66
Appendix – III – (Flow chart for running the experiment).....	71
Appendix – IV – Replication Combinations.....	72
Appendix – V – Data	73

List of Figures

Figure 1 – Slide gate damper similar to those used in this study (Guffey, 2005).....	4
Figure 2 – Flow around a slide gate damper (Guffey, 2005).....	5
Figure 3 – Different leading edges of sliding gate dampers	6
Figure 4 – Laminar flow and turbulent flow velocity profile	11
Figure 5 – Change in resistance with damper insertion depth (Guffey, 1999).....	12
Figure 6 – Graph of Idelchik (1972) Table Values.....	14
Figure 7 – Log (X_{damper}) V/S Insertion Depth/Duct Diameter (Idelchik, 1972)	15
Figure 8 – Influence of face velocity on C_o (Robert Van Becelaere 2005)	16
Figure 9 – Variation of C_o with opposed blade damper (Robert Van Becelaere 2005)....	16
Figure 10– Variation of C_o with parallel blade damper (Robert Van Becelaere 2005)....	17
Figure 12 – Duct system used for the study.....	19
Figure 13 – Slide gate damper (Model No. 3241) used in the study	20
Figure 14 – Pitot tube sketch – similar to the one used in the study.....	20
Figure 15 – Static pressure measurement	21
Figure 16 – Velocity pressure measurement.....	22
Figure 17 – Pitot traverse device (Guffey, 1999)	22
Figure 18 – Digital Manometer (Model 8702)	23
Figure 19 – Hook Gaze (Dwyer Instruments – Model No. 1425)	23
Figure 20 – Exhaust Ventilation System in Ventilation and Exposure Assessment Laboratory (WVU).....	26
Figure 21 – Manometer calibration graph	34
Figure 22 – Velocity Profile for $D=4.85"$, $VP_{\text{COpen}} = 2.103"$ of w.g., Side 1 and Concave Edge.....	36
Figure 24 – X_{damper} V/S (I/D) for original and replicated data.....	38
Figure 25 – Log (X_{damper}) V/S (I/D) for original and replicated data.....	39
Figure 26 – X_{damper} V/S Insertion Depth/Duct Diameter	40
Figure 27 – Log (X_{damper}) V/S Insertion Depth/Duct Diameter	41
Figure 28 – Log cell means for damper edges.....	42

Figure 29 – Log cell means for VP _{CLOpen}	43
Figure 30 – Log cell means for damper orientation.....	44
Figure 31 – Log cell means for duct diameter	45
Figure 32 – Normal Probability Plot for X _{damper}	46
Figure 33 – Normal Probability Plot for Log (X _{damper})	47
Figure 34 – Predicted Log (X _{damper}) V/S Observed Log (X _{damper})	50
Figure 35 – Predicted Log (X _{damper}) V/S Observed Log (X _{damper}) (Reduced Model)	52
Figure 36 – Observed and Predicted (X _{damper}) V/S (I/D) (Complete Model)	55
Figure 37 – Residuals (X _{damper}) V/S (I/D) (Complete Model)	56
Figure 38 – Residuals (X _{damper}) V/S Predicted (X _{damper}) (Complete Model)	56
Figure 39 – Percent Error (X _{damper}) V/S (I/D) (Complete Model)	57
Figure 40 – Observed and Predicted (X _{damper}) V/S (I/D) (Reduced Model)	58
Figure 41 – Residuals (X _{damper}) V/S Predicted (X _{damper}) (Reduced Model)	58
Figure 42– Residuals (X _{damper}) V/S (I/D) (Reduced Model).....	59
Figure 43 – Percent Error (X _{damper}) V/S (I/D) (Reduced Model).....	59
Figure 44 – Percent Error in Airflow V/S (I/D) (Reduced Model).....	60
Figure 45 – Back draft Damper and Outlet Control Damper.....	64
Figure 46 – Parallel Blade and Opposed Blade Outlet Dampers.....	65
Figure 47 – Nested Inlet Vane Damper and External Inlet Vane Damper	65

List of Tables

Table 1 – Independent variables used in the study	3
Table 2 – Damper insertion depth for 4.85” and 3.85” duct diameters	3
Table 3 – Recommended damper resistance values (Idelchik, 1972).....	13
Table 4: - Analysis of Variance with all Independent Variables	48
Table 5: - Analysis of Variance with Significant Independent Variables	49
Table 6: - R ² Analysis for Reduced Regression Model	51

Abbreviations

A_{open}	Open area of the duct
A_{total}	Total area of the duct
C_o	Local loss coefficient
D	Diameter of duct
df	Density Factor
Edge	Damper Edge
F	Damper Resistance (Bernoulli)
I	Insertion depth
(I/D)	Insertion Depth/Duct Diameter (Relative Insertion Depth)
Orient	Damper Orientation
P	Pressure
P_{bar}	Barometric Pressure
PF	Pipe Factor
$P_{std.}$	Standard atmospheric pressure
Q	Air Flow
Re.	Reynolds Number
SP_{end}	Static Pressure at the end of the duct
SP_h	Hood Static Pressure
T	Temperature
TP_{loss}	Total Pressure Loss
$T_{std.}$	Standard atmospheric temperature
V	Velocity of air in duct
V_{CL}	Centerline Velocity
$V_{avg.}$	Average Velocity
VP	Velocity Pressure
$VP_{avg.}$	Average Velocity Pressure
VP_{CLopen}	Air flow level

X_{br}	Branch Resistance
X_{damper}	Damper Resistance
$X_{endwithdamper}$	Damper Resistance with damper partially inserted
X_{elbow}	Elbow Resistance
$X_{Friction}$	Resistance due to friction
X_{hood}	Hood Resistance
$X_{endwithoutdamper}$	Damper resistance with damper fully open
ΔTP	Change in Total Pressure
ρ	Density
ν	Viscosity of air

Chapter 1 Background

Dampers are ventilation devices that can be used to adjust the airflows through the branches in a duct system. Dampers have been used in ventilation systems for at least fifty years (Geiger). SMACNA (1993) defines a damper as a device that varies the volume of air passing through an air outlet, air inlet, or duct. Dampers reduce the airflow to a given branch by adding to its resistance to flow. Increasing resistance of a branch duct reduces the flows to that branch and increases flows in all other branches (Guffey, 1993). Withdrawing the dampers has the reverse effect. According to Robert Van Becelaere (2005), an ideal damper is one which produces no resistance to airflow when wide open and can provide substantial resistance to the system upon partial closure. By proper adjustment of all dampers in a system, the user can force the airflows through the different branches to achieve a desired distribution of airflows.

There are different designs of adjustable dampers that can be used in exhaust ventilation systems including butterfly dampers, splitter dampers and shutter dampers (Haines, 1988). Butterfly dampers are used in branches and resemble flue dampers found in residential chimneys. Butterfly dampers swivel about an axis to block airflow either completely or partially. If the axis of the butterfly dampers is perpendicular to the duct then the resistance is maximum and if it is aligned to the duct then there is minimal resistance. Splitter dampers are used in “Y” shaped junctions to block airflow from one branch, but their use is discouraged in favor of dampers in each branch. Shutter dampers are commonly used for control of smoke, fire, and hot gases at points where ductwork passes through one wall into another area (Geiger).

The most common dampers used for contaminant control ventilation are slide-gate dampers. Slide-gate dampers are preferred in exhaust ventilation because of their ease of adjustment. Butterfly dampers are more likely to promote plugging and also vibrate at high velocities unless rigidly constructed. As demonstrated by Crowder and Loudermilk (1982) and by Idelchik (1972), as the damper insertion depth increases, damper resistance

(X_{damper}) also increases. However the mathematical relationship between damper insertion depth and X_{damper} to which this increase takes place has not been shown. Further it is not clear to what design of dampers their results apply. This study investigates slide gate damper resistance.

1.1 Purpose of Study

The study determines the relationship between damper resistance and damper insertion depth for slide gate dampers. The study will analyze the following statistical model.

Statistical model:

$$\text{Log } (X_{\text{damper-ijklm}}) = C_0 + C_1 * (I)_i + C_2 * (1/D)_j + C_3 * (\text{VP}_{\text{CLopen}})_k + C_4 * (\text{Edge})_l + C_5 * (\text{Orient})_m + e_{ijklm}$$

Where $C_0, C_1, C_2, C_3, C_4, C_5$ = Constants,

e = Residual error,

Edge = Damper edge

$\text{VP}_{\text{CLopen}}$ = Open level of airflow (inches of w.g.)

Orient = Damper Orientation

I = Insertion depth (inches),

D = Duct diameter (inches)

Where $i = 1, 2, 3, 4, 5, 6, 7, 8; j = 1, 2; k = 1, 2, 3, 4; l = 1, 2;$ and $m = 1, 2;$

Damper insertion depth (I), airflow level ($\text{VP}_{\text{CLopen}}$), duct diameter (D), damper orientation (Orient) and edge of the damper (Edge) are the independent variables considered for this study. The levels for each are shown in Table 1. Two levels of diameter (3.85 and 4.85 inches) have been used for the study as the fan used to provide the airflow in the study has capacity to pull air for duct diameters up to 4.85 inches. Two edges (straight and concave) have been considered as they are used in the industry. Orientation has been used as a variable to see if the side of the test damper has any significance on X_{damper} . Both 4.85" and 3.85" diameter duct damper slides were inserted to eight insertion depths, including having the damper in fully open position. The eight

damper insertion depths were obtained on the assumption that the damper resistance is proportional to the log insertion depth. If that is true, then the insertion depths will be evenly spaced in a logarithm (I/D) relationship. The damper insertion depths for both the duct diameters are shown in Table 2.

Table 1 – Independent variables used in the study

Number	Independent Variables	Levels			
		Level 1	Level 2	Level 3	Level 4
1	Duct Diameter	3.85"	4.85"	-	-
2	Damper Edge	Concave	Straight	-	-
3	VP _{CLopen} - Level of Air Flow	2.103" of w.g.	1.01" of w.g.	0.51" of w.g.	0.255" of w.g.
4	Damper Orientation	Side 1	Side 2	-	-
5	Insertion Depth	Eight Insertion depths including the damper fully open position			

Table 2 – Damper insertion depth for 4.85" and 3.85" duct diameters

Number	Insertion Depth (inch)		(I/D) %
	4.85" duct	3.85" duct	
1	0	0	0
2	0.65	0.5	13
3	0.85	0.7	18
4	1.2	0.9	24
5	1.5	1.2	32
6	2.3	1.8	47
7	3.1	2.5	63
8	4.1	3.2	84

1.2 Characteristics of Slide-Gate Dampers

In a slide-gate damper (see Figure 1), the slide is inserted perpendicular to the flow. As the air flows around the slide, it separates from the duct downstream of the slide. The slide-gate, also called “blast-gate or cut-off” damper, is completely out of the air stream when open, yet effectively seals the branch when shut (Haines, 1988). The region where

the air separates from the duct downstream of the slide when the slide is inserted in to the duct is called the “separation region”.

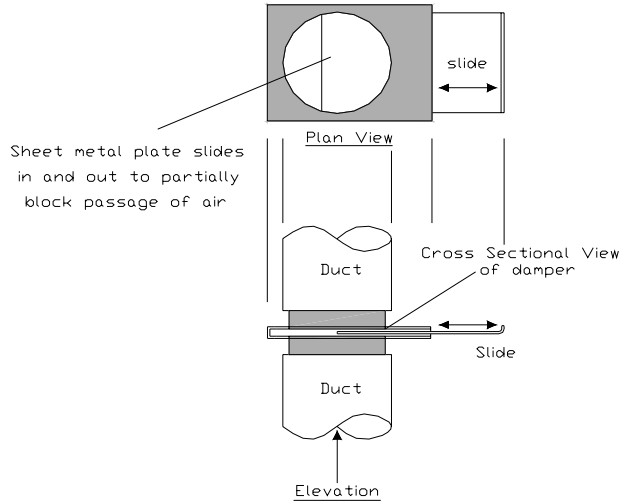


Figure 1 – Slide gate damper similar to those used in this study (Guffey, 2005)

There are energy losses in the separation region as air flows around the slide of a slide gate damper (see Figure 2). Slide gate edge sharpness (blunt or sharp), the velocity pressure (VP) of the airflow upstream of the damper, the shape of the edge of the damper (convex edge, straight edge or concave edge), and the fraction of the duct cross-section blocked by the damper (I/D – insertion depth/duct diameter) affect the energy losses in the separation region. In addition, energy losses in the separation region may be affected by upstream and downstream disturbances (e.g. elbows, hood connections, etc) (Guffey, 2005). These energy changes produce static pressure changes downstream of the damper.

Damper resistance is calculated as the difference between the resistance with and without the damper. The resistance of the damper (X_{damper}) can be defined as the ratio of the change in total pressure (TP) across the damper divided by the upstream velocity pressure. Since it is difficult to measure resistance across a damper accurately it is calculated in the following manner:

$$X_{damper} = \left(\frac{VP_2 + SP_2}{VP_2} \right) - \left(\frac{VP_1 + SP_1}{VP_1} \right) \quad (1)$$

Where I = without damper inserted

2 = with damper inserted to some amount

SP = Static pressure measured downstream of damper

VP = Average velocity pressure

Equation 1 can further be simplified to:

$$X_{damper} = X_{endwithdamper} - X_{endwithoutdamper} \quad (2)$$

Where $X_{endwithoutdamper}$ = damper resistance value with damper fully open

$X_{endwithdamper}$ = damper resistance with damper partially inserted in the duct

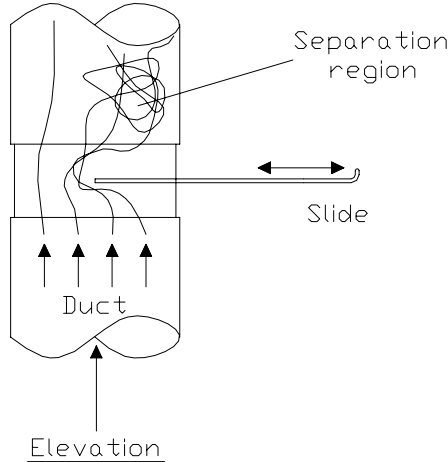


Figure 2 – Flow around a slide gate damper (Guffey, 2005)

Required values of X_{damper} on the same system for different branches typically range from 0.2 to 5 (Guffey, 1993). X_{damper} values less than 0.2 would have little effect on airflow. For a duct that has a diameter much larger than needed, the value of X_{damper} could reach 100 or even more (Guffey, 2005).

It is likely that slide gate dampers for different geometries of the edge of the slide have very different X_{damper} values for a given insertion depth. There are many possible

geometries for the leading edge of the gate of the damper but the two major ones are straight line and curved (convex/concave) (see Figure 3). A concave shape of the edge prevents complete blockage of flow in the duct, which is sometimes desirable.

The sharpness of the leading edge is another factor. As is known by analogy to orifice plates used for airflow measurement, the sharper the leading edge of the damper, the greater the value of X_{damper} at a given insertion depth (Guffey, 2005).

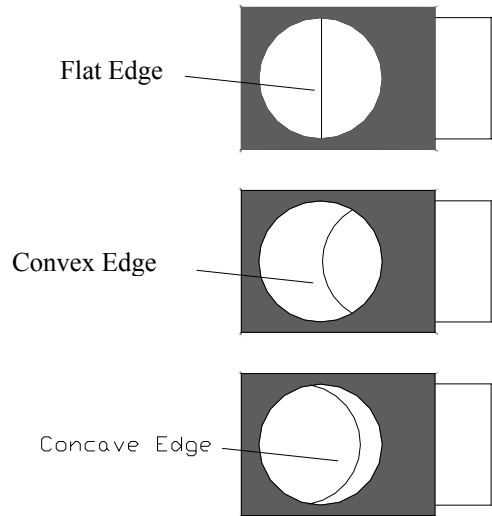


Figure 3 – Different leading edges of sliding gate dampers

Abrasive wear of a previously sharp edge of a damper can reduce the resistance of the damper at a given insertion depth. It is also possible for the damper resistance to vary due to accumulation of contaminants on the slide or just upstream or downstream of the slide. Accumulation of contaminants on the downstream side would substantially reduce the resistance. On the other hand any accumulation that extends beyond the reach of the gate could increase the resistance.

1.3 Derivation of X_{damper} from Bernoulli's Equation

Damper resistance can be derived from Bernoulli's equation in the following manner; Bernoulli's equation is stated as:

$$SP_1 + VP_1 + P_{bar1} = SP_2 + VP_2 + P_{bar2} \quad (3)$$

Where SP = Static pressure measured downstream of damper

VP = Velocity pressure

P_{bar} = Barometric pressure

1 = Inlet condition

2 = Outlet condition

Assuming $P_{bar1} = P_{bar2}$

$$SP_1 + VP_1 = SP_2 + VP_2 \quad (3a)$$

$$TP_1 = TP_2 \quad (3b)$$

Where TP = Total pressure = $SP + VP$

This relationship is incorrect for turbulent conditions of ventilation system ducts since it assumes zero energy losses. It has been extended by adding a ‘lost pressure’ term.

$$TP_{loss} = TP_1 - TP_2 \quad (4)$$

Where TP_{loss} = Total pressure loss

It has been shown that for many components

$$TP_{loss} = F * VP_1 \quad (4a)$$

Where F = Damper resistance

$$\text{Thus } F = \frac{TP_1 - TP_2}{VP_1} \quad (4b)$$

However that Kludged correction is not correct from energy per time point of view.

$$\text{Energy}_1 = \text{Energy}_2 + \text{Energy Loss} \quad (5)$$

For ventilation systems, changes in P_{bar} are trivial,

$$\text{Energy} = Q * TP \quad (6)$$

Where Q = Air flow

Hence from Equation 6 and 7,

$$Q_1 * TP_1 = Q_2 * TP_2 + \text{Energy Loss} \quad (7)$$

$$\text{Energy Loss} = Q_1 * TP_1 - Q_2 * TP_2 \quad (8)$$

Experimentally it has been demonstrated that for serial flow (Guffey, 1993)

$$\text{Energy Loss} \approx X * Q * VP \quad (9)$$

Where X = Damper resistance

Hence from Equation (8) and Equation (9)

$$X = \frac{Q_1 * TP_1 - Q_2 * TP_2}{Q_1 * VP_1} \quad (10)$$

Since changes in pressure are generally small fractions of P_{bar} ,

Then $\rho_1 = \rho_2$, thus $Q_1 = Q_2$

Hence Equation 10 can be further simplified to,

$$X = \frac{TP_1 - TP_2}{VP_1} \quad (11)$$

This is the basis of predicted pressures in ventilation and hydraulic systems.

A more robust relationship can be defined using energy relationships. Energy equation is as follows:

$$\text{Energy Loss}_{A+B} = \text{Energy Loss}_A + \text{Energy Loss}_B \quad (12)$$

$$\text{Then } X_{A+B} = X_A + X_B \quad (13)$$

Where X = damper resistance

In this case,

$$X_{br + \text{damper}} = X_{br} + X_{\text{damper}} \quad (14)$$

Where $X_{br + \text{damper}}$ = Total resistance

X_{br} = Branch resistance

X_{damper} = Damper resistance

Hence from Equation 14,

$$X_{\text{damper}} = X_{br + \text{damper}} - X_{br} \quad (14a)$$

$$X_{\text{damper}} = X_{\text{endwithdamper}} - X_{\text{endwithoutdamper}} \quad (15)$$

Where $X_{endwithoutdamper}$ = damper resistance with damper fully open

$X_{endwithdamper}$ = damper resistance with damper partially inserted in the duct

$X_{endwithdamper}$ can be further simplified to,

$$X_{endwithdamper} = X_{hood} + X_{elbow} + X_{Friction} + X_{damper} \quad (16)$$

Where X_{hood} = Hood resistance = 0.2 (ACGIH, 1997)

X_{elbow} = Elbow resistance = 0.93 (ACGIH, 1997)

$X_{Friction}$ = Resistance due to friction

X_{damper} = damper resistance

$X_{Friction}$ is a function of velocity because TP is proportional to $V^{1.9}$ instead of V^2 (Guffey)

Hence,

$$X_{Friction1} = X_{Friction2} * \left(\frac{V_2}{V_1} \right)^{0.1} \quad (17)$$

Statistically in terms of velocity pressure, Equation 17 can be written as,

$$X_{Friction1} = X_{Friction2} * \left(\frac{VP_2}{VP_1} \right)^{0.05} \quad (18)$$

1.4 Problems Due to Use of Dampers

There are many problems associated with the use of dampers. Dampers increase the total resistance of the duct system. Fan airflow output decreases with increasing resistance. Therefore increasing the damper insertion depth reduces the airflow from the fan and increases the pressure produced by the fan. High resistances may require an increase in fan speed, which increases the operating costs of fan. Fan efficiency also may be affected if the fan was not selected with the additional resistance in mind (Guffey, 2005).

If the dampers are used both to achieve required distribution and to reduce airflow, the pressure required at the fan can be substantial. However this is true only if the fan speed is unnecessarily high. If dampers are employed only to produce the desired distribution

and the fan is adjusted properly, the pressure requirement for the system will be nearly always lower than without the dampers (Guffey, 1993).

The friction between the slide and the damper should not be too high or too low for easy slide movement. Also the duct with the slide gate damper should be supported rigidly to avoid the duct movement when pulling on the slide especially if there is high friction between the slide and the damper.

Dampers should be cleaned regularly as sticky or stringy contaminants can be caught on the slide of the damper. Plugging might likely occur due to rags, pieces of paper and other material that are sucked in to the duct by the fan. Flammable materials caught on a damper could create a fire hazard. Hence care should be taken to avoid flammable materials.

The location of damper on a duct is also important for proper operation of the system. The damper should never be located near elbows and other disturbances that may influence the pressure drop. Dampers can become sources for material build up if not located properly.

Chapter 2 Literature Review

Despite a diligent search for articles on damper resistance and damper insertion depths very little was found in the literature on the relationship of X_{damper} to insertion depth of dampers. Four articles (Guffey, 1999; Idelchik, 1972; Crowder and Loudermilk, 1982; and Robert Van Becelaere, 2005) did cover damper resistance versus damper insertion depths, but there is no mention of any relationship between the two parameters. In addition to the four articles there are some publications that discuss issues relevant to investigation of damper resistances.

2.1 Velocity Profile

In research involving pressure and flow measurements it is important to have suitable measurement conditions. If the velocity profile is symmetric it is very likely that measured conditions are good.

The drag developed at the surface of the duct retards the airflow the most at the skin and lesser amounts as the distance from the surface increases. For air flowing undisturbed in a long straight duct, the velocity of air in the duct will vary from zero at microscopic distance from the duct to a maximum at the centerline of the duct. A turbulent flow develops a flattened parabolic velocity contour (see Figure 4), whereas a laminar flow develops a parabolic velocity contour far downstream flow (Guffey). At velocities typical of ventilation systems, the average velocity equals 90% of the centerline velocity at seven duct diameters from an upstream disturbance (Guffey). Velocity profile for the data collected will be drawn to check whether the data collected is in accordance with the literature mentioned above.



Figure 4 – Laminar flow and turbulent flow velocity profile

2.2 Published Damper Resistance Values

Guffey (1999) found that values of damper resistance changed with different damper insertion depth for different branches but did not describe the mathematical relationship between damper insertion depth and X_{damper} . However Guffey demonstrated that values of damper resistance for a particular branch (X_{br}) with a given damper insertion depth remained nearly constant as airflow velocities were doubled and as other branch dampers were adjusted.

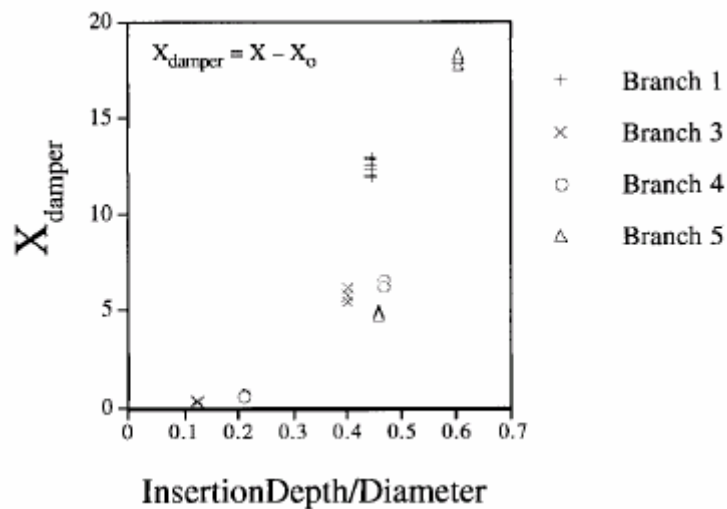


Figure 5 – Change in resistance with damper insertion depth (Guffey, 1999)

According to Guffey (1999) the change in the value of X_{damper} for a branch increased steadily as the damper insertion depth was increased (see Figure 5). The values of the damper resistance increased steadily for all the branches as shown Figure 5. The values of X_{damper} for the different dampers did not follow a smooth curve with increasing relative insertion depths. A possible reason might be due to the damper being inserted partially even when the damper handle was pulled to its most open position. Also there was little scatter in the data points (see Figure 5) which indicates that there is no relationship between damper resistance and airflow level.

Guffey concluded that the values of damper resistance was independent of airflow change in the branch, whether the change was caused by overall system airflow (i.e., changing fan speed) or the adjustment of the damper in another branch. This suggests that level of airflow should not be an important factor in the proposed study.

The graph of damper insertion depth and the damper resistance for all the branches except branch number 1 (see Figure 5) is similar to the graph (see Figure 6) obtained by Idelchik (1972). One reason for a different pattern for branch number 1 in Figure 5 could be the damper slide being inserted in to the duct to some extent even though the damper was in fully open position.

Idelchik (1972) provided a table of recommended values for a damper (see Table 3), but there was no explanation to how the values were produced and no description of the dampers and measuring conditions. Plotting the values showed a highly non-linear relationship (see Figure 6).

Table 3 – Recommended damper resistance values (Idelchik, 1972)

(I/D)	X _{damper}
0.1	0
0.2	0
0.3	1
0.4	2
0.5	3
0.6	6
0.7	11
0.8	37

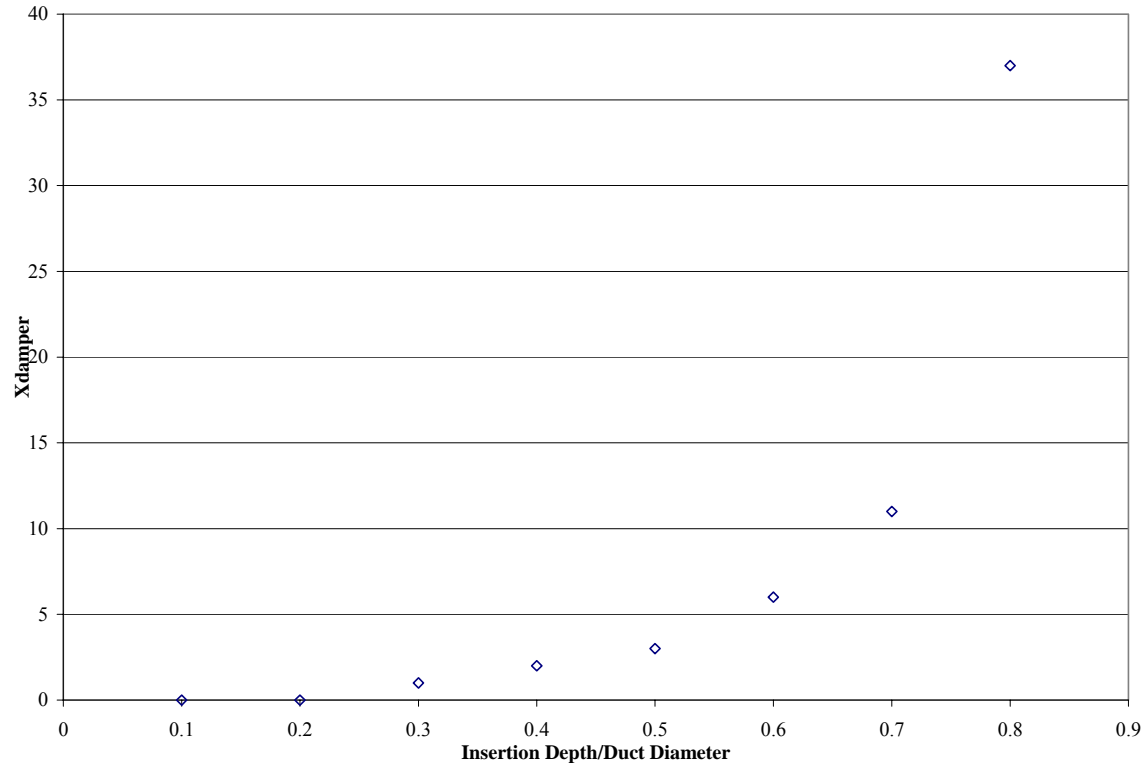


Figure 6 – Graph of Idelchik (1972) Table Values

Log transforming the values will not completely linearize them (see Figure 7). The resistance increases much more than linearly because: 1) as the damper insertion depth increases, the opening of the airflow through the duct becomes progressively smaller, increasing the air velocity past the edge of the slide (Guffey, 2005), and 2) the region of separation becomes larger (see Figure 2).

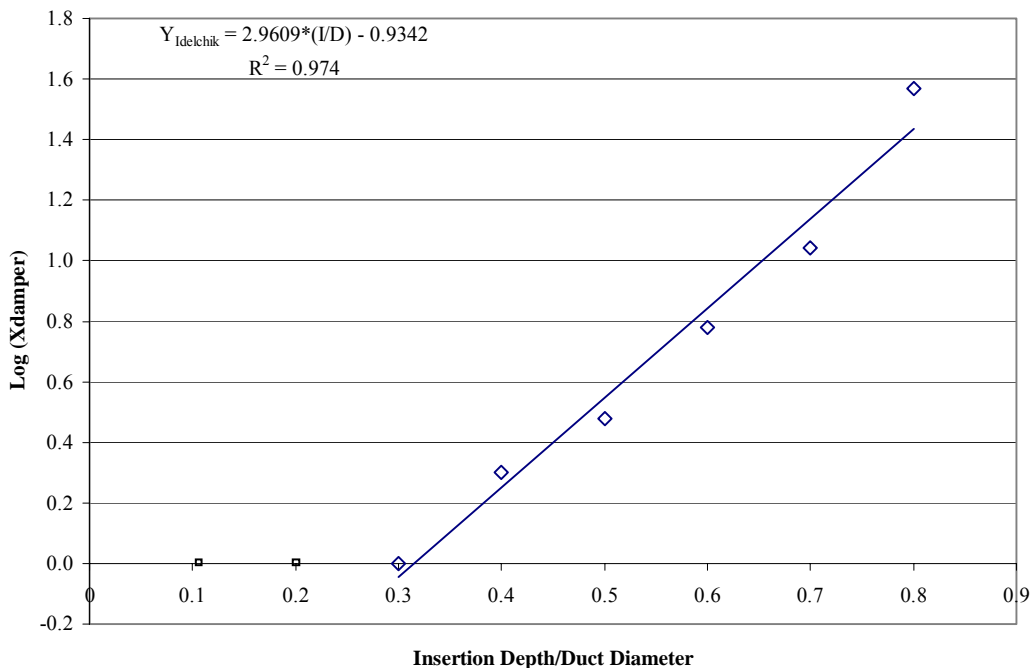


Figure 7 – Log (X_{damper}) V/S Insertion Depth/Duct Diameter (Idelchik, 1972)

Different dampers may follow different curves based on damper blade design (straight or curved). It can be seen that the X_{damper} (see Figure 6) changes little until the damper is more than one third closed. At insertions greater than three quarters of the diameter, the change in the damper resistance is very high. Crowder and Loudermilk (1982) published a table of insertion depths to achieve different pressures at a given velocity but did not show mathematical equation and did not describe the design.

Robert Van Becelaere (2005) demonstrated the effects of type of damper, blade movement, manufacturer, installation, approach velocity, and total system pressure drop on parallel and opposed blade dampers. Resistance to flow was caused by the damper blades, the frame members, and also by the operating linkage. Damper blade positions were expressed in number of degrees from the closed position. The damper blade position was varied by varying the damper louver by 10-degree increments from closed to 90 degrees (open) in the test.

However from figure (see Figure 8), with face velocity as the parameter, it could be seen that the face velocity does have some influence on the loss coefficient at smaller

openings. This disagrees with Guffey (1999) as mentioned earlier. The possible reason might be the manner in which the slide gate dampers and parallel and opposed blade dampers operate is different. However the proposed study can determine whether the air flow velocity does have or does not have an effect on the damper resistance.

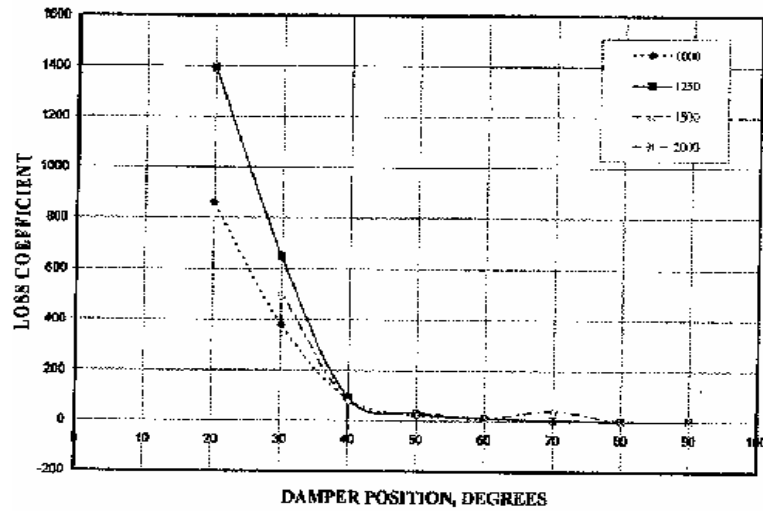


Figure 8 – Influence of face velocity on C_o (Robert Van Becelaere 2005)

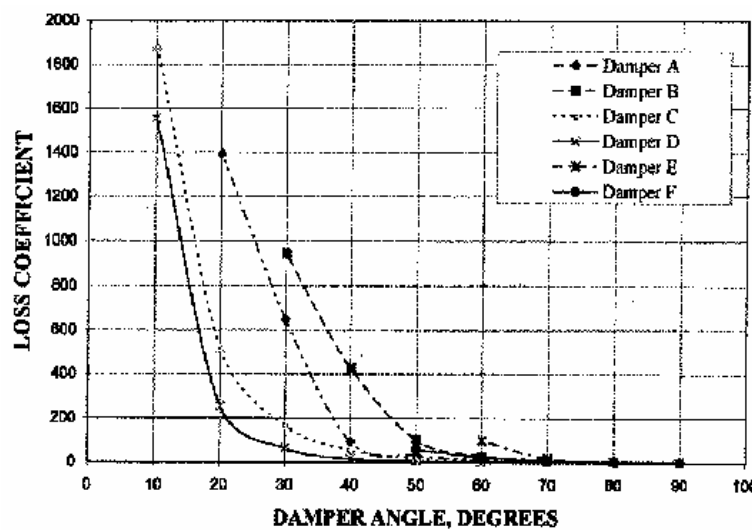


Figure 9 – Variation of C_o with opposed blade damper (Robert Van Becelaere 2005)

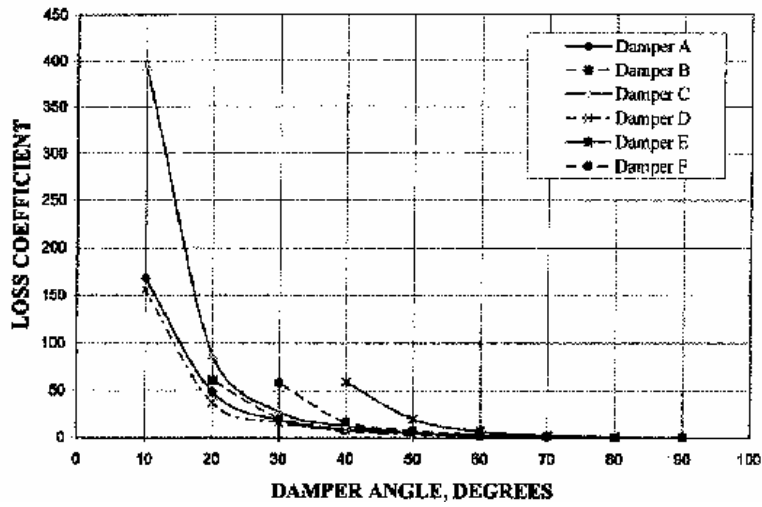


Figure 10– Variation of C_o with parallel blade damper (Robert Van Becelaere 2005)

From the above two graphs (see Figure 9 and Figure 10) it can be seen that the system performs differently with different dampers, although Becelaere did not determine a mathematical relationship between the loss coefficient and blade position.

Chapter 3 Apparatus

The study was performed in the West Virginia University Ventilation and Exposure Assessment Laboratory on the experimental exhaust ventilation system located in the laboratory. An Aerovent Fan (No. 315B1-SWCB-3435-3 Type SWCB Ser. 8708562-001) provided the airflow.

3.1 Test Duct System

A schematic of the test system is shown in Figure 11. It was assembled from 5' lengths of straight ducts (Model No. 3201) and a two 90° elbow (Model No. 3211). They were manufactured and donated by Nordfab (Thomasville, N.C.).

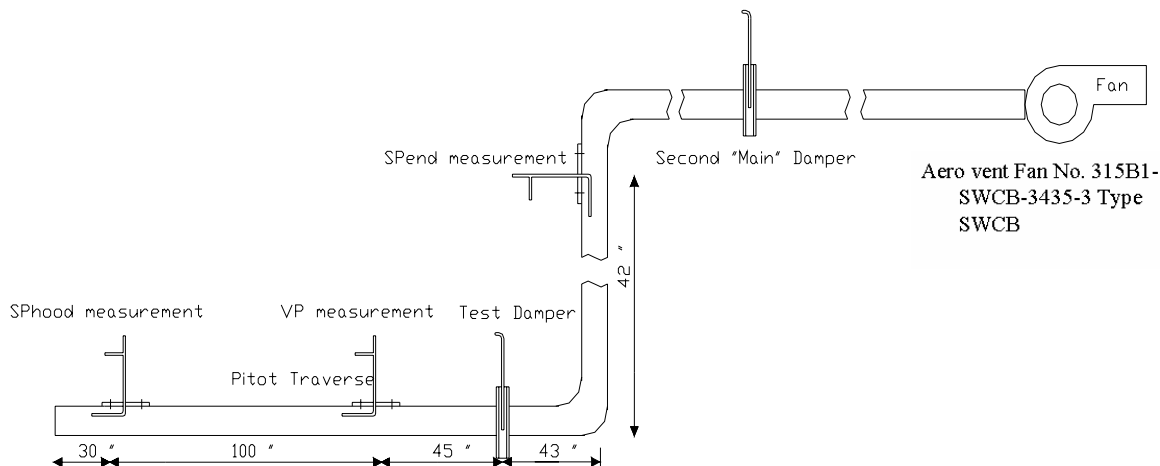


Fig 11 – Schematic of test duct system

The elbow was stamped from 20 – gauge sheet metal in a smooth, full 90° turn. The 5' duct sections were clamped to other duct sections using a clamp manufactured by Nordfab.

Before testing, the sliding gate damper and the elbow were caulked to eliminate air leakage. Ducts were supported at 2 feet intervals using duct tape and nylon strings (see Figure 12). Two duct diameters were tested, 4.85" and 3.85".



Figure 12 – Duct system used for the study

3.2 Dampers Tested

Two sealed slide-gate dampers (Model No. 3241 – see Figure 13) were used for the study. One was used to fit a 4.85" diameter duct and the other to fit a 3.85" duct diameter. Two damper edges for each duct diameter were used, one was straight edge and the other was concave edge. Duct tape was used to seal the joints of dampers. Insertion depths were measured (see Figure 13) from the displacement of the handle from the fully open position of the damper. The sliding gate damper was marked with eight insertion depths, including the fully open position (see Table 2). The damper is symmetric on both sides, and the difference in manufacturing is so subtle that it is practically impossible for a practitioner to see the gasket on side 2. Hence orientation of damper was also considered as a variable to see if there is any difference in damper orientation.



Figure 13 – Slide gate damper (Model No. 3241) used in the study

3.3 Pitot Tube and Traverse Device

Standard Pitot tubes (see Figure 14) were used to obtain the SP_{hood} , and SP_{end} as well as 10-point log linear Pitot traverses. A TSI manometer (Model: 8702) was used to measure the (average flow velocity) velocity pressures and static pressures.

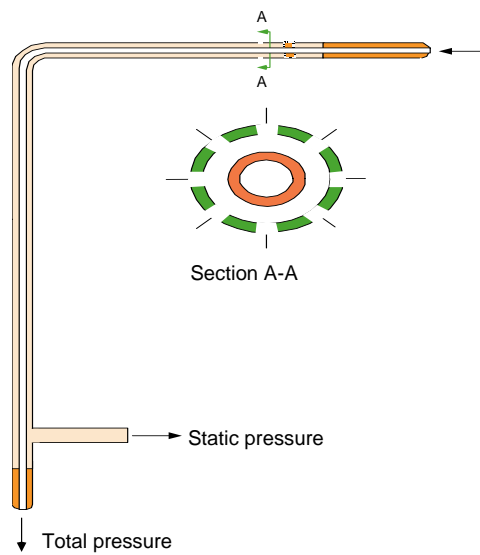


Figure 14 – Pitot tube sketch – similar to the one used in the study

The static pressure (see Figure 15) is measured by connecting the manometer to the static pressure leg. The velocity pressure can be measured by (see Figure 16) connecting the manometer to both the legs of the Pitot tube. Pitot tubes were connected to the pressure sensor using Tygon ® plastic tubing of the digital manometer. All static pressures were measured at duct centerlines.

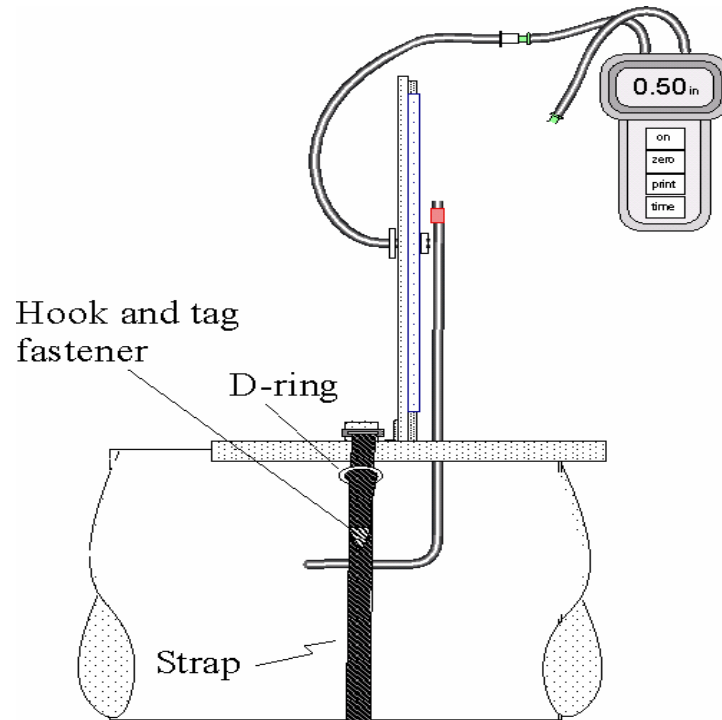


Figure 15 – Static pressure measurement

Custom-made devices (Guffey, 1990) were used to hold each Pitot tube in place (see Figure 17). Each traverse device was attached to the duct using an adjustable strap looped through a D – ring and held in place with tag straps and duct tapes.

The hood static pressures were measured seven duct diameters downstream from the start of the straight duct and the end static pressure was measured nine duct diameters downstream from the 90° elbow. Velocity pressures were measured twenty-six duct diameters from the beginning of the duct opening to allow the air stream to stabilize. According to Guffey and Booth (1999), two perpendicular Pitot traverses can be taken as close as three duct diameters from disturbances with acceptable ($\leq 5\%$) deviations from

measurements. In the study Pitot traverses have been taken more than seven duct diameters from disturbances.

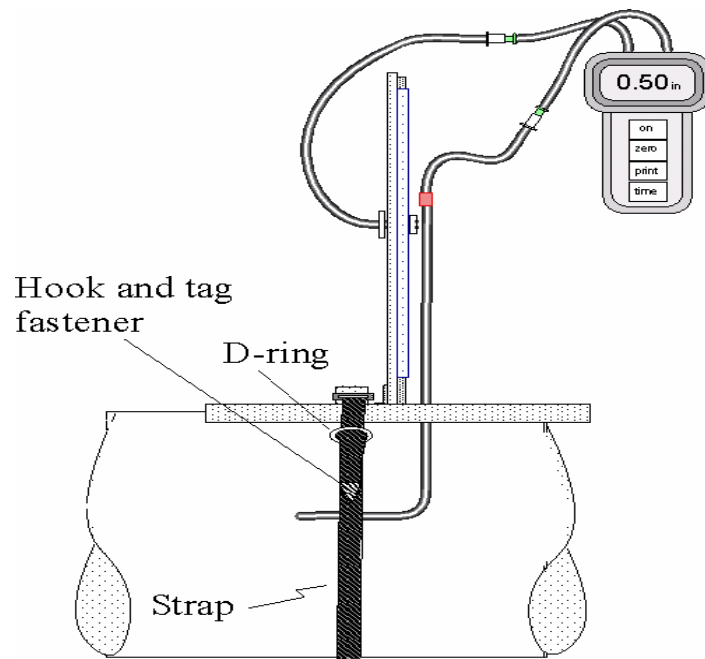


Figure 16 – Velocity pressure measurement

Also Industrial Ventilation (1998) recommends that Pitot traverses be taken at least seven duct diameters of distance downstream from disturbances.

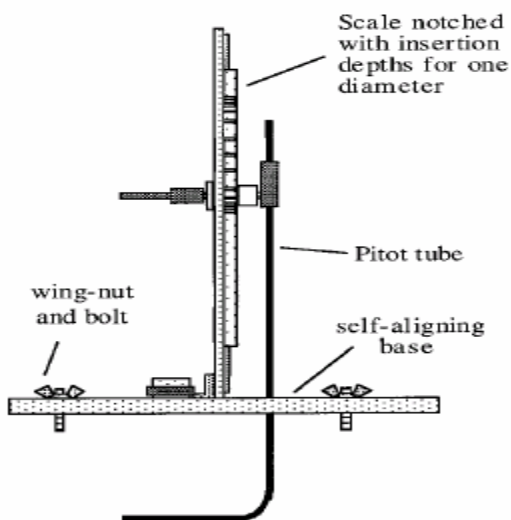


Figure 17 – Pitot traverse device (Guffey, 1999)

3.4 Pressure Sensor

A TSI DP-Calc digital manometer (Model: 8702 – see Figure 18) was used to measure the hood static pressure, end static pressure, and velocity pressures. The digital manometer was calibrated using a Dwyer Instruments Inc. No. 1425 Hook gage (see Figure 19).



Figure 18 – Digital Manometer (Model 8702)



Figure 19 – Hook Gaze (Dwyer Instruments – Model No. 1425)

3.5 Devices to Measure Environmental Conditions

Environmental conditions, such as temperature and pressure, were measured during the study in the laboratory every time the data was collected. The temperature in the laboratory was measured using a calibrated dry bulb thermometer and the barometric pressure was measured using a standard laboratory barometer inside the laboratory. The duct temperature was measured with a calibrated digital thermometer. The later was always within three degrees of room temperature.

Chapter 4 Methods

This study determines the relationship between the damper resistance and damper insertion depth. This section includes study design, parameter calculations, and the test procedure followed by the author.

4.1 Study Design

Insertion depth, duct diameter, airflow velocity, damper orientation and damper edge were considered as variables in the study to determine the relationship between the damper insertion depth and damper resistance. For every test run, values of SP_{end} , SP_{hood} , and 20 velocity pressure readings along with the centerline velocity pressure readings were measured using the digital manometer and Pitot tubes.

This study is a factorial design with the following variables:

Dependant variables: X_{damper}

Independent variables: Insertion depth (I), duct diameter (D), damper edge (Edge), damper orientation (Orient) and level of airflow (VP_{CLopen})

Levels of Independent variables are shown in Table 1 and Table 2.

It was not feasible to adjust the fan in the laboratory to vary airflow velocity. Instead the level of airflow (VP_{CLopen}) was changed by adjusting a second (“Main”) damper (see Figure 20) that was well downstream of the test damper. This was achieved by setting the system centerline velocity at four different ranges shown in Table 1 with the damper in open position. Velocity pressure readings for different insertion depths were measured for each of the main damper settings.



Figure 20 – Exhaust Ventilation System in Ventilation and Exposure Assessment Laboratory (WVU)

4.2 Calculations

This section shows the formulae and the order in which the different parameters are calculated, required for analysis of the data collected by the author.

4.2.1 Density Factor Calculation

Density factor is defined as the ratio of actual density to standard density. Density factor can be expressed in terms of component density for the effects of pressure, temperature and humidity on air density as shown below;

$$df = \left(\frac{P_{bar} + SP_{duct}}{P_{std}} \right) * \left(\frac{T_{std}}{T_{act}} \right) \quad (19)$$

Where $P_{std} = 407$ " w.g. or 760 mmHG or 101 kPa or 29.92" of Hg

$$T_{std} = 530 \text{ R or } 294.3 \text{ K (} 70^{\circ}\text{F or } 21^{\circ}\text{C})$$

$$T_{act} = (460 \text{ R} + T_F) \text{ or } (273 + T_C)$$

df = Density factor

4.2.2 Average Velocity Calculation

Air velocity can be computed from observed velocity pressures if the air density is known or can be determined using density factor (Guffey). For velocity at a single point, i

$$V_i = 1096 \sqrt{\frac{VP_i}{\rho}} \quad (20)$$

$$Vi = 4005 \sqrt{\frac{VP_i}{df}} \quad (21)$$

Where V_i = velocity in fpm at a single location i ($i = 1, 2, 3 \dots 20$)

VP_i = Velocity pressure in inches of water gauze measured at a single location i

ρ = Density of air in lb/ft^3

df = density factor

Although a point velocity can be computed from a point velocity pressure, the average velocity cannot be computed from each individual velocity pressure. Instead the average velocity is computed by calculating individual velocity from individual velocity pressure measurements and then taking the average of all the velocities as shown below.

$$V_{avg.} = \frac{1}{n} \sum_{i=1}^n V_i \quad (22)$$

Where n = number of samples taken across a section

V_i = Point velocity at i ($i = 1, 2 \dots 20$)

4.2.3 Average Velocity Pressure Calculation

Average velocity pressure is calculated from average velocity, which is equivalent to;

$$VP_{avg.} = \left(\frac{\sum_{i=1}^{i=20} \sqrt{VP_i}}{20} \right)^2 \quad (23)$$

Where $VP_{avg.}$ = Average velocity pressure

This method used to calculate the average velocity pressure is mathematically identical to computing it from the density and the mean velocity (Guffey, 1999). Note that the centerline velocity pressure is not included in the calculation of average velocity pressure.

4.2.4 Total Pressure (ΔTP) Calculation

The change in total pressure is calculated as;

$$\Delta TP = SP_{end} + VP_{avg.} \quad (24)$$

Where $VP_{avg.}$ = Average velocity pressure calculated excluding the centerline
Velocity pressure reading

SP_{end} = Static pressure at the end of the branch

4.2.5 Damper Resistance (X_{damper}) Calculation

Damper resistance is calculated as the difference between the resistance with and without the damper. The resistance of the damper (X_{damper}) can be defined as the ratio of the change in total pressure (TP) across the damper divided by the upstream velocity pressure. Since it is difficult to measure resistance across a damper accurately it is calculated in the following manner:

$$X_{damper} = \left(\frac{VP_2 + SP_2}{VP_2} \right) - \left(\frac{VP_1 + SP_1}{VP_1} \right) \quad (25)$$

Where 1 = without damper inserted

2 = with damper inserted to some amount

SP = Static pressure measured downstream of damper

VP = Average velocity pressure

Equation 25 can further be simplified to:

$$X_{damper} = X_{endwithdamper} - X_{endwithoutdamper}$$

Where $X_{endwithoutdamper}$ = damper resistance value with damper fully open

$X_{endwithdamper}$ = damper resistance with damper partially inserted in the duct

$X_{endwithdamper}$ can be further simplified to,

$$X_{endwithdamper} = X_{hood} + X_{elbow} + X_{Friction} + X_{damper}$$

Where X_{hood} = Hood resistance = 0.2 (ACGIH, 1997)

X_{elbow} = Elbow resistance = 0.93 (ACGIH, 1997)

$X_{Friction}$ = Resistance due to friction

X_{damper} = damper resistance

$$\text{Where } X_{Friction} = X_{Hood} - X_{Elbow} - \left[1 - \left(\left(\frac{VP_{Avg.}}{VP_{COpen}} \right)^{0.5} \right)^{0.1} \right] \quad (26)$$

Errors in shifts in airflow are determined in the following manner. Consider two branches ‘a’ and ‘b’ with damper in branch a.

$$\frac{Q_b}{Q_a} \alpha \left(\frac{1 + X_{enda} + X_{damper}}{1 + X_{enda}} \right)^{0.5} \quad (27)$$

Where Q_b = Airflow in branch b

Q_a = Airflow in branch a

X_{enda} = End damper resistance

X_{damper} = Damper resistance

Percent error can be calculated in the following manner:

$$\left(\frac{\frac{Q_a}{Q_b}}{\frac{Q_{bt}}{Q_{at}}} \right) \alpha \left(\frac{1 + X_{enda} + X_{damper} + Error}{1 + X_{enda} + X_{damper}} \right)^{0.5} \quad (28)$$

Where Q_{bt} = Target airflow in branch b

Q_{at} = Target airflow in branch a

Typically $X_{end} = 2$

Substituting X_{end} value in Equation 28,

$$Error = \left(\frac{3 + X_{damp} + (1 + Error\%)}{3 + X_{damp}} \right)^{0.5} - 1 \quad (29)$$

4.2.6 Reynolds Number Calculations

Reynolds Number is used to determine the type of flow. Based on the value of Reynolds Number, flow may be laminar or turbulent. Reynolds Number is defined as the ratio of inertial force to viscous force. It is calculated as;

$$Re = \frac{\rho * V * d}{\nu} \quad (30)$$

Where Re = Reynolds Number, dimensionless,

ρ = Density of medium lbs/ft³,

V = Velocity in ft/min.

d = Diameter of duct in inches,

ν = Viscosity of air in lbs-min. /ft²,

Reynolds number has been calculated in this study to determine whether the flow is laminar or turbulent. The results for the Reynolds number have been included in the results section.

4.2.7 Pipe Factor Calculations

Pipe factor (PF) is defined as the ratio of the average velocity to the centerline velocity. There is a rule of thumb that the pipe factor is typically 0.90 (Guffey). Thus the average velocity will equal 90% or some other fixed percentage of the centerline velocity.

$$PF = \frac{V_{avg.}}{V_{CL}} \quad (31)$$

Where PF = Pipe factor,

$V_{avg.}$ = Average velocity in ft/min.

V_{cl} = Centerline Velocity in ft/min. (from data collected)

4.3 Test Procedure

The test procedure included calibration (see Appendix II); steps taken prior to measurements, and steps taken during measurements.

4.3.1 Calibration

The digital manometer was calibrated against Dwyer hook gauge using about 20 calibration points over the range of interest. The manometer was calibrated to record positive readings. A small hand pump supplied positive pressures for these calibrations, connected through the plastic static pressure manifold to the digital manometer. The manometer was checked against water levels at $2/5$, $3/5$, $4/5$, 1 , $1\frac{2}{5}$, $1\frac{3}{5}$, $1\frac{4}{5}$, 2 , $2\frac{3}{5}$, 3 , $3\frac{4}{5}$, 4 , $4\frac{2}{5}$, 5 , 6 , 7 , 8 , 9 , 10 , 11 and 12 inches of water gauge to cover the range of pressure readings during measurement of the ventilation system (see Appendix for calibration data).

4.3.2 Leak Tests

Before any experiments were conducted, the duct inlet was all capped and the fan was left running to detect the presence of any leaks in the duct connections, the damper insertion and elbow connections. The white powder smoke tube was sprayed around the duct connections, elbow connections and around the sliding gate damper to detect any flow in to the ducts, seams or joints in the ductwork. Flexible caulking and duct tape were used to seal the leaks present. Duct tape was also taped around the sliding gate damper to avoid any leak through the damper slide.

4.3.3 Preparation for Data Collection

The laboratory temperature and barometric pressure were measured every time before the experiments were conducted and data measured. When measuring the static pressure, the manometer time constant was set to 5 seconds and while measuring the velocity pressure reading, the manometer time constant was set to 1 second since 20 velocity pressure readings were measured for every damper insertion depth. The digital manometer was switched on for a half hour before measurements to allow the manometer to stabilize before it was used to take measurements.

4.3.4 Running the Experiment

The following steps were followed to run the entire experiment to determine the relationship between damper insertion depth and damper resistance (see Appendix III for flowchart).

Steps:

- 1.** Calibrate TSI digital manometer.
- 2.** Select duct diameter (D) randomly.
- 3.** Select damper edge (Concave/Straight) randomly.
- 4.** Select damper orientation (Side 1/Side 2) randomly.
- 5.** Set the system to one of the four airflow levels (VP_{CLopen}) randomly.
- 6.** Measure the velocity pressures and static pressures at one of the eight insertion depths randomly.
- 7.** Repeat step 6 until all eight insertion depths are tested
- 8.** Repeat steps 5 – 7 for each of the remaining three VP_{CLopen} levels.
- 9.** Repeat steps 4 – 7 for the second damper orientation (reverse the side of damper).
- 10.** Repeat steps 3 – 7 for the second damper edge.
- 11.** Repeat steps 2 – 7 for the second duct diameter.
- 12.** Replicate steps 1 – 11 to check the consistency in the data measured.

4.3.5 Running a Test

The following procedure was followed every time for running a test in the study for one diameter duct system, one damper edge, one air flow level and one damper insertion depth.

Steps:

1. Measure static pressure readings at the hood face, and at the end of the duct
2. Measure velocity pressure readings across the two 10-point log linear Pitot traverses
3. Calculate average velocity pressure, total pressure and damper resistance.

4.3.6 Replications

Replications were taken only for certain set of conditions (see Appendix IV). Idelchik (1972) found an exponential relationship between X_{damper} and insertion depth. A plot of his table values with Log (X_{damper}) versus insertion depth (see Figure 6) produced a linear relationship over most of the range.

If log-transformed values of X_{damper} are linear with insertion depth then error can be determined from the derivations from a straight line and replications are not required greatly reducing time and effort required to conduct the study. However in case the relationship between X_{damper} and insertion depth proved non linear the remaining subset of data was replicated.

Chapter 5 Results

The following results have been obtained from the data collection.

5.1 Manometer Calibration

Statistical regression of the manometer readings and the hook gauge readings produced a linear predictive equation (see Figure 21) used to compute pressures from manometer readings. R^2 values were typically 0.997 or better.

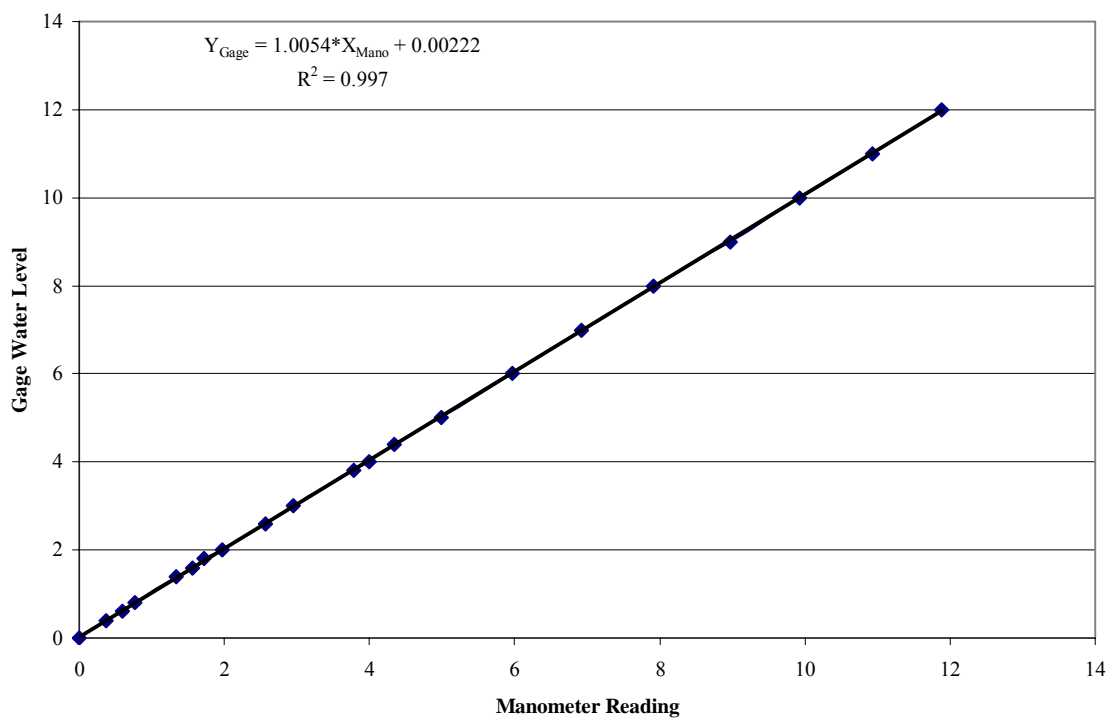


Figure 21 – Manometer calibration graph

5.2 Characteristics of Velocity Measurements

The fitness measurement condition is demonstrated with velocity profile and pipe factor. The range of Reynolds number is also computed.

5.2.1 Reynolds Number

Reynolds number was calculated for the data measured (refer to Equation 30). The Reynolds number varied from 34,000 to 716,000 indicating a highly turbulent flow. At high Reynolds number one would expect flattened parabolic velocity contours. The broad range of Reynolds number values suggests the possibility that damper resistances could vary with velocity and diameter.

5.2.2 Velocity Profile

As mentioned in the literature review, the graph of velocity with respect to the distance from the duct centerline in a turbulent flow should follow a flattened, symmetric parabolic contour. Figure 22 shows the velocity profile found for 4.85 inches duct diameter, concave edge damper, air flow level of 2.103 inches of water gaze, and for side 1. Note that graphs are most parabolic at the highest velocity and are more flattened at lower velocities. The symmetry of each plot suggests that measurement conditions were conducive to high accuracy (Guffey and Booth, 1999).

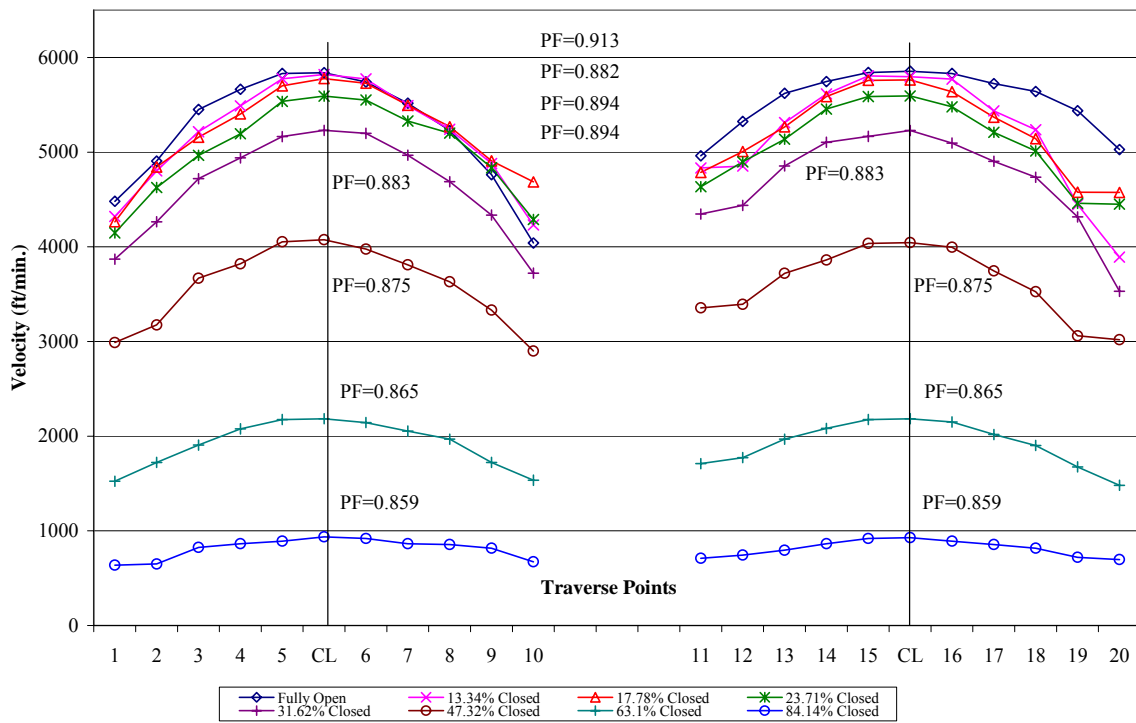


Figure 22 – Velocity Profile for $D=4.85"$, $VP_{CLopen} = 2.103"$ of w.g., Side 1 and Concave Edge

5.2.3 Pipe Factor

Pipe factor was calculated for the data collected (refer to Equation 31). Maximum pipe factor obtained for the collected data was 0.935 and the least was 0.679. The average pipe factor for the data measured was 0.870 which is fairly equal to the thumb rule pipe factor value of 0.9. A plot of pipe factor against Reynolds number (Re) (see Figure 23) indicates that the pipe factor has been consistently more than 0.85 for Re greater than 300,000. The pipe factor appears to increase with Re in an exponential relationship. It appears to converge on a value of about 0.9. It can be noted that pipe factor for both diameters are scattered in a similar fashion when plotted against Re .

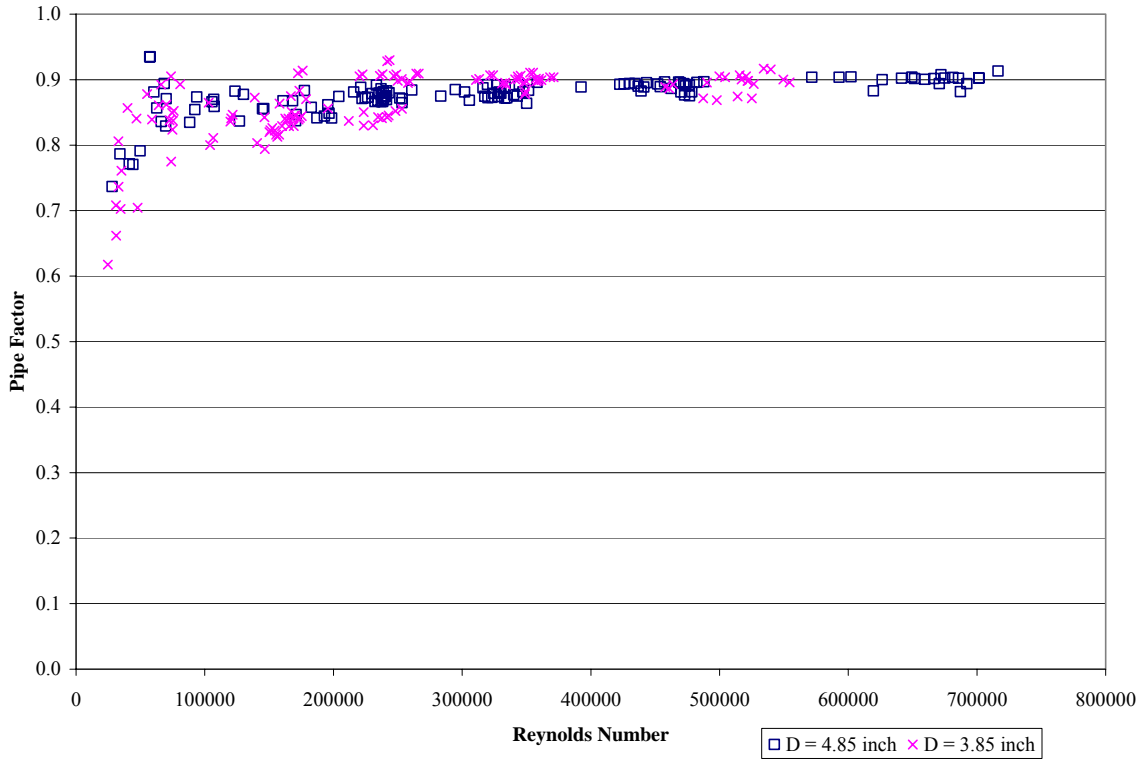


Figure 23 – Pipe Factor V/S Reynolds Number

5.3 Results of Replicated Data

Data collection was replicated only for certain combinations initially to see if there was a linear relationship between $\log(X_{\text{damper}})$ and insertion depth as was found by Idelchik (1972). As can be seen from the plot of X_{damper} and (I/D) (see Figure 24), appear to be exponential.

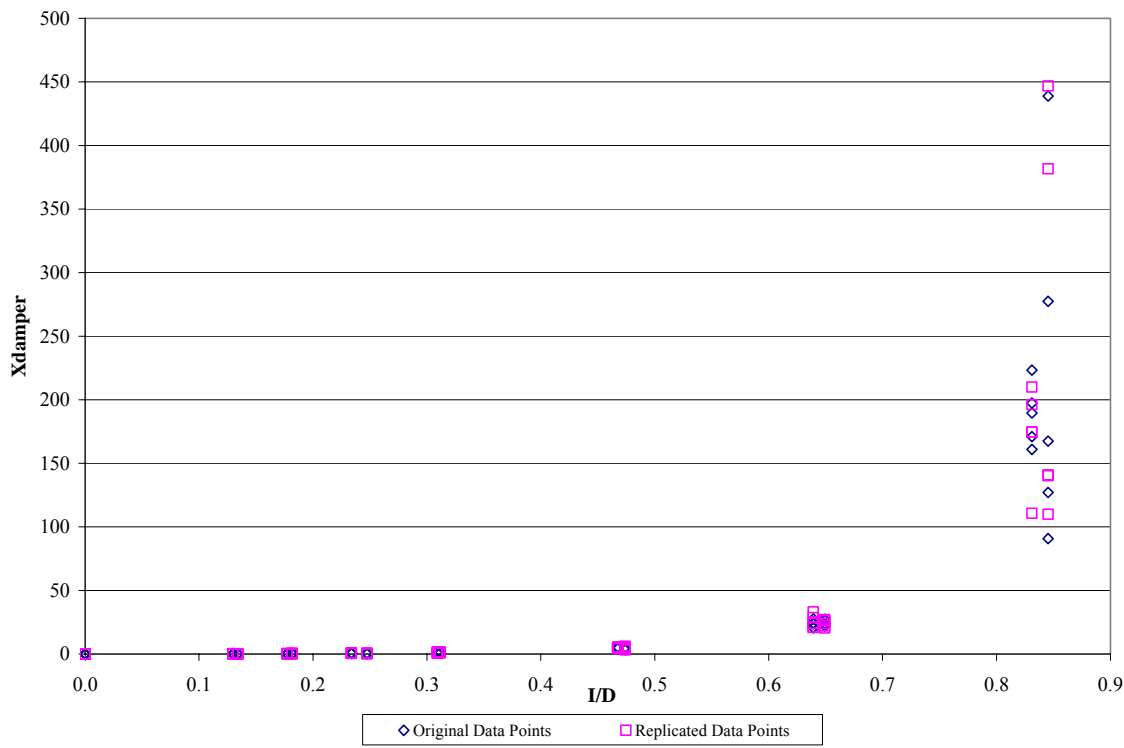


Figure 24 – X_{damper} V/S (I/D) for original and replicated data

Log transforming the X_{damper} and plotting it against (I/D) gives a linear relationship for both the original data set and replicated data set (see Figure 25). With reason for confidence that a linear relationship exists, it was not necessary to take second replications for other conditions.

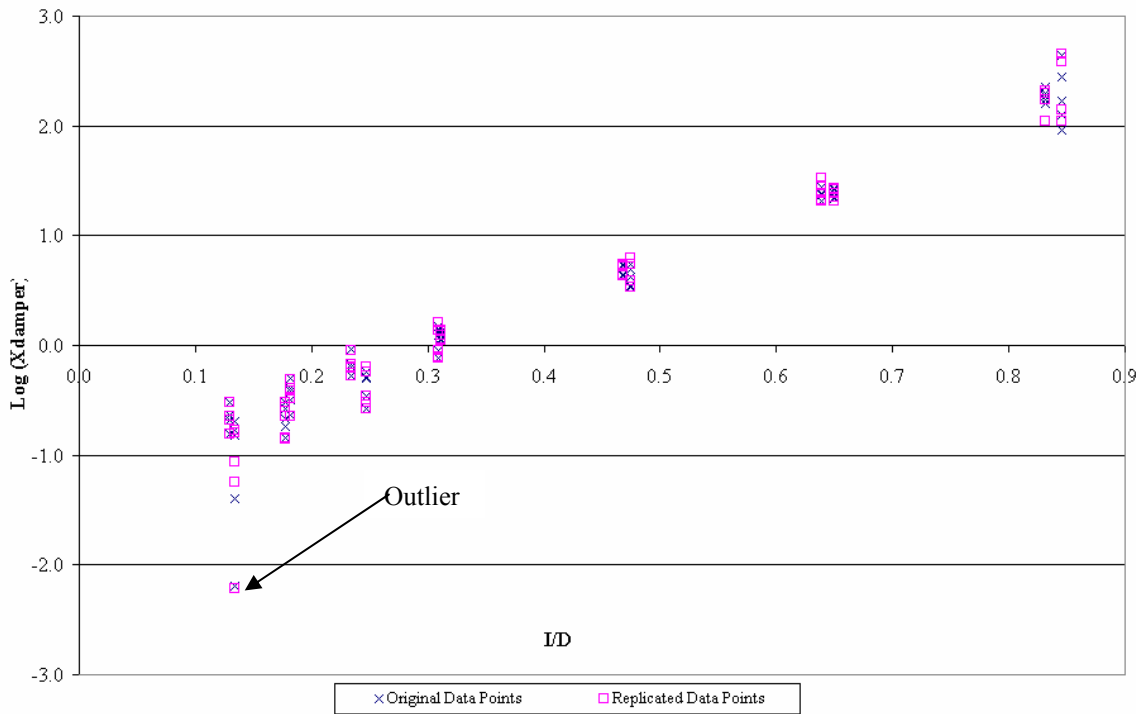


Figure 25 – Log (X_{damper}) V/S (I/D) for original and replicated data

5.4 Results of Relationship between X_{damper} and Relative Insertion Depth (I/D) – For All Data

X_{damper} is plotted against relative insertion depth i.e. Insertion depth/Duct diameter (I/D) (see Figure 26). As can be seen from the figure there is an exponential increase in X_{damper} as the relative insertion depth (I/D) increases, which is similar to the graph obtained by Idelchik (see Figure 6). The variability in X_{damper} is increasing as (I/D) is increasing and there is very little variability when the damper is 50% shut (see Figure 26).

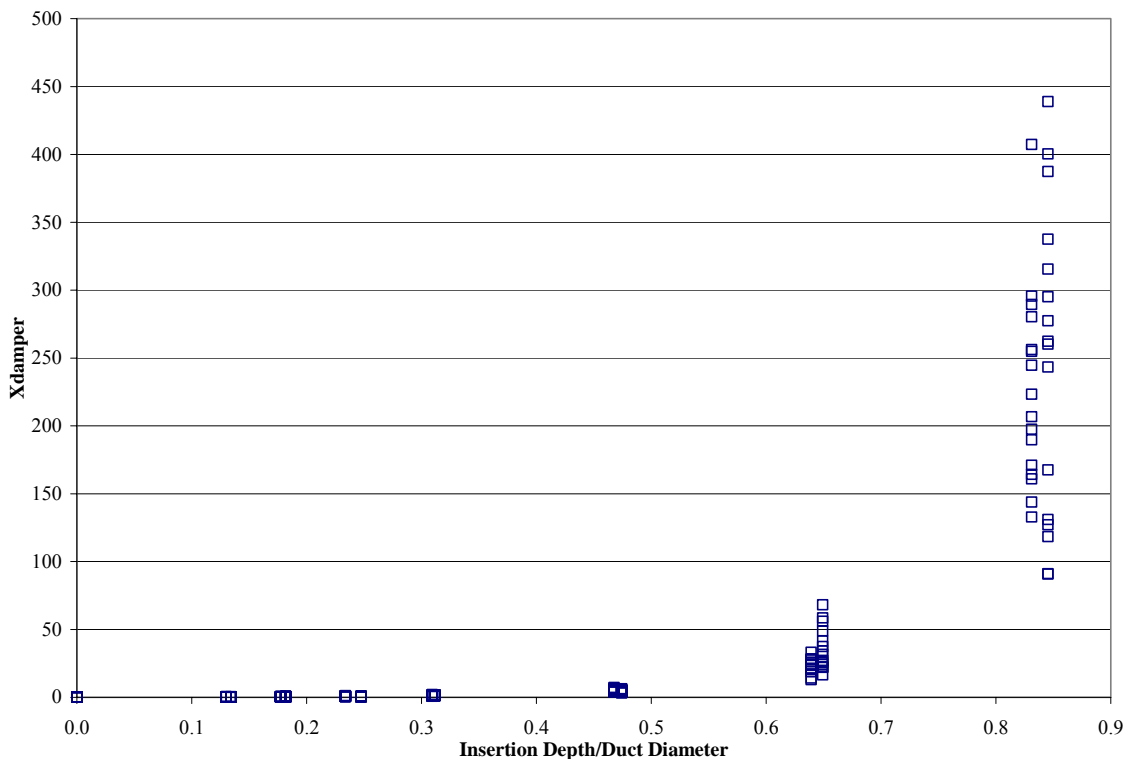


Figure 26 – X_{damper} V/S Insertion Depth/Duct Diameter

However, as shown in Figure 27, $\log(X_{\text{damper}})$ is highly linear with insertion depth/duct diameter which is also similar to the graph obtained by log transforming the plot obtained by Idelchik (see Figure 27). Authors slope is much more linear than Idelchik. The authors plot is in confirmation with Idelchik plot. Note that the variability is much more uniform over (I/D) after log transforming. It can also be observed that there is one outlying data point in the author's data set, which indicates that there is variation in log-transformed X_{damper} when (I/D) is 13%. Note that outlier was consistent over both the replications for the data point. However the data point was excluded from statistical analysis for two reasons: 1) they represent X_{damper} values less than 0.0064, which is too low to be of interest and 2) they would skew the regression fit. Log-transformed Idelchik values have also been plotted in Figure 27. Idelchik values have been consistently below the author's data points, however measuring conditions for Idelchik values are not known.

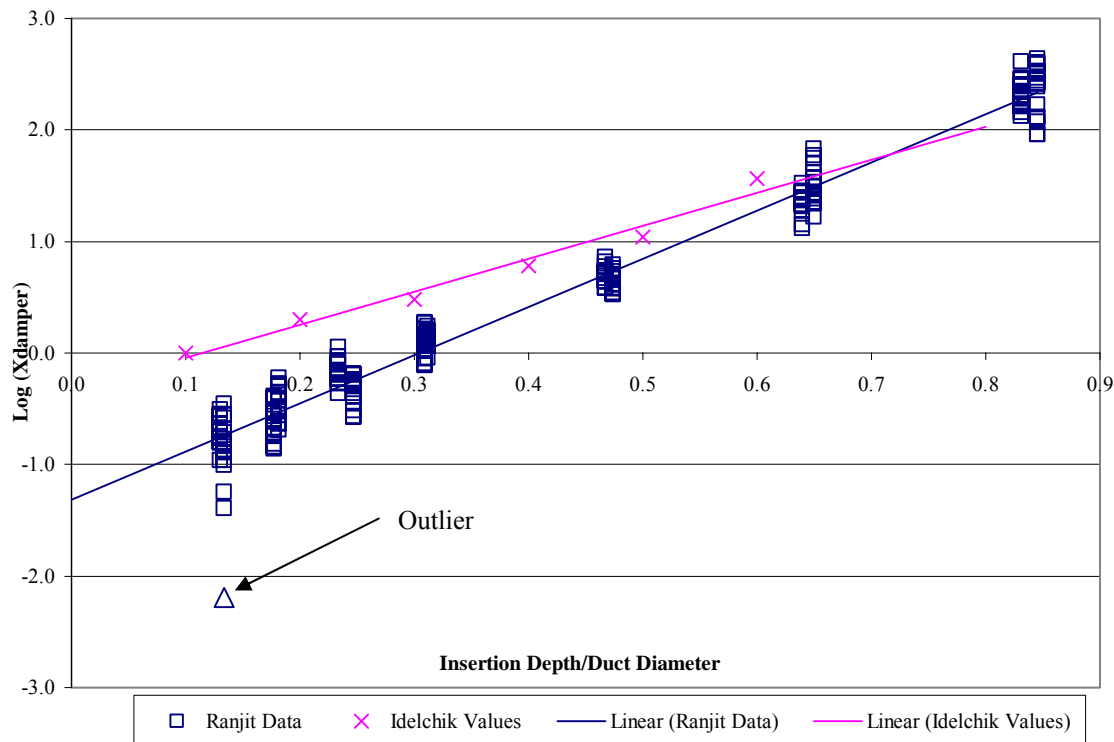


Figure 27 – Log (X_{damper}) V/S Insertion Depth/Duct Diameter

5.5 Effect of (I/D) and remaining Independent Variables on Log(X_{damper})

Statistical analysis of the data is done considering log-transformed X_{damper}, individually for every independent variable along with Insertion Depth/Duct (I/D) to determine the presence of any interaction effect of (I/D) and the respective independent variable. Check for presence of interaction effect is done by comparing the slope of independent variable cell means which is calculated considering (I/D) for Log (X_{damper}).

5.5.1 Effect of (I/D) and Damper Edges (Edge) on Log (X_{damper})

Plotting the log of the X_{damper} means for the two damper edges (straight/concave) against (I/D) leads to two regression lines with nearly identical slopes (see Figure 28) and slightly different intercepts.

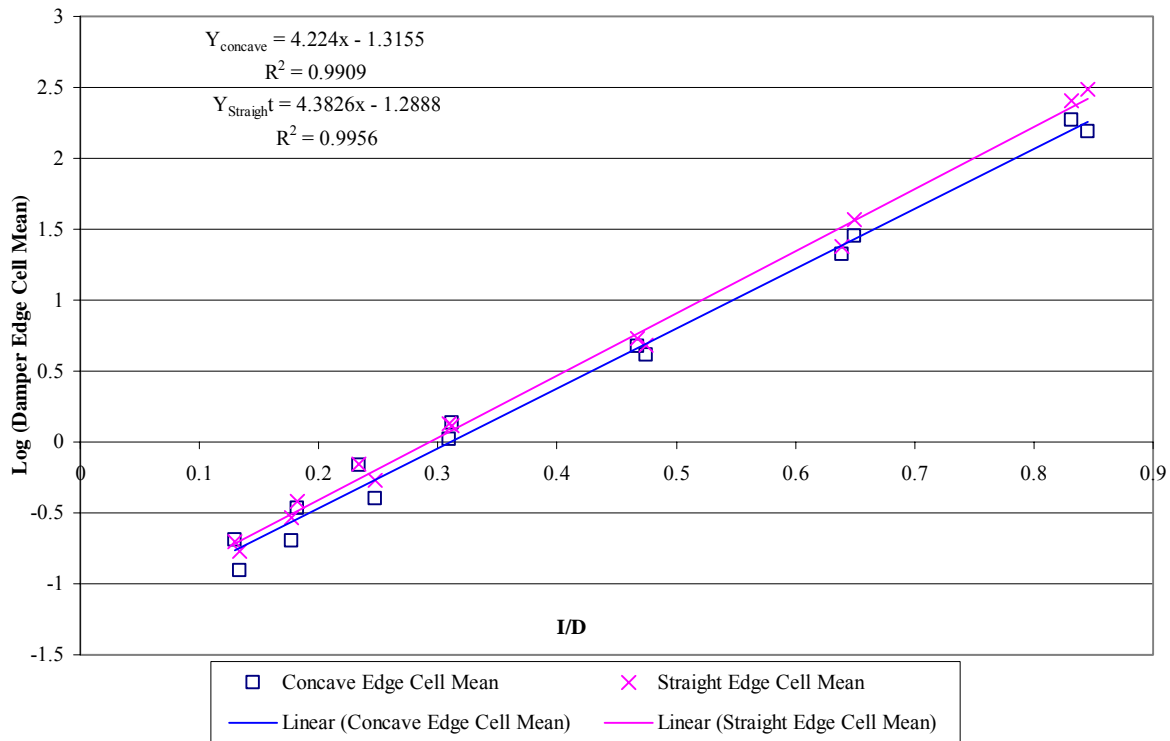


Figure 28 – Log cell means for damper edges

The concave damper edge regression line is consistently below the straight edge regression line. The slope of log cell means for straight edge is 3.6% more than the log cell means for concave edge. The similarity of the slopes suggests that if there is an interaction between edge and (I/D), it is weak.

5.5.2 Effect of (I/D) and Air Flow Levels (VP_{CLOpen}) on Log (X_{damper})

The cell means for Log (X_{damper}) and the four different levels of air flow are plotted against (I/D) and the regression lines are fitted in to the data for the four levels of VP_{CLOpen} (see Figure 29).

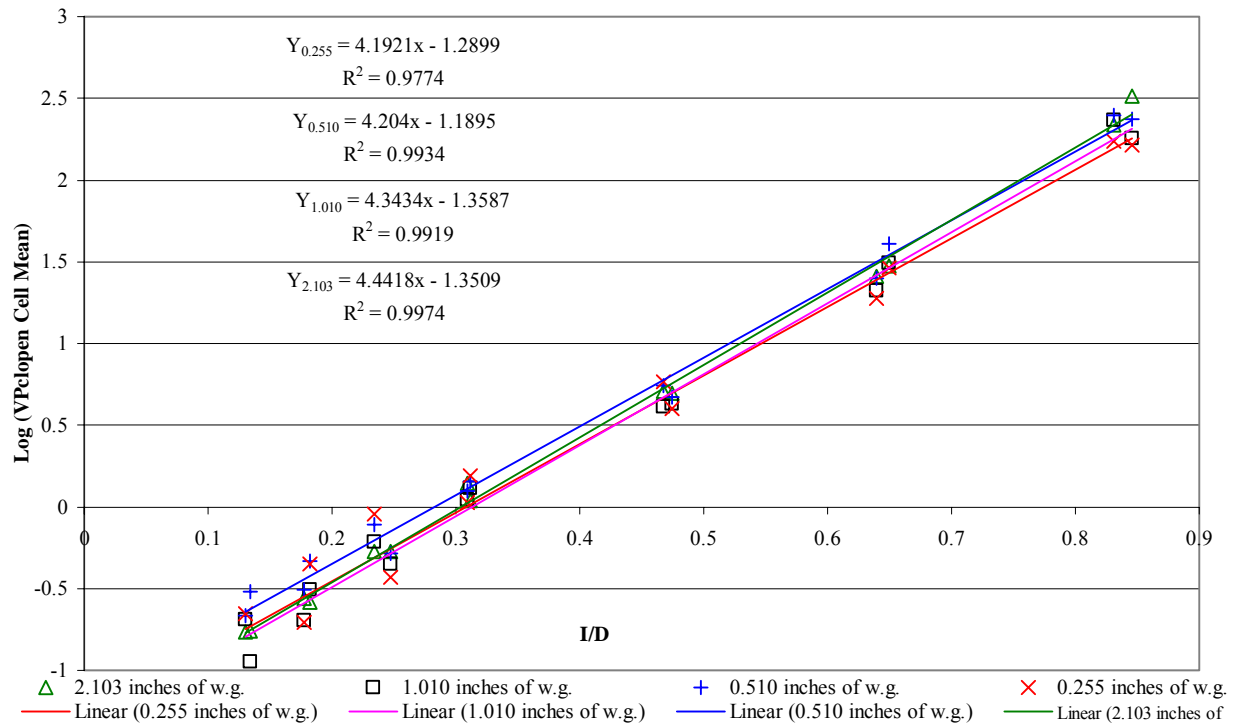


Figure 29 – Log cell means for VP_{CLOpen}

It can be seen from Figure 29 that the regression lines for all levels of VP_{CLOpen} have nearly identical slopes and slightly different intercepts. The value of slope of the mean regression lines for the four levels increased as the air flow level is increased. The regression lines are not parallel to each other. The slope value is increasing by approximately 5.9% from 0.255 inches of water gaze of velocity pressure to 2.103 inches of water gaze of velocity pressure. This suggests the possibility of presence of interaction effect between VP_{CLOpen} and (I/D).

5.5.3 Effect of (I/D) and Damper Orientation (Orient) on Log (X_{damper})

Plotting the cell means of Log (X_{damper}) for the two damper orientations against (I/D) leads to two regression lines with nearly identical slopes (see Figure 30).

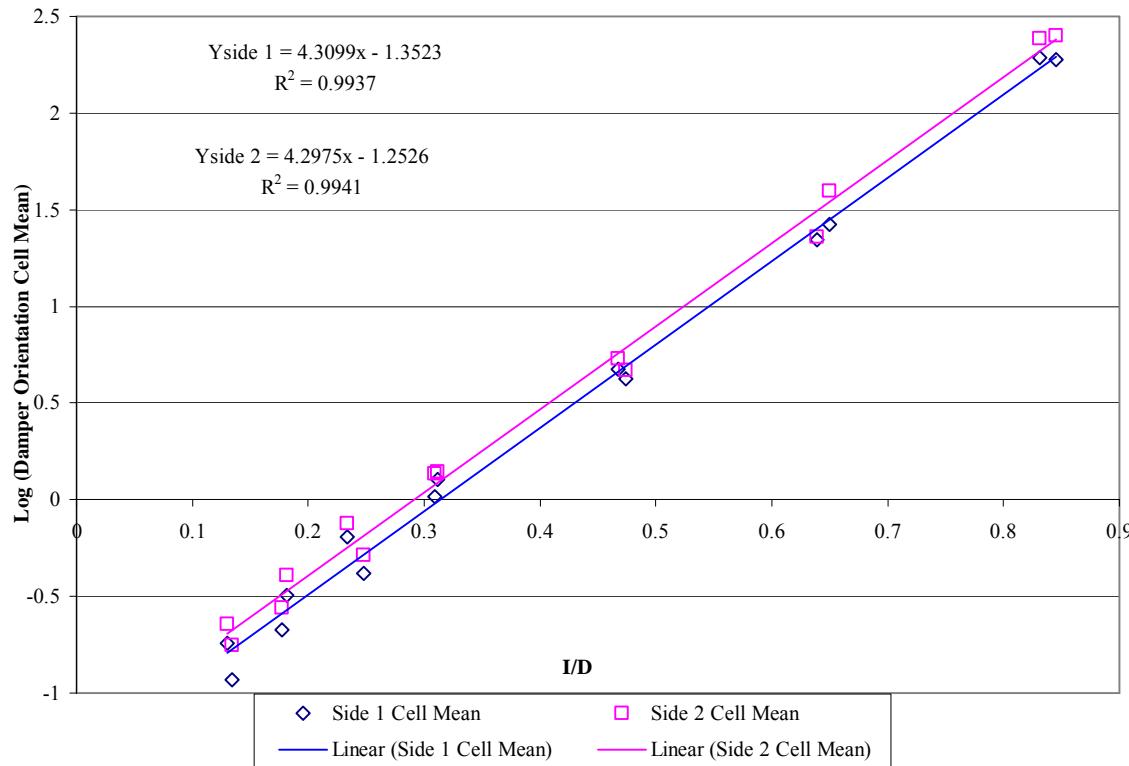


Figure 30 – Log cell means for damper orientation

The X_{damper} values for the second orientation (side 2) are consistently above the values for first orientation (Side 1). The slope increases by a minimal amount of 0.47% from second orientation to first orientation. This suggests that the interaction affect of (I/D) and damper orientation is not significant.

5.5.4 Effect of (I/D) and Duct Diameter (D) on Log (X_{damper})

Plotting the cell means of Log (X_{damper}) for the two duct diameters against percentage relative insertion depth (see Table 2) leads to two regression lines with slightly different slopes (see Figure 31) suggesting a weak interaction between duct diameter and (I/D).

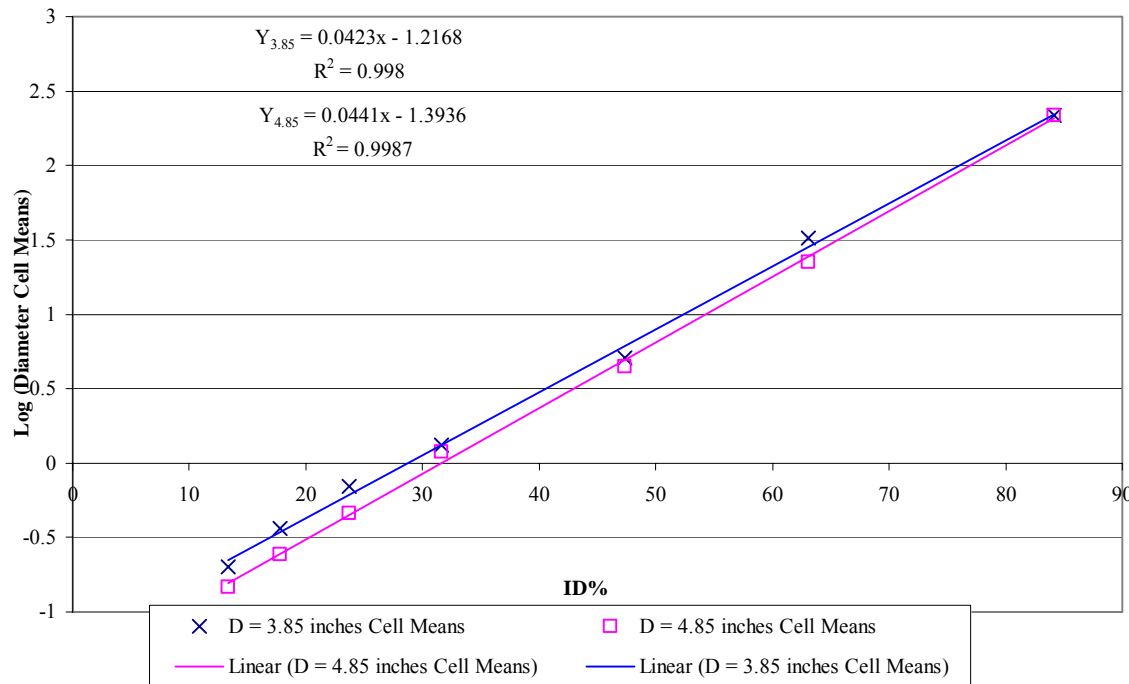


Figure 31 – Log cell means for duct diameter

The regression line for duct diameter of 3.85 inches is consistently above the regression line for duct diameter of 4.85 inches. Percentage change in slope of from 3.85 inches to 4.85 inches cell mean regression lines is about 4.3%. Intercepts for both duct diameter log cell means are also different and every value for the larger diameter is slightly lower than the corresponding value of smaller diameter, suggesting that (I/D) does not fully explain the effects of diameter on X_{damper}.

Chapter 6 Discussion

Data analysis was done using a commercial software package, Data-Desk (Version 5.0, Data-desk of Ithaca, N.Y.), to determine the relationship between X_{damper} and damper insertion depth (I) considering variables damper edge (Edge), air flow levels (VP_{CLopen}), damper orientation (Orient) and duct diameter (D).

6.1 Normality of Residuals for Log-transformed Data

A normal probability plot of residuals for X_{damper} did not give a straight line (see Figure 32) which suggests that the error distribution was not normal and that X_{damper} should be transformed for analysis.

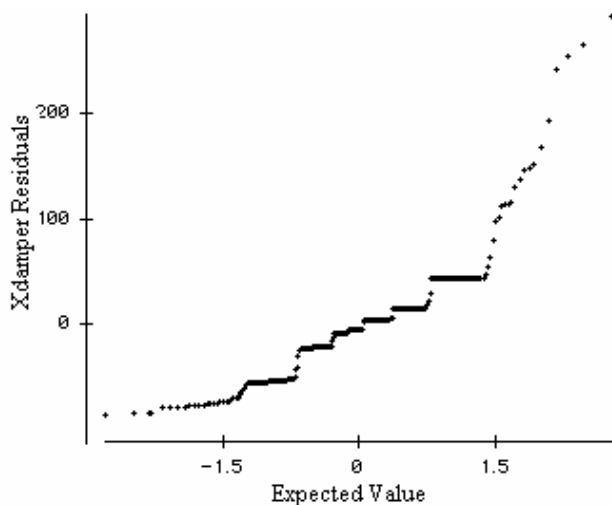


Figure 32 – Normal Probability Plot for X_{damper}

The normal probability plot of the residuals (see Figure 33) for $\text{Log}(X_{\text{damper}})$ gives a straight line, which confirms normality and validates the fact that $\text{Log}(X_{\text{damper}})$ should be analyzed instead of X_{damper} .

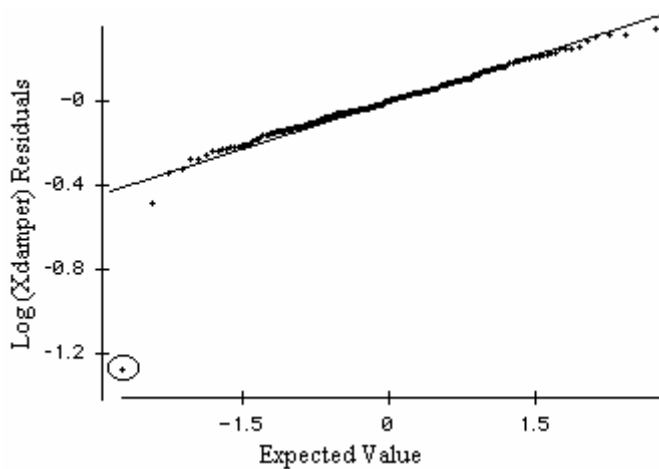


Figure 33 – Normal Probability Plot for Log (X_{damper})

6.2 Identifying Outlying Observations

Figure 33 shows the outlying observations (see circled values in Figure 33). This outlying observation corresponds to concave edge dampers for an air flow level of 0.510 inches of w.g., a duct diameter of 4.85 inches, side 1 and a relative insertion depth (I/D) of 13.34%. This outlying point was measured again to check the validity of data collection. The results were consistent with previous values. However, the value of X_{damper} for this point is 0.0064 which is a uselessly low value for application. Rather than have this outlier strongly influence ANOVA and regression analyses, it is omitted from all statistical analyses.

6.3 Analysis of Variance

Analysis of variance was done (see Table 4) initially with all the independent variables (I/D), D, Edge, Orient, and VP_{CLopen} plus all two-way interactions. As shown in Table 4 relative insertion depth (I/D) contributed 97.6% of the total sum of squares explained by ANOVA. The remaining sum of squares for the other variables was minimal in comparison to (I/D). The error sum of squares was also very small compared to the (I/D) sum of squares.

Table 4: - Analysis of Variance with all Independent Variables

Source of Variation	Sums of Squares	df	Mean Square	F-ratio	P Value
Constant	42.199	1	42.199	3552.20	0.0001*
(I/D)	241.705	1	241.705	20346.00	0.0001*
D	0.466	1	0.466	39.21	0.0001*
(I/D)*D	0.069	1	0.069	5.80	0.0170*
Orient	0.135	1	0.135	11.32	0.0009*
(I/D)*Orient	0.000	1	0.000	0.01	0.9224
D*Orient	0.000	1	0.000	0.03	0.8635
VP _{CLopen}	0.227	3	0.076	6.38	0.0004*
(I/D)*VP _{CLopen}	0.126	3	0.042	3.54	0.0156*
D*VP _{CLopen}	0.542	3	0.181	15.21	0.0001*
Orient*VP _{CLopen}	0.024	3	0.008	0.67	0.5688
Edge	0.008	1	0.008	0.69	0.4063
(I/D)*Edge	0.087	1	0.087	7.32	0.0074*
D*Edge	0.100	1	0.100	8.45	0.0041*
Orient*Edge	0.00045	1	0.000	0.01	0.9272
VP _{CLopen} *Edge	0.334	3	0.111	9.38	0.0001*
Error	2.340	197	0.012		
Total	247.436	222			

When insignificant independent variables ($P > 0.05$) were removed from the model, terms were reduced to the values shown in Table 5. It can be observed that (I/D) still contributed 97.6% of the sum of squares explained by ANOVA, whereas the remaining sum of squares for the other significant variables was minimal. Error sum of squares contributed 1% to the total sum of squares which is very low when compared to (I/D) sum of squares. As shown in Table 5, I/D, D, (I/D)*D, Orient, I/D*VP_{CLopen}, Edge, D*VP_{CLopen}, (I/D)*Edge, D*Edge, VP_{CLopen}*Edge were significant. The fact that D and VP_{CLopen} were significant (but not substantial), suggests modest Reynolds number effects. Orientation was significant (but not substantial), can perhaps be explained by the difference in construction of the inlet and outlet due to the gasket protruding on side 2. However orientation is an impractical variable in a predictive model for two reasons: 1) the asymmetry was too subtle for a practitioner to notice and 2) the manufacturer did not

mark the direction of flow. For that reason Orientation and Orientation interactions were removed from the regression analyses.

Table 5: - Analysis of Variance with Significant Independent Variables

Source of Variation	Sums of Squares	df	Mean Square	F-ratio	P Value
Constant	42.199	1	42.199	2954.40	0.0001
Edge	0.444	1	0.444	31.07	0.0001
I/D	241.945	1	241.945	16939.00	0.0001
VP _{CLopen}	0.417	3	0.139	9.72	0.0001
D	0.512	1	0.512	35.84	0.0001
I/D*D	0.068	1	0.068	4.76	0.0302
D*Edge	0.097	1	0.097	6.81	0.0097
I/D*VP _{CLopen}	0.124	1	0.124	8.67	0.0036
VP _{CLopen} *Edge	0.341	3	0.114	7.96	0.0001
D*VP _{CLopen}	0.425	1	0.425	29.73	0.0001
I/D*Edge	0.092	1	0.092	6.48	0.0117
Error	2.971	208	0.014		
Total	247.436	222			

6.4 Regression Analysis

Regression analysis was done for the 10 significant variables (see Table 4) to come up with a regression model for Log (X_{damper}). Regression coefficients for the significant variables have been written in an equation (see Equation 32). R² is also calculated to determine the fit of the regression equation which was found to be 0.985. R² value of 0.985 indicates that the degree of linear association between the log-transformed X_{damper} the 10 significant independent variables is high and the model is a good fit to the data.

$$\begin{aligned}
 Y_{\text{Log}(X_{\text{damper}})} = & 0.524 - 0.310 * (\text{Edge}) + 3.286 * \left(\frac{I}{D}\right) - 0.531 * (\text{VP}_{\text{Clopen}}) - 0.431 * D + \\
 & 0.151 * \left(\frac{I}{D} * D\right) + 0.087 * (\text{Edge} * D) + 0.133 * \left(\frac{I}{D} * \text{VP}_{\text{Clopen}}\right) - 0.042 * (\text{Edge} * \text{VP}_{\text{Clopen}}) + \\
 & 0.124 * (\text{VP}_{\text{Clopen}} * D) + 0.159 * \left(\frac{I}{D} * \text{Edge}\right)
 \end{aligned}
 \tag{32}$$

Equation (32)

As shown in Figure 34, the variance does not appear to change with level of $\text{Log}(X_{\text{damper}})$. R^2 for the plot is 0.985.

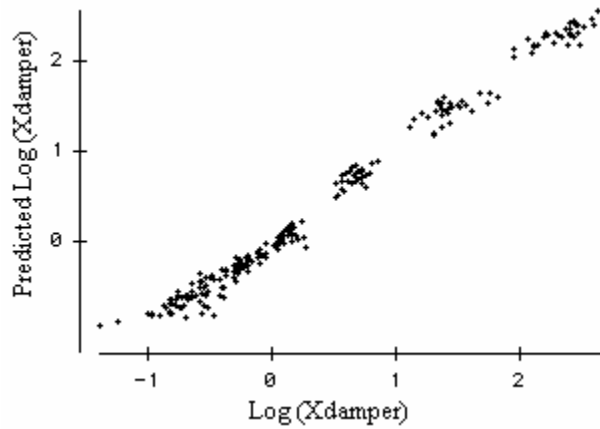


Figure 34 – Predicted Log (X_{damper}) V/S Observed Log (X_{damper})

6.4 Reduced Regression Analysis Based on R²

Further regression analysis for the model derived in Equation 32 was done to reduce the number of independent variables. Variables were removed from the regression model on their contribution to R^2 (see Table 6).

Table 6: - R² Analysis for Reduced Regression Model

Independent Variables	Variable Removed	R-Square	% Change in R ²
Edge, I/D, VP _{CLopen} , D, (I/D*D), (Edge*D), (I/D*VP _{CLopen}), (Edge*VP _{CLopen}), (VP _{CLopen} *D), (I/D*Edge)	None	0.9850	-
Edge, I/D, VP _{CLopen} , D, (I/D*D), (Edge*D), (I/D*VP _{CLopen}), (Edge*VP _{CLopen}), (VP _{CLopen} *D),	(I/D*Edge)	0.9850	0.00%
Edge, I/D, VP _{CLopen} , D, (Edge*D), (I/D*VP _{CLopen}), (Edge*VP _{CLopen}), (VP _{CLopen} *D),	(I/D*D)	0.9850	0.00%
Edge, I/D, VP _{CLopen} , D, (I/D*VP _{CLopen}), (Edge*VP _{CLopen}), (VP _{CLopen} *D),	(Edge*D)	0.9840	0.10%
Edge, I/D, VP _{CLopen} , D, (Edge*VP _{CLopen}), (VP _{CLopen} *D),	(I/D*VP _{CLopen})	0.9840	0.10%
Edge, I/D, VP _{CLopen} , D, (VP _{CLopen} *D),	(Edge*VP _{CLopen})	0.9830	0.20%
I/D, VP _{CLopen} , Edge, D,	(VP _{CLopen} *D)	0.9820	0.30%
I/D, Edge, D,	VP _{CLopen}	0.9820	0.30%
I/D, Edge	D	0.9780	0.71%
I/D	Edge	0.9770	0.81%

The R² decreases from 0.985 with all the significant independent variables to 0.977 with the model explained by just (I/D) (see Table 6). The overall percentage drop from R² of 0.987 to R² of 0.977 was about .81% which can be considered negligible. Hence regression model can be explained with (I/D) and Edge with an R² of 0.978. The overall drop of R² from 0.985 to 0.978 is about .71% which can be considered negligible.

Edge has been included along with (I/D) in the reduced regression model for two reasons: 1) other edge shapes may have more substantial effects and 2) both straight and concave edges cannot be used at the same time. Thus log-transformed X_{dumper} can be explained only in terms of (I/D) and Edge (see Equation 33). The R² for the model was 0.978.

$$Y_{Log(X_{damper})} = -1.434 + 0.089 * (Edge) + 4.30 * \left(\frac{I}{D}\right) \quad (33)$$

As shown in Figure 35, the variance does not appear to change with level of $\text{Log}(X_{\text{damper}})$ for the reduced model. R^2 for the plot is 0.978.

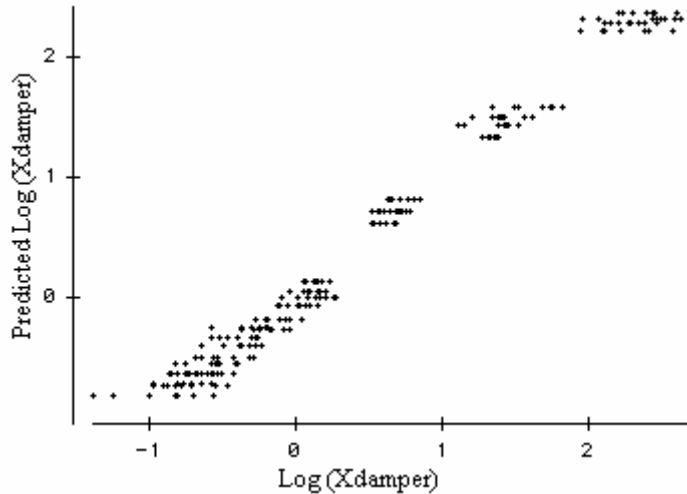


Figure 35 – Predicted Log (X_{damper}) V/S Observed Log (X_{damper}) (Reduced Model)

Reduced regression model (see Equation 33) was further broken down in to two models, each model representing a damper edge as both edges cannot be used at the same time to adjust airflow. Regression model for straight edge is as follows:

$$Y_{Log(X_{damper})} = -1.289 + 4.383 * \left(\frac{I}{D}\right) \quad (34)$$

R^2 value for the model in Equation 34 was 0.986, which indicates a good fit.

Regression model for concave edge is as follows:

$$Y_{Log(X_{damper})} = -1.311 + 4.217 * \left(\frac{I}{D}\right) \quad (35)$$

R^2 value for the model in Equation 35 was 0.971, which indicates a good fit.

Plots of the residuals of Equations 32 and 33 show high normality and linearly uniform variance with different levels of each independent variable.

Further analysis was done after removing VP_{CLopen} and D and including Reynolds Number as one of the independent variable. However using Reynolds Number as an independent variable for analysis lead to a regression model similar to the reduced regression model (see Equation 33) making Reynolds Number highly insignificant.

Regression analysis was also done considering damper percentage open area as one of the independent variables instead of insertion depth for the straight edge damper as damper percentage open area cannot be calculated for concave edge damper. Regression analysis was done considering (A_{open}/A_{total}) as the independent variable for straight edge, as tested in Equation 36. The model R^2 was found to be 0.987.

$$Y_{Log(X_{damper})} = 3.108 - 4.401 * \left(\frac{A_{open}}{A_{total}} \right) \quad (36)$$

$$\text{Where } A_{open} = D^2 * \left[\frac{\left(\frac{S * 2}{D} \right) - \text{Sine}\left(\frac{S * 2}{D} \right)}{8} \right] \quad (37)$$

Where S = Arc length with the chord

D = Duct diameter

Regression analysis for straight edge damper using relative insertion depth instead of percentage open area (see Equation 38) resulted in a R^2 of 0.986.

$$Y_{Log(X_{damper})} = -1.289 + 4.383 * \left(\frac{I}{D} \right) \quad (38)$$

Comparing both models (see Equation 36 and 38) it can be seen that both models have the same R^2 and hence percentage open area has the same effect on X_{damper} as relative insertion depth.

6.5 Non Log-Transformed Predictive Models

The two regression models listed in Equation 32 and Equation 33 are compared on the basis of residual error plots against (I/D). The residuals are untransformed in both cases in order to determine the untransformed error rather than the log-transformed error.

6.5.1 Predictive Models for X_{damper}

For application, Equations 32, 33, 34, and 35, should be transformed to the following non-log versions: The untransformed predicted model for X_{damper} for complete model from Equation 32 is as follows:

$$X_{\text{damper}} = 10^{\left(\begin{array}{l} 0.524 - 0.310 * (\text{Edge}) + 3.286 * \left(\frac{I}{D}\right) - 0.531 * (\text{VPCopen}) - 0.431 * D + \\ 0.151 * \left(\frac{I}{D}\right) * D + 0.087 * (\text{Edge} * D) + 0.133 * \left(\frac{I}{D}\right) * \text{VPCopen} - 0.042 * (\text{Edge} * \text{VPCopen}) + \\ 0.124 * (\text{VPCopen} * D) + 0.159 * \left(\frac{I}{D}\right) * \text{Edge} \end{array} \right)} \quad (39)$$

$$X_{\text{damper}} = 3.342 * 10^{\left(\begin{array}{l} -0.310 * (\text{Edge}) + 3.286 * \left(\frac{I}{D}\right) - 0.531 * (\text{VPCopen}) - 0.431 * D + \\ 0.151 * \left(\frac{I}{D}\right) * D + 0.087 * (\text{Edge} * D) + 0.133 * \left(\frac{I}{D}\right) * \text{VPCopen} - 0.042 * (\text{Edge} * \text{VPCopen}) + \\ 0.124 * (\text{VPCopen} * D) + 0.159 * \left(\frac{I}{D}\right) * \text{Edge} \end{array} \right)} \quad (39a)$$

The untransformed predicted model for X_{damper} for reduced model from Equation 33 is as follows:

$$X_{\text{damper}} = 10^{\left(-1.434 + 0.089 * (\text{Edge}) + 4.3 * \frac{I}{D} \right)} \quad (40)$$

$$X_{\text{damper}} = 0.037 * 10^{\left(0.089 * (\text{Edge}) + 4.3 * \frac{I}{D} \right)} \quad (40a)$$

The predicted model for X_{damper} for straight edge from Equation 34 is as follows:

$$X_{\text{damper}} = 10^{\left(-1.289 + 4.383 * \frac{I}{D} \right)} \quad (41)$$

$$X_{\text{damper}} = 0.051 * 10^{\left(4.383 * \frac{I}{D} \right)} \quad (41a)$$

The predicted model for X_{damper} for concave edge from Equation 35 is as follows:

$$X_{\text{damper}} = 10^{\left(-1.311 + 4.217 \frac{I}{D}\right)} \quad (42)$$

$$X_{\text{damper}} = 0.049 * 10^{\left(4.217 \frac{I}{D}\right)} \quad (42\text{a})$$

Where X_{damper} is damper resistance

Edge is damper edge

(I/D) is insertion depth/duct diameter

6.5.2 Complete Regression Model

It can be noted from Figure 36 that the observed and predicted X_{damper} behave similarly with (I/D).

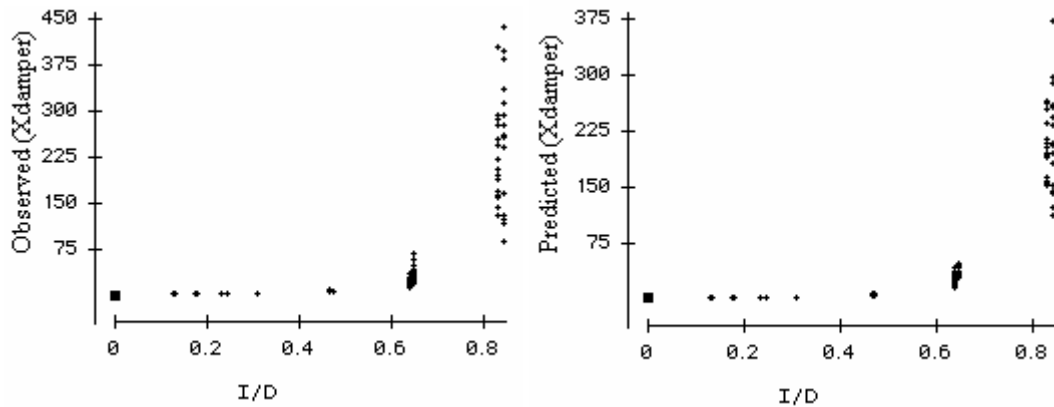


Figure 36 – Observed and Predicted (X_{damper}) V/S (I/D) (Complete Model)

A plot of X_{damper} residuals (obtained by transforming the Log (X_{damper}) residuals back to X_{damper} residuals) against (I/D) indicates that the absolute error (see Figure 37) increases sharply with (I/D).

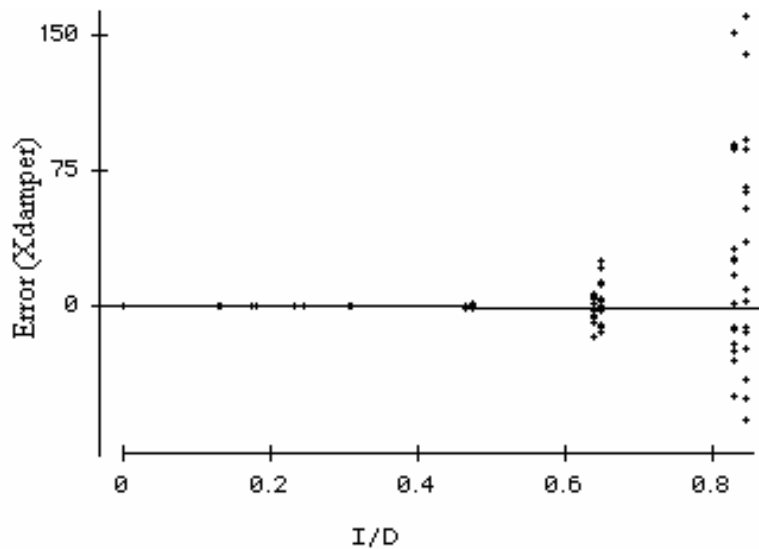


Figure 37 – Residuals (X_{damper}) V/S (I/D) (Complete Model)

As would be expected from Figure 37, a plot of X_{damper} residuals against predicted (X_{damper}) indicates that the absolute error (see Figure 38) increases sharply with predicted (X_{damper}).

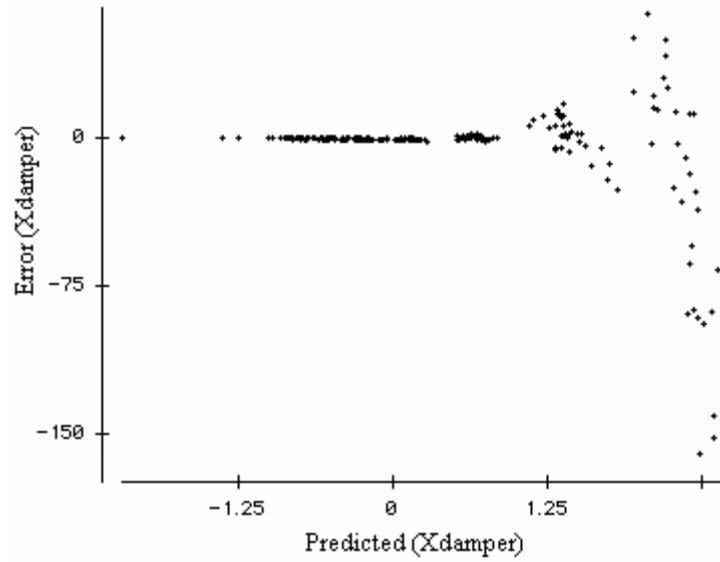


Figure 38 – Residuals (X_{damper}) V/S Predicted (X_{damper}) (Complete Model)

The maximum percent error of X_{damper} is around 125% (see Figure 39), which is very high. As shown in Figure 39, errors commonly exceed $\pm 25\%$ throughout the range of X_{damper} . The ratio of airflows for ducts at a junction fitting is proportional to square root of the ratios of their end damper resistance (X_{end}) (Guffey, 1993). Hence the errors in achieving airflows would be proportional to the square root of X values. For low values of X_{damper} , the X_{end} values typically range from 1 to 3 when no dampers are present. As noted in Equation 28 and 29, X_{damper} adds to X_{end} when a damper is inserted.

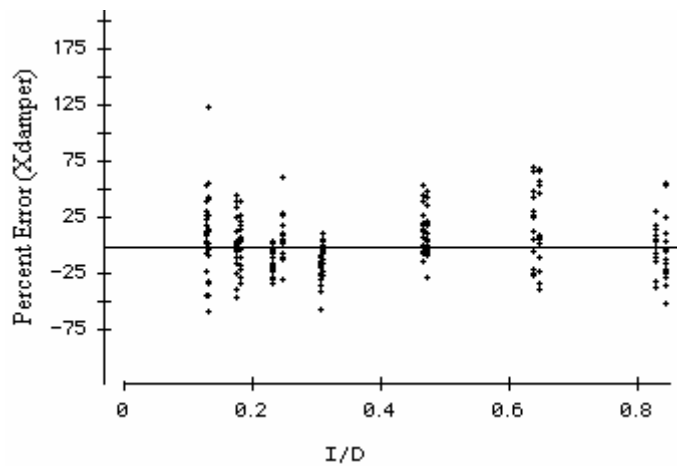


Figure 39 – Percent Error (X_{damper}) V/S (I/D) (Complete Model)

6.5.3 Reduced Regression Model

Reduced model is expected to behave in a similar manner as the complete model as shown in the following section. It can be noted from Figure 40 that the observed and predicted X_{damper} behave similarly with (I/D). However most of the X_{damper} values in the predicted plot are clustered around only few points as the reduced model is explained only in terms of Edge and (I/D).

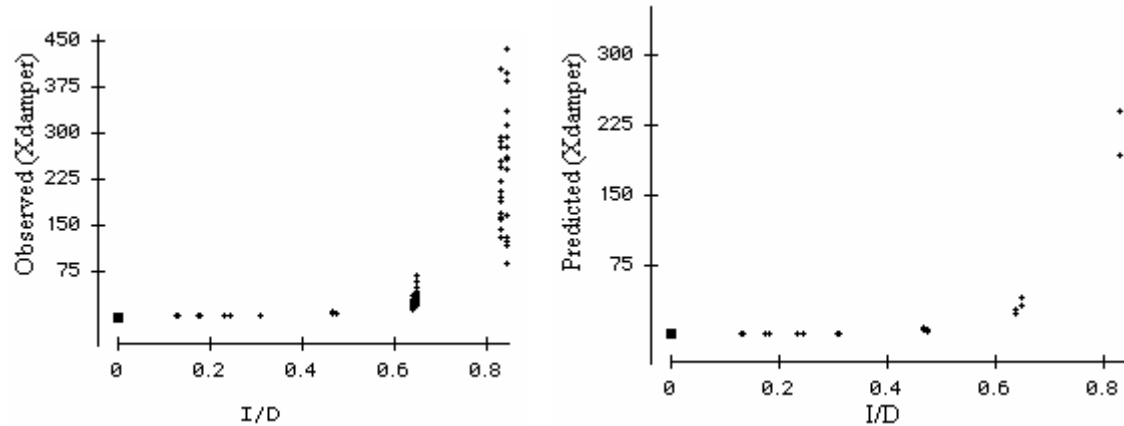


Figure 40 – Observed and Predicted (X_{damper}) V/S (I/D) (Reduced Model)

A plot of X_{damper} residuals (obtained by transforming the Log (X_{damper}) residuals back to X_{damper} residuals) against (I/D) indicates that the absolute error (see Figure 41) increases sharply with (I/D).

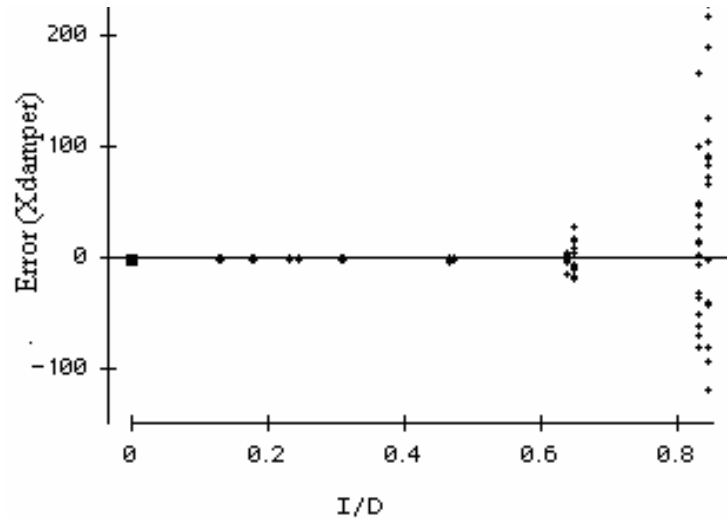


Figure 41 – Residuals (X_{damper}) V/S Predicted (X_{damper}) (Reduced Model)

As would be expected from Figure 41, a plot of X_{damper} residuals against predicted (X_{damper}) indicates that the absolute error (see Figure 42) increases sharply with predicted (X_{damper}).

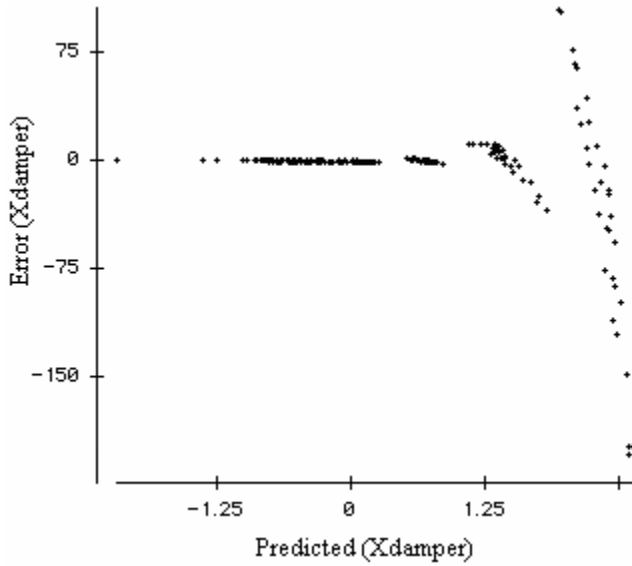


Figure 42– Residuals (X_{damper}) V/S (I/D) (Reduced Model)

The maximum percent error of X_{damper} is about 125% which is very high (see Figure 43). As shown in Figure 43, errors commonly exceed $\pm 25\%$ throughout the range of X_{damper} .

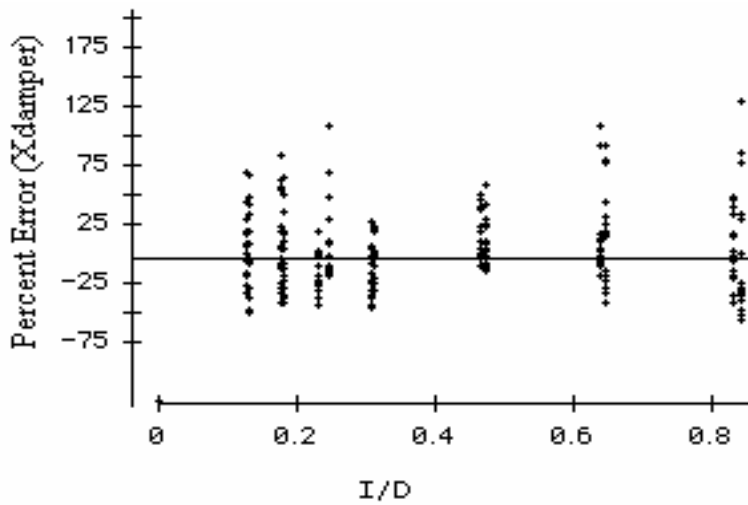


Figure 43 – Percent Error (X_{damper}) V/S (I/D) (Reduced Model)

Complete and reduced regression models derived earlier (see Equation 32 and 33) have approximately the same absolute and percent error. R^2 value is high and approximately same for both models hence both models are statistically accurate even though the

absolute and percent error is high. Both models can be used to define X_{damper} . However the reduced model is selected to determine the log-transformed X_{damper} as it has lesser number of variables.

Percent error in shifts in air flow (refer Equation 28 and 29) were plotted against (I/D) for the reduced model (see Figure 44). It can be noted from Figure 44, that for adjusting airflows (X_{damper}), the percent errors in shifts in airflow would reach a maximum value of 40%.

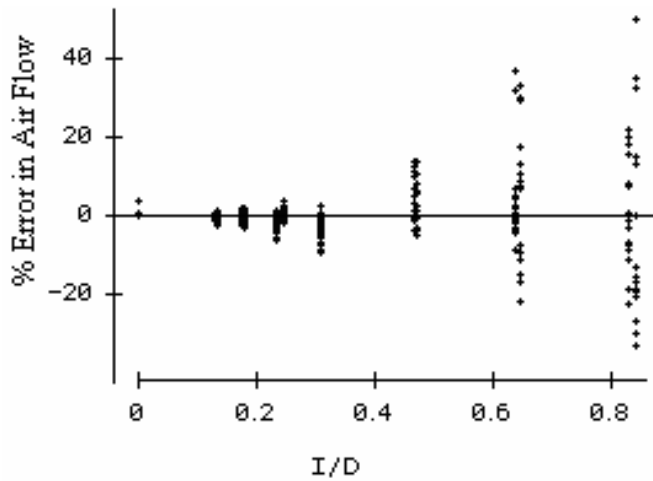


Figure 44 – Percent Error in Airflow V/S (I/D) (Reduced Model)

Chapter 7 Conclusions

Values of X_{damper} varied exponentially with the relative insertion depth (I/D) as demonstrated by the highly linear relationship between $\text{Log}(X_{\text{damper}})$ and I/D ($R^2 = 0.978$). Orientation, Edge, duct diameter, and level of airflow were individually highly significant ($p < 0.01$) with $\text{Log}(X_{\text{damper}})$ as were most two-way interactions of independent variables. However, including all independent variables and all significant interactions increased the R^2 by a very small amount for an R^2 of 0.985. Since Orientation, diameter, and airflow level significantly complicate the predictive model without adding much predictive power, they and their interactions were omitted from the “Reduced Model.” The latter included Edge since other edge shapes may have more substantial effects.

$$Y_{\text{Log}(X_{\text{damper}})} = -1.434 + 0.089 * (\text{Edge}) + 4.30 * \left(\frac{I}{D}\right)$$

Although the log-transformed model fits the data with an $R^2 = 0.978$, the recommended predictive models (Equations 32 and 33) each have errors that increase sharply with increasing I/D values with percent errors as high as 75% across the range of I/D . However non log-transformed X_{damper} errors in shifts in airflows would be as large as 40%. This suggests that it would be nearly impossible to make substantial adjustment to airflow by setting insertion depth using only the predicted models for X_{damper} . However the predicted models may be useful for an initial rough adjustment. Final adjustments could be done by trial and error adjustment to goal airflow.

Given the very good fit ($R^2 = 0.978$) for $\text{Log}(X_{\text{damper}})$, it is unlikely that superior methods can produce a substantially more useful predictive model for X_{damper} .

Bibliography

1. **Steven E. Guffey and Jeffrey G. Spann (1999):** Experimental Investigation of Power Loss Coefficients and Static Pressure Ratios in an Industrial Exhaust Ventilation System. American Industrial Hygiene Association Journal (May/June 1999): 60:367 – 376.
2. **Michael Winifred Dodrill:** Experimental Validation of the “Target Hood Static Pressure” Balancing Method for Exhaust Ventilation Systems. Masters Thesis, West Virginia University (2004)
3. **Robert Van Becelaere, Harry J. Sauer and Fathi Finaish (January 2005):** Flow Resistance Characteristics of Airflow Control Dampers. HVAC&R Research: RP – 1157
4. **Steven E. Guffey (1993):** Airflow Redistribution in Exhaust Ventilation Systems Using Dampers and Static Pressure ratios. Applied Occupational Environmental Hygiene 8(3): 168 – 177 (1993b)
5. **Haines, R. W.:** HVAC Systems Design Handbook. Blue Ridge Summit, PA, 1988.
6. **Holly M. Geiger:** Evaluation of Proposed Static Pressure Ratio Balancing Method for Exhaust Ventilation Systems. Masters Thesis, University of Washington.
7. **Sheet Metal and Air Conditioning Contractors’ National Association. Inc.** (1993). HVAC Systems Testing, Adjusting, & Balancing. Published by SMACNA.
8. **American Conference of Governmental Industrial Hygienists (ACGIH) Committee on Industrial Ventilation:** Industrial Ventilation: A Manual of Recommended Practice, 23rd ed. Cincinnati, OH:ACGIH, 1997.
9. **Steven E. Guffey (1994):** Quantitative Troubleshooting of Industrial Exhaust Ventilation Systems. Applied Occupational Environmental Hygiene. 9:267 – 280 (1994)

- 10. Crowder, J.W., & Loudermilk, K.J.:** Balancing of Industrial Ventilation Systems. *Control Technology News*. (1982) Vol. 32, No. 1
- 11. Steven E. Guffey, Derrick W. Booth:** Comparison of Pitot Traverses Taken at Varying Distances Downstream of Obstructions. *American Industrial Hygiene Association Journal*. (1999) 60: 165 – 174.
- 12. American Conference of Governmental Industrial Hygienists (ACGIH) Committee on Industrial Ventilation:** Industrial Ventilation: A Manual of Recommended Practice, 23rd ed. Cincinnati, OH:ACGIH, 1998.
- 13. Ower, E., and Parkhurst, R.C.:** The Measurement of Air Flow, 5th edition. New York: Pergamon, 1977.
- 14. Hugh E. McLoone, Steven E. Guffey, & James P. Curran:** Effects of Shape, Size, and Air Velocity on Entry Loss Factors of Suction Hoods. *American Industrial Hygiene Association Journal*. (1993) 54(3): 87 – 94
- 15. Steven E. Guffey:** Unpublished Manuscript. (2005)
- 16. Idelchik, I.E. (1972):** Handbook of Hydraulic Resistance Coefficients of Local Resistance and Friction. *US Atomic Energy Commission*, AEC – TR – 6630, 1972.

Appendix I: HVAC Regulation Dampers

In addition to the exhaust ventilation dampers there are other heating, ventilation and air conditioning (HVAC) dampers used to control the flow of air used for HVAC. HVAC installation dampers are generally installed on the fan inlet or outlet. Based on the fan performance, there are two types of dampers namely outlet dampers and inlet dampers. Outlet dampers mount on the fan outlet to add resistance to the system when partially closed. These dampers are available with either Back-draft or with outlet volume control dampers (see Figure 45). Outlet volume control dampers are further classified in to parallel and opposed blade dampers.

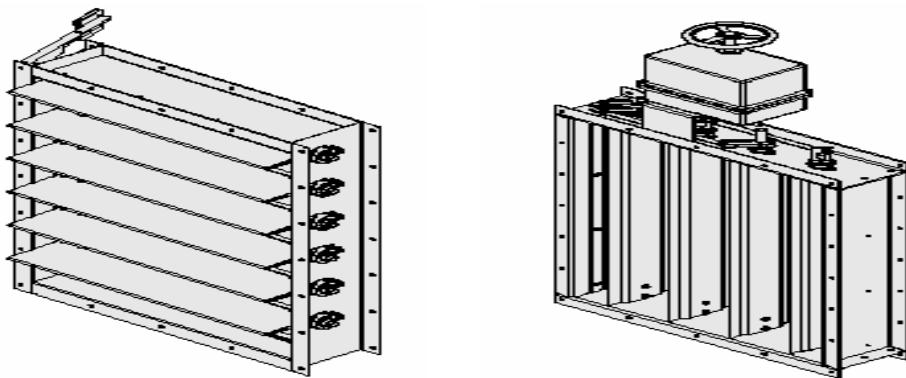


Figure 45 – Back draft Damper and Outlet Control Damper

Back draft dampers allow air to pass air in one direction and restrict the flow in opposite direction. Outlet volume control dampers regulate the airflow by modulating of damper blades. Actuators may be manual or pneumatic and are mounted out of the air stream. Control dampers are specially designed so blades are all perpendicular to the fan shaft. Parallel blade dampers (see Figure 46) have excellent control over the range of 75% to 100% wide-open volume due to the amount of control arm swing required to modulate the blades. Opposed blade dampers (see Figure 46) offer the best control over the entire operating range.

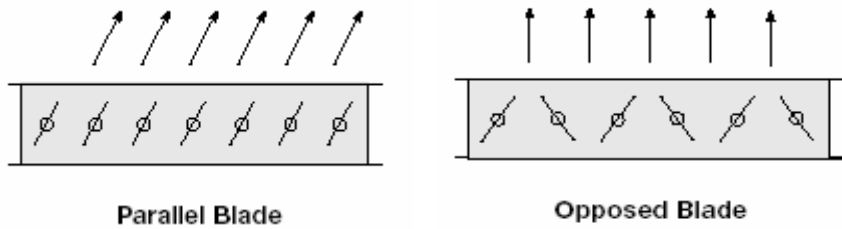


Figure 46 – Parallel Blade and Opposed Blade Outlet Dampers

Inlet dampers mount on the fan inlet to pre-spin air into the impeller. This reduces fan output and lowers operating horsepower. Because of the power savings, inlet dampers should be considered when the fan would operate for longer periods at reduced capacities. Inlet dampers include nested inlet vane, external inlet vane and inlet box dampers. Nested Inlet vane dampers (see Figure 47) are primarily used in non-ducted applications with space constraints. External Inlet Vane damper (see Figure 47) is intended for ducted applications and those with higher pressures and velocities. These dampers are mounted in the air stream or directly to the fan housing. Inlet box damper are used in standard or heavy-duty clean air applications with inlet boxes.

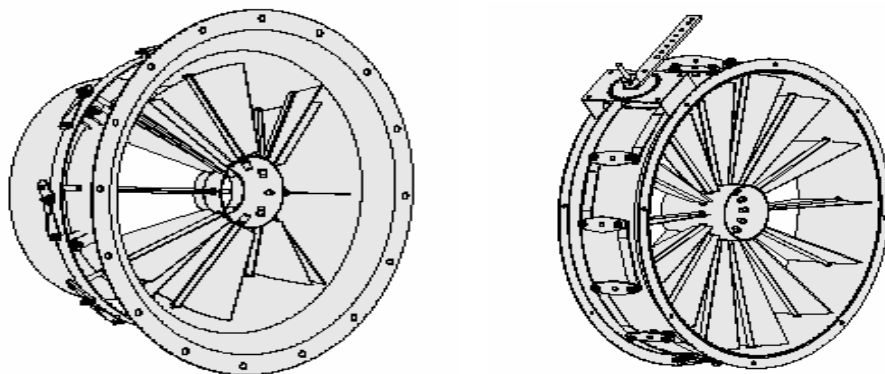


Figure 47 – Nested Inlet Vane Damper and External Inlet Vane Damper

Appendix II: Calibration of Digital Manometer

Equipment Used:

Digital Manometer: TSI DP – Calc. Digital manometer Model: 8702 Serial: 96071045

Hook Gauge: Dwyer Instruments Inc. Pressure No. 1425 Hook Gauge.

The manometer was calibrated before data measurement was made and was verified after collecting the data. The manometer was calibrated first on 30 August 2005 and was calibrated again on the 10 September 2005, 30 September 2005 and 11 January 2006.

**Calibration Data for the Determination of the Original Distribution and Calibration
Verification**

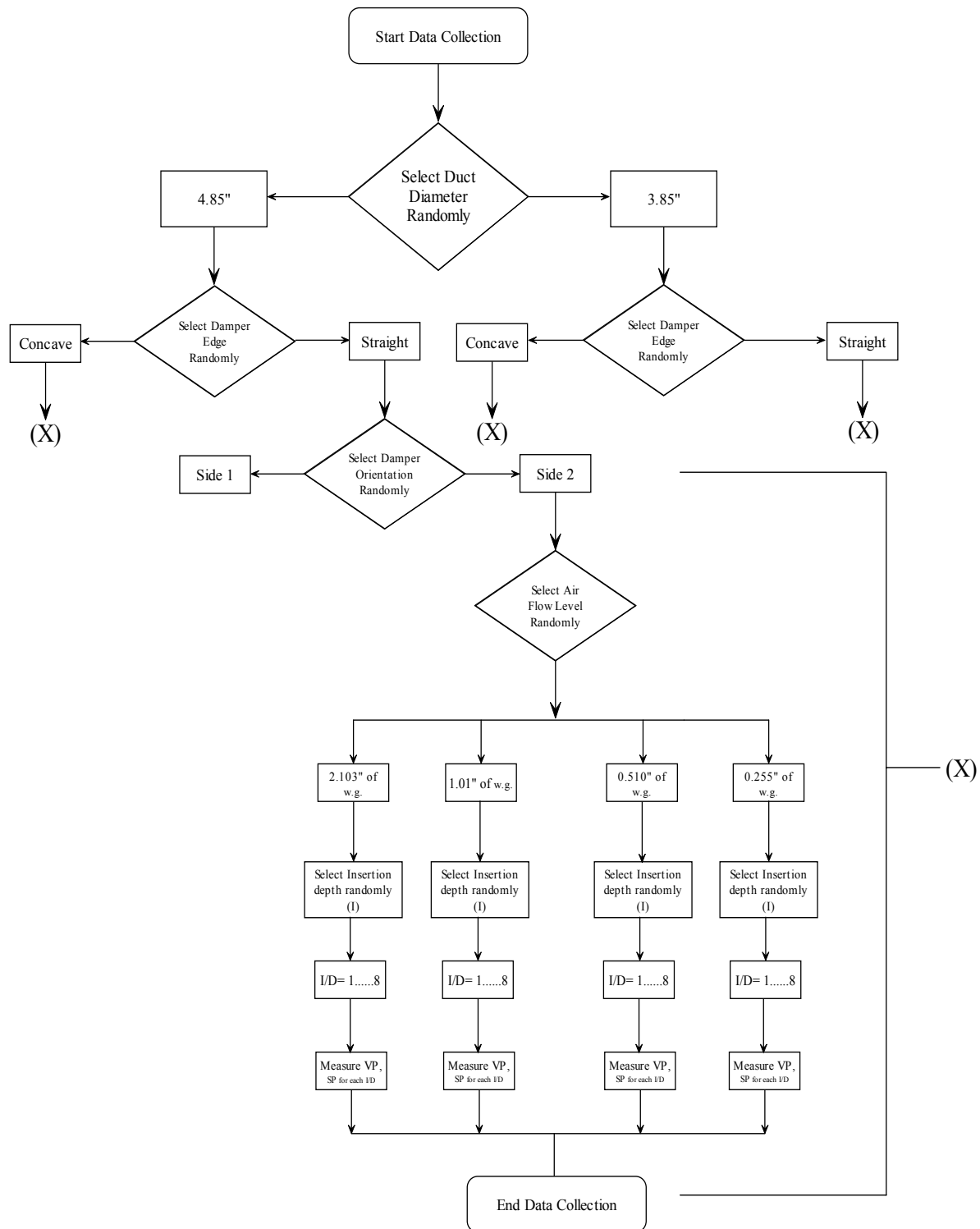
Trial	Date	Time	Gage Water Level	Manometer Reading
	mm/dd/yyyy		(Inches)	(Inches)
Original	8/30/2005	11:50 P.M.	0	0
			0.4	0.377
			0.6	0.59
			0.8	0.761
			1.4	1.342
			1.6	1.56
			1.8	1.722
			2	1.968
			2.6	2.569
			3	2.947
			3.8	3.779
			4	3.995
			4.4	4.338
			5	4.986
			6	5.967
			7	6.917
			8	7.911
			9	8.968
			10	9.922
			11	10.93
			12	11.88

Trial	Date mm/dd/yyyy	Time	Gage Water Level	Manometer Reading
			(Inches)	(Inches)
Original	9/10/2005	9:15 P.M.	0	0
			0.4	0.387
			0.6	0.61
			0.8	0.771
			1.4	1.354
			1.6	1.57
			1.8	1.729
			2	1.977
			2.6	2.578
			3	2.959
			3.8	3.788
			4	3.999
			4.4	4.349
			5	4.996
			6	5.973
			7	6.925
			8	7.918
			9	8.976
			10	9.934
			11	10.98
			12	11.92

Trial	Date mm/dd/yyyy	Time	Gage Water Level	Manometer Reading
			(Inches)	(Inches)
Calibration Verification	9/30/2005	8.00 P.M.	0	0
			0.4	0.396
			0.6	0.72
			0.8	0.793
			1.4	1.362
			1.6	1.58
			1.8	1.733
			2	1.979
			2.6	2.68
			3	2.971
			3.8	3.81
			4	4.01
			4.4	4.392
			5	5.11
			6	6.09
			7	6.946
			8	7.939
			9	9.161
			10	9.987
			11	11.231
			12	12.19

Trial	Date	Time	Gage Water Level	Manometer Reading
	mm/dd/yyyy		(Inches)	(Inches)
Calibration Verification	1/11/2006	6.00 P.M.	0	0
			0.4	0.386
			0.6	0.599
			0.8	0.77
			1.4	1.351
			1.6	1.569
			1.8	1.731
			2	1.977
			2.6	2.578
			3	2.956
			3.8	3.788
			4	4.004
			4.4	4.347
			5	4.995
			6	5.976
			7	6.926
			8	7.92
			9	8.977
			10	9.931
			11	10.939
			12	11.889

Appendix – III – (Flow chart for running the experiment)



Appendix – IV – Replication Combinations

Iteration	Duct Diameter	Damper Edge	Damper Orientation	Air Flow Level	Replicated
1	4.85	Concave	Side 1	0.255" of w.g.	Yes
2	4.85	Concave	Side 1	0.510" of w.g.	Yes
3	4.85	Concave	Side 1	1.010" of w.g.	No
4	4.85	Concave	Side 1	2.103" of w.g.	Yes
5	4.85	Concave	Side 2	0.255" of w.g.	No
6	4.85	Concave	Side 2	0.510" of w.g.	No
7	4.85	Concave	Side 2	1.010" of w.g.	No
8	4.85	Concave	Side 2	2.103" of w.g.	No
9	4.85	Straight	Side 1	0.255" of w.g.	No
10	4.85	Straight	Side 1	0.510" of w.g.	No
11	4.85	Straight	Side 1	1.010" of w.g.	No
12	4.85	Straight	Side 1	2.103" of w.g.	No
13	4.85	Straight	Side 2	0.255" of w.g.	No
14	4.85	Straight	Side 2	0.510" of w.g.	No
15	4.85	Straight	Side 2	1.010" of w.g.	Yes
16	4.85	Straight	Side 2	2.103" of w.g.	Yes
17	3.85	Concave	Side 1	0.255" of w.g.	No
18	3.85	Concave	Side 1	0.510" of w.g.	No
19	3.85	Concave	Side 1	1.010" of w.g.	No
20	3.85	Concave	Side 1	2.103" of w.g.	Yes
21	3.85	Concave	Side 2	0.255" of w.g.	Yes
22	3.85	Concave	Side 2	0.510" of w.g.	No
23	3.85	Concave	Side 2	1.010" of w.g.	Yes
24	3.85	Concave	Side 2	2.103" of w.g.	No
25	3.85	Straight	Side 1	0.255" of w.g.	No
26	3.85	Straight	Side 1	0.510" of w.g.	Yes
27	3.85	Straight	Side 1	1.010" of w.g.	No
28	3.85	Straight	Side 1	2.103" of w.g.	Yes
29	3.85	Straight	Side 2	0.255" of w.g.	No
30	3.85	Straight	Side 2	0.510" of w.g.	No
31	3.85	Straight	Side 2	1.010" of w.g.	No
32	3.85	Straight	Side 2	2.103" of w.g.	No

Appendix – V – Data

Data collected in Ventilation Exposure Laboratory is as follows with their abbreviations:

I – Insertion depth

D – Duct diameter

VP_{CLopen} – Airflow levels

Orient – Damper orientation (0 – Side1, 1 – Side2)

Edge – Damper edge (Con – Concave, Strt. – Straight)

SP_{end} – End static pressure

SP_{hood} – Hood static pressure

$VP_1 \dots VP_{20}$ – Velocity traverses (Velocity pressure)

VP_{CL} – Centerline velocity pressure

TP – Total Pressure

$X_{w/o}$ – Resistance without damper

X_{end} – End damper resistance

X_{damper} – Damper resistance

$V_{avg.}$ – Average velocity

Re – Reynolds number

Seq.	Year	Month	Date	Time	T_{act}	P_{bar}	I	D	VP_{CLopen}	Orient	Edge	ID
1	2005	8	31	12.75	72	29.70	0	4.85	2.103	0	Con	0.000
2	2005	8	31	12.75	72	29.70	0.65	4.85	2.103	0	Con	0.134
3	2005	8	31	12.75	72	29.70	0.86	4.85	2.103	0	Con	0.177
4	2005	8	31	12.75	72	29.70	1.2	4.85	2.103	0	Con	0.247
5	2005	8	31	12.75	72	29.70	1.5	4.85	2.103	0	Con	0.309
6	2005	8	31	12.75	72	29.70	2.3	4.85	2.103	0	Con	0.474
7	2005	8	31	12.75	72	29.70	3.1	4.85	2.103	0	Con	0.639
8	2005	8	31	12.75	72	29.70	4.1	4.85	2.103	0	Con	0.845
9	2005	8	31	15.00	72	29.70	0	4.85	1.010	0	Con	0.000
10	2005	8	31	15.00	72	29.70	0.65	4.85	1.010	0	Con	0.134
11	2005	8	31	15.00	72	29.70	0.86	4.85	1.010	0	Con	0.177
12	2005	8	31	15.00	72	29.70	1.2	4.85	1.010	0	Con	0.247
13	2005	8	31	15.00	72	29.70	1.5	4.85	1.010	0	Con	0.309
14	2005	8	31	15.00	72	29.70	2.3	4.85	1.010	0	Con	0.474
15	2005	8	31	15.00	72	29.70	3.1	4.85	1.010	0	Con	0.639
16	2005	8	31	15.00	72	29.70	4.1	4.85	1.010	0	Con	0.845
17	2005	8	31	16.25	73	29.80	0	4.85	0.510	0	Con	0.000
18	2005	8	31	16.25	73	29.80	0.65	4.85	0.510	0	Con	0.134
19	2005	8	31	16.25	73	29.80	0.86	4.85	0.510	0	Con	0.177
20	2005	8	31	16.25	73	29.80	1.2	4.85	0.510	0	Con	0.247
21	2005	8	31	16.25	73	29.80	1.5	4.85	0.510	0	Con	0.309
22	2005	8	31	16.25	73	29.80	2.3	4.85	0.510	0	Con	0.474
23	2005	8	31	16.25	73	29.80	3.1	4.85	0.510	0	Con	0.639
24	2005	8	31	16.25	73	29.80	4.1	4.85	0.510	0	Con	0.845
25	2005	8	31	17.50	72	29.80	0	4.85	0.255	0	Con	0.000
26	2005	8	31	17.50	72	29.80	0.65	4.85	0.255	0	Con	0.134
27	2005	8	31	17.50	72	29.80	0.86	4.85	0.255	0	Con	0.177
28	2005	8	31	17.50	72	29.80	1.2	4.85	0.255	0	Con	0.247
29	2005	8	31	17.50	72	29.80	1.5	4.85	0.255	0	Con	0.309
30	2005	8	31	17.50	72	29.80	2.3	4.85	0.255	0	Con	0.474
31	2005	8	31	17.50	72	29.80	3.1	4.85	0.255	0	Con	0.639
32	2005	8	31	17.50	72	29.80	4.1	4.85	0.255	0	Con	0.845
33	2005	9	13	11.75	72	30.13	0	4.85	2.103	1	Con	0.000
34	2005	9	13	11.75	72	30.13	0.65	4.85	2.103	1	Con	0.134
35	2005	9	13	11.75	72	30.13	0.86	4.85	2.103	1	Con	0.177
36	2005	9	13	11.75	72	30.13	1.2	4.85	2.103	1	Con	0.247
37	2005	9	13	11.75	72	30.13	1.5	4.85	2.103	1	Con	0.309
38	2005	9	13	11.75	72	30.13	2.3	4.85	2.103	1	Con	0.474
39	2005	9	13	11.75	72	30.13	3.1	4.85	2.103	1	Con	0.639
40	2005	9	13	11.75	72	30.13	4.1	4.85	2.103	1	Con	0.845
41	2005	9	13	13.00	72	30.13	0	4.85	0.510	1	Con	0.000
42	2005	9	13	13.00	72	30.13	0.65	4.85	0.510	1	Con	0.134
43	2005	9	13	13.00	72	30.13	0.86	4.85	0.510	1	Con	0.177
44	2005	9	13	13.00	72	30.13	1.2	4.85	0.510	1	Con	0.247

Seq.	SP_{end}	SP_{Hood}	VP₁	VP₂	VP₃	VP₄	VP₅	VP_{CLa}	VP₆	VP₇	VP₈	VP₉	VP₁₀
1	5.099	3.202	1.238	1.484	1.832	1.978	2.097	2.102	2.032	1.876	1.686	1.398	1.007
2	5.044	3.150	1.151	1.422	1.677	1.858	2.057	2.088	2.055	1.859	1.694	1.468	1.103
3	5.128	3.093	1.121	1.447	1.641	1.800	2.004	2.058	2.023	1.862	1.712	1.485	1.354
4	5.267	2.913	1.061	1.320	1.520	1.663	1.890	1.928	1.900	1.751	1.667	1.442	1.134
5	5.234	2.550	0.923	1.121	1.374	1.505	1.644	1.687	1.666	1.522	1.355	1.159	0.854
6	5.561	1.518	0.551	0.622	0.830	0.900	1.013	1.024	0.975	0.895	0.813	0.684	0.518
7	5.861	0.412	0.143	0.183	0.224	0.266	0.292	0.294	0.283	0.260	0.239	0.183	0.145
8	6.735	0.077	0.025	0.026	0.042	0.046	0.049	0.054	0.052	0.046	0.045	0.041	0.028
9	2.432	1.478	0.568	0.683	0.855	0.914	1.006	1.010	0.988	0.933	0.874	0.695	0.524
10	2.428	1.483	0.532	0.628	0.805	0.851	0.963	0.998	0.967	0.906	0.773	0.697	0.504
11	2.462	1.448	0.571	0.628	0.783	0.858	0.954	0.980	0.961	0.868	0.823	0.705	0.560
12	2.503	1.391	0.474	0.505	0.752	0.812	0.910	0.928	0.923	0.842	0.793	0.690	0.564
13	2.584	1.259	0.470	0.570	0.688	0.778	0.828	0.853	0.816	0.757	0.732	0.588	0.446
14	2.935	0.820	0.296	0.307	0.439	0.497	0.547	0.563	0.536	0.512	0.450	0.370	0.288
15	3.528	0.251	0.091	0.101	0.133	0.143	0.162	0.178	0.172	0.157	0.134	0.114	0.085
16	3.917	0.050	0.018	0.019	0.030	0.031	0.037	0.039	0.037	0.034	0.029	0.027	0.023
17	1.206	0.748	0.277	0.294	0.427	0.450	0.501	0.511	0.482	0.452	0.412	0.345	0.242
18	1.203	0.730	0.286	0.324	0.416	0.428	0.484	0.499	0.475	0.453	0.385	0.331	0.250
19	1.233	0.708	0.269	0.297	0.376	0.419	0.463	0.481	0.475	0.439	0.388	0.341	0.253
20	1.255	0.682	0.227	0.290	0.358	0.393	0.452	0.471	0.456	0.422	0.383	0.333	0.252
21	1.300	0.619	0.215	0.237	0.325	0.372	0.411	0.421	0.407	0.374	0.344	0.309	0.221
22	1.460	0.422	0.154	0.183	0.227	0.256	0.283	0.289	0.268	0.252	0.253	0.207	0.146
23	1.747	0.140	0.049	0.056	0.076	0.077	0.095	0.099	0.094	0.083	0.079	0.064	0.046
24	1.960	0.025	0.010	0.013	0.015	0.018	0.019	0.021	0.020	0.019	0.018	0.016	0.015
25	0.649	0.383	0.153	0.165	0.208	0.230	0.256	0.263	0.258	0.236	0.209	0.174	0.139
26	0.643	0.383	0.143	0.149	0.200	0.230	0.253	0.260	0.254	0.235	0.213	0.175	0.125
27	0.683	0.367	0.142	0.156	0.200	0.228	0.249	0.260	0.254	0.233	0.212	0.187	0.148
28	0.693	0.377	0.145	0.150	0.197	0.222	0.246	0.259	0.252	0.230	0.211	0.175	0.143
29	0.686	0.327	0.114	0.148	0.178	0.198	0.219	0.223	0.220	0.200	0.181	0.157	0.120
30	0.767	0.225	0.081	0.097	0.127	0.135	0.146	0.155	0.153	0.129	0.124	0.096	0.081
31	0.928	0.070	0.026	0.028	0.039	0.043	0.050	0.052	0.050	0.044	0.040	0.035	0.025
32	1.070	0.014	0.005	0.007	0.009	0.010	0.012	0.013	0.013	0.012	0.010	0.010	0.010
33	4.928	3.172	1.319	1.600	1.844	1.942	2.065	2.107	2.061	1.876	1.690	1.401	1.351
34	4.981	2.968	1.280	1.492	1.725	1.807	1.936	1.976	1.924	1.711	1.598	1.412	1.292
35	5.032	2.920	1.233	1.432	1.644	1.751	1.886	1.917	1.868	1.683	1.569	1.410	1.243
36	5.176	2.718	1.132	1.354	1.509	1.640	1.788	1.799	1.735	1.566	1.441	1.377	1.142
37	5.543	2.254	0.909	1.111	1.296	1.378	1.475	1.512	1.455	1.297	1.214	1.121	0.941
38	5.995	1.209	0.483	0.587	0.688	0.744	0.810	0.828	0.783	0.729	0.643	0.531	0.473
39	6.450	0.332	0.128	0.155	0.184	0.214	0.235	0.236	0.226	0.206	0.186	0.146	0.126
40	6.780	0.027	0.012	0.014	0.015	0.020	0.021	0.027	0.021	0.020	0.019	0.017	0.014
41	1.206	0.753	0.327	0.374	0.439	0.471	0.513	0.524	0.511	0.470	0.416	0.358	0.316
42	1.232	0.712	0.244	0.251	0.381	0.416	0.468	0.488	0.481	0.449	0.407	0.357	0.267
43	1.245	0.678	0.287	0.335	0.387	0.423	0.459	0.468	0.451	0.399	0.368	0.331	0.272
44	1.274	0.644	0.262	0.319	0.367	0.401	0.435	0.448	0.422	0.384	0.359	0.319	0.261

Seq.	VP₁₁	VP₁₂	VP₁₃	VP₁₄	VP₁₅	VP_{CLb}	VP₁₆	VP₁₇	VP₁₈	VP₁₉	VP₂₀	VP_{avg.}	TP
1	1.518	1.748	1.948	2.036	2.104	2.114	2.096	2.021	1.962	1.823	1.559	1.758	3.341
2	1.440	1.452	1.740	1.944	2.078	2.072	2.053	1.822	1.691	1.219	0.933	1.617	3.427
3	1.412	1.545	1.710	1.925	2.044	2.048	1.961	1.777	1.631	1.291	1.290	1.640	3.488
4	1.324	1.479	1.627	1.834	1.925	1.930	1.851	1.673	1.549	1.226	1.221	1.541	3.726
5	1.165	1.214	1.453	1.606	1.646	1.686	1.601	1.482	1.382	1.149	0.768	1.315	3.919
6	0.694	0.710	0.853	0.919	1.004	1.009	0.984	0.865	0.766	0.577	0.562	0.778	4.783
7	0.180	0.194	0.239	0.267	0.292	0.294	0.285	0.251	0.223	0.173	0.135	0.220	5.641
8	0.031	0.034	0.039	0.046	0.052	0.053	0.049	0.045	0.041	0.032	0.030	0.039	6.696
9	0.680	0.690	0.866	0.955	1.001	1.009	0.955	0.832	0.737	0.578	0.522	0.784	1.648
10	0.703	0.725	0.821	0.918	0.994	0.995	0.930	0.858	0.731	0.572	0.584	0.766	1.662
11	0.596	0.614	0.764	0.910	0.959	0.969	0.932	0.842	0.766	0.592	0.583	0.757	1.705
12	0.640	0.662	0.753	0.833	0.928	0.934	0.906	0.827	0.754	0.608	0.592	0.732	1.771
13	0.578	0.591	0.699	0.799	0.849	0.841	0.807	0.722	0.631	0.492	0.487	0.660	1.924
14	0.371	0.375	0.465	0.511	0.552	0.562	0.537	0.470	0.397	0.297	0.287	0.420	2.515
15	0.116	0.119	0.131	0.164	0.167	0.175	0.176	0.159	0.143	0.107	0.081	0.131	3.397
16	0.024	0.027	0.031	0.035	0.038	0.041	0.038	0.036	0.033	0.024	0.020	0.029	3.888
17	0.327	0.329	0.400	0.453	0.495	0.499	0.485	0.435	0.392	0.296	0.278	0.384	0.822
18	0.343	0.345	0.403	0.453	0.500	0.503	0.483	0.400	0.371	0.276	0.284	0.381	0.822
19	0.326	0.339	0.385	0.430	0.478	0.486	0.468	0.430	0.366	0.307	0.292	0.374	0.859
20	0.298	0.336	0.383	0.419	0.464	0.469	0.445	0.397	0.366	0.283	0.274	0.358	0.897
21	0.272	0.280	0.334	0.380	0.426	0.429	0.413	0.366	0.306	0.249	0.240	0.320	0.980
22	0.188	0.193	0.232	0.263	0.289	0.292	0.280	0.247	0.223	0.156	0.154	0.220	1.240
23	0.061	0.065	0.077	0.087	0.099	0.100	0.097	0.089	0.072	0.057	0.053	0.073	1.674
24	0.011	0.011	0.012	0.014	0.018	0.022	0.019	0.017	0.016	0.012	0.011	0.015	1.945
25	0.168	0.172	0.217	0.219	0.263	0.266	0.253	0.223	0.205	0.155	0.137	0.200	0.449
26	0.161	0.175	0.215	0.226	0.257	0.259	0.249	0.219	0.200	0.143	0.126	0.195	0.448
27	0.160	0.173	0.219	0.226	0.255	0.259	0.249	0.220	0.200	0.145	0.152	0.198	0.485
28	0.165	0.169	0.202	0.227	0.250	0.258	0.249	0.225	0.204	0.158	0.147	0.196	0.497
29	0.143	0.146	0.178	0.193	0.215	0.224	0.211	0.187	0.178	0.123	0.121	0.170	0.516
30	0.090	0.095	0.130	0.122	0.152	0.157	0.145	0.134	0.117	0.087	0.080	0.115	0.652
31	0.032	0.038	0.040	0.046	0.053	0.050	0.047	0.044	0.039	0.030	0.026	0.038	0.890
32	0.006	0.007	0.009	0.010	0.012	0.013	0.012	0.011	0.011	0.010	0.070	0.011	1.059
33	1.501	1.558	1.802	1.986	2.054	2.089	2.033	1.827	1.636	1.421	1.416	1.710	3.218
34	1.399	1.458	1.717	1.842	1.967	1.976	1.889	1.698	1.542	1.369	1.341	1.612	3.369
35	1.365	1.395	1.648	1.783	1.850	1.893	1.852	1.685	1.622	1.312	1.308	1.569	3.463
36	1.269	1.305	1.544	1.647	1.740	1.787	1.702	1.532	1.416	1.321	1.270	1.465	3.711
37	1.044	1.084	1.296	1.366	1.447	1.479	1.440	1.332	1.228	1.096	1.021	1.221	4.322
38	0.568	0.595	0.697	0.760	0.809	0.811	0.784	0.721	0.679	0.557	0.545	0.655	5.340
39	0.154	0.156	0.187	0.212	0.230	0.232	0.222	0.202	0.172	0.135	0.129	0.178	6.272
40	0.012	0.014	0.017	0.018	0.021	0.022	0.021	0.018	0.017	0.015	0.013	0.017	6.763
41	0.331	0.364	0.435	0.469	0.505	0.511	0.484	0.431	0.377	0.363	0.341	0.412	0.794
42	0.330	0.333	0.422	0.446	0.484	0.492	0.474	0.411	0.371	0.290	0.287	0.374	0.858
43	0.309	0.322	0.401	0.422	0.455	0.465	0.452	0.392	0.375	0.322	0.307	0.371	0.874
44	0.300	0.311	0.373	0.407	0.423	0.443	0.421	0.379	0.365	0.321	0.310	0.355	0.919

Seq.	X_{w/o}	X_{end}	X_{damper}	Log(X_{damper})	V_{avg.}	Re	Pipe Factor
1	1.9012	1.901	0.0000		5339.21	716426.25	0.913
2	1.9012	2.120	0.2054	-0.687	5121.00	687146.32	0.882
3	1.9012	2.126	0.2124	-0.673	5158.28	692149.39	0.894
4	1.9012	2.417	0.5007	-0.300	4999.90	670896.79	0.894
5	1.9012	2.981	1.0564	0.024	4618.03	619657.27	0.883
6	1.9012	6.144	4.1944	0.623	3553.25	476783.14	0.875
7	1.9012	25.670	23.6615	1.374	1888.00	253335.35	0.865
8	1.9012	169.661	167.5800	2.224	800.06	107354.08	0.859
9	2.1015	2.101	0.0000		3566.32	478536.18	0.881
10	2.1015	2.171	0.0563	-1.250	3523.83	472834.98	0.877
11	2.1015	2.254	0.1380	-0.860	3503.26	470074.74	0.881
12	2.1015	2.421	0.3033	-0.518	3445.02	462259.71	0.887
13	2.1015	2.915	0.7928	-0.101	3271.77	439013.34	0.883
14	2.1015	5.991	3.8463	0.585	2609.55	350154.85	0.864
15	2.1015	25.920	23.7217	1.375	1457.97	195632.98	0.862
16	2.1015	133.219	130.9555	2.117	688.01	92318.07	0.854
17	2.1393	2.139	0.0000		2494.37	334699.52	0.872
18	2.1393	2.160	0.0064	-2.195	2483.01	333175.39	0.872
19	2.1393	2.299	0.1447	-0.839	2460.16	330110.03	0.879
20	2.1393	2.506	0.3493	-0.457	2407.75	323077.41	0.873
21	2.1393	3.057	0.8950	-0.048	2278.02	305669.96	0.868
22	2.1393	5.630	3.4499	0.538	1888.47	253398.83	0.871
23	2.1393	22.976	20.7439	1.317	1086.33	145765.52	0.856
24	2.1393	129.418	127.1175	2.104	493.36	66199.42	0.836
25	2.2460	2.246	0.0000		1797.80	241232.75	0.869
26	2.2460	2.299	0.0401	-1.396	1774.91	238160.47	0.867
27	2.2460	2.441	0.1829	-0.738	1791.18	240343.95	0.875
28	2.2460	2.527	0.2678	-0.572	1782.26	239147.05	0.872
29	2.2460	3.042	0.7763	-0.110	1656.28	222243.18	0.871
30	2.2460	5.687	3.4019	0.532	1361.68	182712.97	0.857
31	2.2460	23.248	20.9116	1.320	786.55	105541.54	0.866
32	2.2460	93.181	90.7908	1.958	428.55	57504.02	0.935
33	1.8826	1.883	0.0000		5228.07	701513.64	0.903
34	1.8826	2.090	0.1939	-0.712	5076.89	681227.67	0.903
35	1.8826	2.206	0.3092	-0.510	5009.19	672142.92	0.908
36	1.8826	2.533	0.6326	-0.199	4839.71	649402.05	0.904
37	1.8826	3.539	1.6291	0.212	4418.91	592938.77	0.904
38	1.8826	8.155	6.2156	0.793	3235.70	434173.10	0.894
39	1.8826	35.157	33.1586	1.521	1688.82	226609.43	0.873
40	1.8826	402.403	400.3054	2.602	518.38	69557.14	0.829
41	1.9257	1.926	0.0000		2567.20	344472.21	0.893
42	1.9257	2.292	0.3511	-0.455	2446.04	328215.03	0.874
43	1.9257	2.355	0.4131	-0.384	2435.96	326862.23	0.892
44	1.9257	2.589	0.6454	-0.190	2382.30	319662.22	0.893

Seq.	Year	Month	Date	Time	T_{act}	P_{bar}	I	D	VP_{CLopen}	Orient	Edge	I/D
45	2005	9	13	13.00	72	30.13	1.5	4.85	0.510	1	Con	0.309
46	2005	9	13	13.00	72	30.13	2.3	4.85	0.510	1	Con	0.474
47	2005	9	13	13.00	72	30.13	3.1	4.85	0.510	1	Con	0.639
48	2005	9	13	13.00	72	30.13	4.1	4.85	0.510	1	Con	0.845
49	2005	9	14	11.50	74	30.19	0	4.85	1.010	1	Con	0.000
50	2005	9	14	11.50	74	30.19	0.65	4.85	1.010	1	Con	0.134
51	2005	9	14	11.50	74	30.19	0.86	4.85	1.010	1	Con	0.177
52	2005	9	14	11.50	74	30.19	1.2	4.85	1.010	1	Con	0.247
53	2005	9	14	11.50	74	30.19	1.5	4.85	1.010	1	Con	0.309
54	2005	9	14	11.50	74	30.19	2.3	4.85	1.010	1	Con	0.474
55	2005	9	14	11.50	74	30.19	3.1	4.85	1.010	1	Con	0.639
56	2005	9	14	11.50	74	30.19	4.1	4.85	1.010	1	Con	0.845
57	2005	9	14	13.00	74	30.19	0	4.85	0.255	1	Con	0.000
58	2005	9	14	13.00	74	30.19	0.65	4.85	0.255	1	Con	0.134
59	2005	9	14	13.00	74	30.19	0.86	4.85	0.255	1	Con	0.177
60	2005	9	14	13.00	74	30.19	1.2	4.85	0.255	1	Con	0.247
61	2005	9	14	13.00	74	30.19	1.5	4.85	0.255	1	Con	0.309
62	2005	9	14	13.00	74	30.19	2.3	4.85	0.255	1	Con	0.474
63	2005	9	14	13.00	74	30.19	3.1	4.85	0.255	1	Con	0.639
64	2005	9	14	13.00	74	30.19	4.1	4.85	0.255	1	Con	0.845
65	2005	9	14	15.25	74	30.19	0	4.85	2.103	0	Strt.	0.000
66	2005	9	14	15.25	74	30.19	0.65	4.85	2.103	0	Strt.	0.134
67	2005	9	14	15.25	74	30.19	0.86	4.85	2.103	0	Strt.	0.177
68	2005	9	14	15.25	74	30.19	1.2	4.85	2.103	0	Strt.	0.247
69	2005	9	14	15.25	74	30.19	1.5	4.85	2.103	0	Strt.	0.309
70	2005	9	14	15.25	74	30.19	2.3	4.85	2.103	0	Strt.	0.474
71	2005	9	14	15.25	74	30.19	3.1	4.85	2.103	0	Strt.	0.639
72	2005	9	14	15.25	74	30.19	4.1	4.85	2.103	0	Strt.	0.845
73	2005	9	25	11.50	84	30.16	0	4.85	1.010	0	Strt.	0.000
74	2005	9	25	11.50	84	30.16	0.65	4.85	1.010	0	Strt.	0.134
75	2005	9	25	11.50	84	30.16	0.86	4.85	1.010	0	Strt.	0.177
76	2005	9	25	11.50	84	30.16	1.2	4.85	1.010	0	Strt.	0.247
77	2005	9	25	11.50	84	30.16	1.5	4.85	1.010	0	Strt.	0.309
78	2005	9	25	11.50	84	30.16	2.3	4.85	1.010	0	Strt.	0.474
79	2005	9	25	11.50	84	30.16	3.1	4.85	1.010	0	Strt.	0.639
80	2005	9	25	11.50	84	30.16	4.1	4.85	1.010	0	Strt.	0.845
81	2005	9	25	13.00	84	30.16	0	4.85	0.510	0	Strt.	0.000
82	2005	9	25	13.00	84	30.16	0.65	4.85	0.510	0	Strt.	0.134
83	2005	9	25	13.00	84	30.16	0.86	4.85	0.510	0	Strt.	0.177
84	2005	9	25	13.00	84	30.16	1.2	4.85	0.510	0	Strt.	0.247
85	2005	9	25	13.00	84	30.16	1.5	4.85	0.510	0	Strt.	0.309
86	2005	9	25	13.00	84	30.16	2.3	4.85	0.510	0	Strt.	0.474
87	2005	9	25	13.00	84	30.16	3.1	4.85	0.510	0	Strt.	0.639
88	2005	9	25	13.00	84	30.16	4.1	4.85	0.510	0	Strt.	0.845

Seq.	SP_{end}	SP_{Hood}	VP₁	VP₂	VP₃	VP₄	VP₅	VP_{CLa}	VP₆	VP₇	VP₈	VP₉	VP₁₀
45	1.352	0.526	0.179	0.216	0.278	0.312	0.352	0.363	0.359	0.331	0.305	0.263	0.196
46	1.532	0.329	0.114	0.140	0.178	0.194	0.222	0.228	0.226	0.207	0.194	0.165	0.128
47	1.791	0.104	0.039	0.051	0.060	0.064	0.073	0.075	0.069	0.067	0.062	0.049	0.039
48	1.892	0.017	0.004	0.005	0.007	0.008	0.009	0.011	0.008	0.007	0.005	0.004	0.003
49	2.312	1.482	0.632	0.749	0.855	0.931	0.986	1.013	0.982	0.893	0.806	0.712	0.621
50	2.323	1.451	0.602	0.708	0.829	0.880	0.963	0.988	0.958	0.839	0.773	0.619	0.600
51	2.336	1.415	0.588	0.708	0.813	0.881	0.955	0.956	0.940	0.835	0.761	0.610	0.581
52	2.368	1.354	0.543	0.681	0.753	0.805	0.886	0.907	0.878	0.787	0.725	0.591	0.540
53	2.521	1.181	0.485	0.593	0.680	0.723	0.790	0.802	0.780	0.697	0.620	0.502	0.482
54	2.784	0.829	0.333	0.412	0.457	0.503	0.549	0.555	0.523	0.476	0.438	0.353	0.329
55	3.263	0.355	0.129	0.169	0.201	0.220	0.244	0.255	0.242	0.211	0.190	0.156	0.112
56	3.706	0.046	0.024	0.030	0.031	0.037	0.038	0.039	0.037	0.034	0.029	0.027	0.023
57	0.611	0.373	0.156	0.180	0.215	0.232	0.251	0.259	0.252	0.225	0.203	0.180	0.154
58	0.617	0.362	0.143	0.149	0.200	0.230	0.253	0.260	0.254	0.235	0.213	0.175	0.125
59	0.621	0.355	0.146	0.170	0.200	0.222	0.243	0.250	0.244	0.212	0.184	0.166	0.148
60	0.625	0.347	0.138	0.165	0.202	0.218	0.240	0.238	0.230	0.213	0.190	0.148	0.133
61	0.653	0.306	0.127	0.148	0.177	0.192	0.213	0.218	0.208	0.190	0.169	0.148	0.125
62	0.744	0.196	0.081	0.099	0.115	0.130	0.141	0.141	0.138	0.119	0.108	0.097	0.079
63	0.853	0.094	0.042	0.046	0.063	0.063	0.069	0.070	0.067	0.060	0.058	0.044	0.041
64	1.070	0.014	0.005	0.007	0.009	0.010	0.012	0.013	0.013	0.012	0.010	0.010	0.010
65	4.920	3.184	1.343	1.536	1.795	1.914	2.056	2.102	2.052	1.817	1.658	1.410	1.299
66	4.970	3.043	1.267	1.504	1.725	1.821	1.972	2.001	1.950	1.743	1.605	1.285	1.198
67	5.050	2.945	1.214	1.464	1.662	1.773	1.925	1.949	1.896	1.692	1.590	1.319	1.227
68	5.141	2.816	1.166	1.418	1.584	1.702	1.852	1.868	1.798	1.620	1.444	1.262	1.114
69	5.487	2.330	0.931	1.143	1.306	1.417	1.526	1.540	1.494	1.365	1.243	1.112	0.960
70	5.867	1.403	0.583	0.699	0.800	0.858	0.932	0.952	0.923	0.827	0.736	0.659	0.571
71	6.226	0.437	0.176	0.209	0.252	0.265	0.298	0.305	0.295	0.265	0.240	0.181	0.171
72	6.654	0.026	0.012	0.015	0.016	0.020	0.021	0.024	0.021	0.017	0.015	0.014	0.012
73	2.352	1.491	0.629	0.735	0.852	0.930	0.990	1.006	0.971	0.851	0.797	0.623	0.620
74	2.377	1.433	0.597	0.698	0.806	0.872	0.951	0.974	0.937	0.843	0.752	0.613	0.599
75	2.406	1.402	0.596	0.667	0.798	0.847	0.913	0.951	0.916	0.829	0.744	0.616	0.589
76	2.459	1.326	0.530	0.650	0.762	0.808	0.863	0.881	0.868	0.777	0.708	0.621	0.539
77	2.601	1.127	0.461	0.563	0.636	0.712	0.761	0.778	0.746	0.664	0.617	0.541	0.447
78	2.960	0.695	0.271	0.335	0.389	0.426	0.469	0.475	0.456	0.410	0.382	0.321	0.286
79	3.455	0.254	0.103	0.124	0.148	0.161	0.170	0.185	0.179	0.158	0.139	0.129	0.114
80	3.938	0.016	0.013	0.014	0.015	0.016	0.018	0.019	0.018	0.017	0.016	0.014	0.013
81	1.264	0.797	0.315	0.391	0.461	0.498	0.537	0.551	0.524	0.466	0.450	0.374	0.306
82	1.351	0.811	0.312	0.380	0.454	0.475	0.519	0.531	0.503	0.459	0.433	0.347	0.301
83	1.359	0.781	0.321	0.379	0.441	0.477	0.511	0.521	0.498	0.451	0.406	0.341	0.291
84	1.405	0.749	0.297	0.360	0.424	0.469	0.506	0.511	0.500	0.434	0.389	0.329	0.263
85	1.435	0.634	0.239	0.307	0.361	0.383	0.421	0.428	0.412	0.371	0.350	0.298	0.221
86	1.687	0.407	0.168	0.198	0.236	0.247	0.281	0.285	0.265	0.239	0.217	0.173	0.152
87	1.957	0.130	0.051	0.063	0.078	0.083	0.097	0.099	0.085	0.081	0.075	0.059	0.050
88	2.243	0.013	0.005	0.007	0.008	0.011	0.012	0.013	0.011	0.009	0.007	0.005	0.004

Seq.	VP₁₁	VP₁₂	VP₁₃	VP₁₄	VP₁₅	VP_{CLb}	VP₁₆	VP₁₇	VP₁₈	VP₁₉	VP₂₀	VP_{avg.}	TP
45	0.238	0.269	0.292	0.327	0.358	0.366	0.352	0.304	0.272	0.219	0.215	0.279	1.073
46	0.144	0.168	0.189	0.211	0.224	0.233	0.220	0.194	0.175	0.128	0.124	0.175	1.357
47	0.047	0.050	0.064	0.072	0.077	0.078	0.075	0.066	0.063	0.056	0.046	0.059	1.732
48	0.004	0.006	0.007	0.009	0.011	0.009	0.008	0.007	0.005	0.003	0.003	0.006	1.886
49	0.678	0.705	0.842	0.901	0.989	0.998	0.969	0.838	0.765	0.712	0.669	0.807	1.505
50	0.664	0.697	0.861	0.900	0.966	0.973	0.925	0.816	0.743	0.689	0.624	0.778	1.545
51	0.659	0.681	0.801	0.861	0.940	0.950	0.913	0.815	0.707	0.683	0.642	0.764	1.572
52	0.617	0.640	0.672	0.848	0.896	0.901	0.866	0.732	0.675	0.635	0.613	0.715	1.653
53	0.531	0.570	0.673	0.737	0.797	0.802	0.766	0.697	0.666	0.594	0.521	0.641	1.880
54	0.365	0.396	0.482	0.517	0.548	0.554	0.543	0.501	0.450	0.412	0.372	0.445	2.339
55	0.159	0.172	0.208	0.224	0.248	0.251	0.239	0.207	0.192	0.179	0.152	0.191	3.072
56	0.024	0.027	0.031	0.035	0.038	0.041	0.038	0.036	0.033	0.024	0.020	0.031	3.675
57	0.167	0.177	0.209	0.231	0.257	0.259	0.249	0.217	0.193	0.169	0.152	0.202	0.409
58	0.161	0.175	0.215	0.226	0.257	0.259	0.249	0.219	0.200	0.143	0.126	0.195	0.422
59	0.156	0.168	0.208	0.230	0.243	0.246	0.233	0.218	0.201	0.179	0.151	0.195	0.426
60	0.159	0.166	0.201	0.219	0.235	0.237	0.230	0.210	0.184	0.169	0.157	0.189	0.436
61	0.141	0.147	0.180	0.194	0.209	0.212	0.203	0.183	0.178	0.145	0.139	0.170	0.483
62	0.087	0.091	0.114	0.123	0.138	0.139	0.131	0.119	0.111	0.096	0.085	0.109	0.635
63	0.042	0.043	0.052	0.057	0.064	0.066	0.063	0.060	0.052	0.041	0.041	0.053	0.800
64	0.006	0.007	0.009	0.010	0.012	0.013	0.012	0.011	0.011	0.010	0.070	0.011	1.059
65	1.466	1.509	1.814	1.927	2.075	2.090	2.077	1.841	1.761	1.576	1.392	1.706	3.214
66	1.424	1.476	1.685	1.833	1.991	2.005	1.988	1.830	1.641	1.479	1.382	1.630	3.340
67	1.362	1.383	1.682	1.815	1.915	1.932	1.926	1.672	1.583	1.484	1.214	1.581	3.469
68	1.273	1.329	1.582	1.714	1.833	1.852	1.817	1.729	1.544	1.368	1.198	1.508	3.633
69	1.088	1.103	1.326	1.417	1.528	1.535	1.496	1.422	1.306	1.120	0.996	1.258	4.229
70	0.655	0.670	0.789	0.863	0.937	0.941	0.913	0.874	0.745	0.646	0.624	0.761	5.106
71	0.195	0.208	0.250	0.278	0.295	0.299	0.293	0.263	0.250	0.191	0.187	0.236	5.990
72	0.016	0.017	0.018	0.019	0.020	0.021	0.020	0.019	0.018	0.017	0.016	0.017	6.637
73	0.682	0.734	0.849	0.920	0.979	1.006	0.961	0.875	0.859	0.747	0.679	0.809	1.543
74	0.678	0.663	0.800	0.885	0.947	0.965	0.913	0.840	0.821	0.671	0.651	0.772	1.605
75	0.655	0.669	0.788	0.863	0.931	0.947	0.910	0.832	0.778	0.660	0.649	0.758	1.648
76	0.600	0.626	0.729	0.801	0.867	0.888	0.853	0.773	0.721	0.621	0.591	0.711	1.748
77	0.504	0.527	0.596	0.688	0.759	0.768	0.758	0.708	0.645	0.572	0.521	0.617	1.984
78	0.315	0.335	0.404	0.436	0.470	0.481	0.454	0.417	0.392	0.341	0.301	0.378	2.582
79	0.114	0.120	0.144	0.164	0.177	0.186	0.172	0.153	0.147	0.122	0.116	0.142	3.313
80	0.014	0.016	0.018	0.019	0.020	0.021	0.019	0.018	0.016	0.014	0.013	0.016	3.922
81	0.347	0.365	0.446	0.473	0.520	0.527	0.517	0.465	0.412	0.315	0.306	0.421	0.843
82	0.341	0.362	0.431	0.466	0.517	0.525	0.510	0.449	0.399	0.313	0.303	0.410	0.941
83	0.325	0.336	0.351	0.473	0.514	0.522	0.502	0.434	0.395	0.311	0.301	0.399	0.960
84	0.336	0.346	0.424	0.462	0.505	0.511	0.486	0.426	0.386	0.303	0.294	0.393	1.012
85	0.287	0.294	0.351	0.384	0.430	0.435	0.427	0.385	0.351	0.301	0.282	0.340	1.095
86	0.181	0.184	0.213	0.243	0.276	0.281	0.271	0.239	0.212	0.179	0.165	0.215	1.472
87	0.057	0.062	0.076	0.082	0.094	0.096	0.096	0.077	0.063	0.059	0.054	0.071	1.886
88	0.007	0.008	0.009	0.012	0.013	0.014	0.012	0.010	0.009	0.008	0.006	0.008	2.235

Seq.	X_{w/o}	X_{end}	X_{damper}	Log(X_{damper})	V_{avg.}	Re	Pipe Factor
45	1.9257	3.846	1.8904	0.277	2112.06	283401.18	0.875
46	1.9257	7.738	5.7599	0.760	1674.31	224661.83	0.872
47	1.9257	29.420	27.3918	1.438	970.22	130186.43	0.877
48	1.9257	317.590	315.4647	2.499	308.14	41346.68	0.772
49	1.8642	1.864	0.0000		3595.66	482473.68	0.896
50	1.8642	1.987	0.1094	-0.961	3529.58	473605.81	0.891
51	1.8642	2.058	0.1797	-0.745	3497.99	469368.15	0.895
52	1.8642	2.313	0.4320	-0.364	3383.32	453980.37	0.889
53	1.8642	2.933	1.0463	0.020	3204.14	429937.85	0.894
54	1.8642	5.256	3.3515	0.525	2669.80	358238.78	0.896
55	1.8642	16.109	14.1651	1.151	1747.75	234516.17	0.868
56	1.8642	120.394	118.3695	2.073	699.26	93828.08	0.874
57	2.0251	2.025	0.0000		1798.61	241340.88	0.883
58	2.0251	2.166	0.1276	-0.894	1766.72	237061.52	0.867
59	2.0251	2.190	0.1515	-0.820	1765.77	236934.70	0.886
60	2.0251	2.309	0.2693	-0.570	1739.24	233374.58	0.892
61	2.0251	2.849	0.8041	-0.095	1648.34	221177.97	0.888
62	2.0251	5.811	3.7449	0.573	1322.67	177478.51	0.883
63	2.0251	15.111	13.0102	1.114	920.87	123564.47	0.882
64	2.0251	93.181	91.0117	1.959	426.57	57238.68	0.935
65	1.8833	1.883	0.0000		5227.81	701478.93	0.902
66	1.8833	2.048	0.1524	-0.817	5110.13	685687.70	0.902
67	1.8833	2.195	0.2974	-0.527	5031.58	675147.23	0.903
68	1.8833	2.409	0.5093	-0.293	4914.63	659454.65	0.900
69	1.8833	3.363	1.4544	0.163	4487.99	602207.60	0.904
70	1.8833	6.715	4.7816	0.680	3490.10	468308.27	0.896
71	1.8833	25.371	23.3845	1.369	1944.56	260925.63	0.884
72	1.8833	389.392	387.2943	2.588	522.49	70108.41	0.871
73	1.9058	1.906	0.0000		3635.94	487878.39	0.897
74	1.9058	2.078	0.1590	-0.798	3551.40	476533.64	0.892
75	1.9058	2.173	0.2532	-0.597	3519.07	472196.79	0.894
76	1.9058	2.458	0.5345	-0.272	3408.14	457311.04	0.897
77	1.9058	3.214	1.2838	0.108	3175.10	426041.53	0.894
78	1.9058	6.832	4.8782	0.688	2484.51	333376.32	0.889
79	1.9058	23.374	21.3748	1.330	1521.56	204166.05	0.874
80	1.9058	245.495	243.4024	2.386	510.81	68542.05	0.894
81	2.0041	2.004	0.0000		2621.48	351756.04	0.884
82	2.0041	2.293	0.2781	-0.556	2588.59	347343.06	0.881
83	2.0041	2.403	0.3869	-0.412	2553.86	342682.90	0.875
84	2.0041	2.573	0.5561	-0.255	2534.24	340049.35	0.877
85	2.0041	3.221	1.1964	0.078	2356.52	316202.27	0.888
86	2.0041	6.842	4.7955	0.681	1874.47	251520.94	0.872
87	2.0041	26.429	24.3317	1.386	1079.48	144847.35	0.855
88	2.0041	264.446	262.2564	2.419	371.50	49848.30	0.791

Seq.	Year	Month	Date	Time	T_{act}	P_{bar}	I	D	VP_{CLopen}	Orient	Edge	I/D
89	2005	9	14	14.00	74	30.19	0	4.85	0.255	0	Strt.	0.000
90	2005	9	14	14.00	74	30.19	0.65	4.85	0.255	0	Strt.	0.134
91	2005	9	14	14.00	74	30.19	0.86	4.85	0.255	0	Strt.	0.177
92	2005	9	14	14.00	74	30.19	1.2	4.85	0.255	0	Strt.	0.247
93	2005	9	14	14.00	74	30.19	1.5	4.85	0.255	0	Strt.	0.309
94	2005	9	14	14.00	74	30.19	2.3	4.85	0.255	0	Strt.	0.474
95	2005	9	14	14.00	74	30.19	3.1	4.85	0.255	0	Strt.	0.639
96	2005	9	14	14.00	74	30.19	4.1	4.85	0.255	0	Strt.	0.845
97	2005	12	29	15.25	25	30.19	0	4.85	2.103	1	Strt.	0.000
98	2005	12	29	15.25	25	30.19	0.65	4.85	2.103	1	Strt.	0.134
99	2005	12	29	15.25	25	30.19	0.86	4.85	2.103	1	Strt.	0.177
100	2005	12	29	15.25	25	30.19	1.2	4.85	2.103	1	Strt.	0.247
101	2005	12	29	15.25	25	30.19	1.5	4.85	2.103	1	Strt.	0.309
102	2005	12	29	15.25	25	30.19	2.3	4.85	2.103	1	Strt.	0.474
103	2005	12	29	15.25	25	30.19	3.1	4.85	2.103	1	Strt.	0.639
104	2005	12	29	15.25	25	30.19	4.1	4.85	2.103	1	Strt.	0.845
105	2005	12	29	17.50	25	30.16	0	4.85	1.010	1	Strt.	0.000
106	2005	12	29	17.50	25	30.16	0.65	4.85	1.010	1	Strt.	0.134
107	2005	12	29	17.50	25	30.16	0.86	4.85	1.010	1	Strt.	0.177
108	2005	12	29	17.50	25	30.16	1.2	4.85	1.010	1	Strt.	0.247
109	2005	12	29	17.50	25	30.16	1.5	4.85	1.010	1	Strt.	0.309
110	2005	12	29	17.50	25	30.16	2.3	4.85	1.010	1	Strt.	0.474
111	2005	12	29	17.50	25	30.16	3.1	4.85	1.010	1	Strt.	0.639
112	2005	12	29	17.50	25	30.16	4.1	4.85	1.010	1	Strt.	0.845
113	2005	12	30	11.00	27	30.16	0	4.85	0.510	1	Strt.	0.000
114	2005	12	30	11.00	27	30.16	0.65	4.85	0.510	1	Strt.	0.134
115	2005	12	30	11.00	27	30.16	0.86	4.85	0.510	1	Strt.	0.177
116	2005	12	30	11.00	27	30.16	1.2	4.85	0.510	1	Strt.	0.247
117	2005	12	30	11.00	27	30.16	1.5	4.85	0.510	1	Strt.	0.309
118	2005	12	30	11.00	27	30.16	2.3	4.85	0.510	1	Strt.	0.474
119	2005	12	30	11.00	27	30.16	3.1	4.85	0.510	1	Strt.	0.639
120	2005	12	30	11.00	27	30.16	4.1	4.85	0.510	1	Strt.	0.845
121	2005	12	30	12.50	27	30.19	0	4.85	0.255	1	Strt.	0.000
122	2005	12	30	12.50	27	30.19	0.65	4.85	0.255	1	Strt.	0.134
123	2005	12	30	12.50	27	30.19	0.86	4.85	0.255	1	Strt.	0.177
124	2005	12	30	12.50	27	30.19	1.2	4.85	0.255	1	Strt.	0.247
125	2005	12	30	12.50	27	30.19	1.5	4.85	0.255	1	Strt.	0.309
126	2005	12	30	12.50	27	30.19	2.3	4.85	0.255	1	Strt.	0.474
127	2005	12	30	12.50	27	30.19	3.1	4.85	0.255	1	Strt.	0.639
128	2005	12	30	12.50	27	30.19	4.1	4.85	0.255	1	Strt.	0.845
129	2005	11	25	11.00	10	30.00	0	3.85	2.103	0	Con	0.000
130	2005	11	25	11.00	10	30.00	0.5	3.85	2.103	0	Con	0.130
131	2005	11	25	11.00	10	30.00	0.7	3.85	2.103	0	Con	0.182
132	2005	11	25	11.00	10	30.00	0.9	3.85	2.103	0	Con	0.234

Seq.	SP_{end}	SP_{Hood}	VP₁	VP₂	VP₃	VP₄	VP₅	VP_{CLa}	VP₆	VP₇	VP₈	VP₉	VP₁₀
89	0.631	0.378	0.159	0.189	0.217	0.235	0.260	0.262	0.250	0.229	0.212	0.154	0.153
90	0.643	0.370	0.145	0.177	0.211	0.219	0.247	0.252	0.245	0.222	0.202	0.171	0.147
91	0.643	0.358	0.142	0.169	0.203	0.227	0.243	0.249	0.244	0.217	0.194	0.150	0.141
92	0.655	0.339	0.136	0.161	0.193	0.209	0.232	0.238	0.231	0.202	0.186	0.150	0.136
93	0.686	0.293	0.117	0.145	0.175	0.187	0.203	0.208	0.197	0.175	0.158	0.140	0.103
94	0.793	0.178	0.072	0.089	0.103	0.112	0.124	0.132	0.124	0.110	0.096	0.075	0.069
95	0.876	0.087	0.028	0.033	0.042	0.043	0.051	0.052	0.050	0.043	0.042	0.032	0.028
96	1.058	0.005	0.002	0.003	0.004	0.005	0.005	0.006	0.005	0.004	0.004	0.003	0.002
97	4.910	3.174	1.333	1.526	1.785	1.904	2.046	2.092	2.042	1.807	1.648	1.400	1.289
98	4.960	3.033	1.257	1.494	1.715	1.811	1.962	1.991	1.940	1.733	1.595	1.275	1.188
99	5.040	2.935	1.204	1.454	1.652	1.763	1.915	1.939	1.886	1.682	1.580	1.309	1.217
100	5.131	2.806	1.156	1.408	1.574	1.692	1.842	1.858	1.788	1.610	1.434	1.252	1.104
101	5.477	2.320	0.921	1.133	1.296	1.407	1.516	1.530	1.484	1.355	1.233	1.102	0.950
102	5.857	1.393	0.573	0.689	0.790	0.848	0.922	0.942	0.913	0.817	0.726	0.649	0.561
103	6.216	0.427	0.166	0.199	0.242	0.255	0.288	0.295	0.285	0.255	0.230	0.171	0.161
104	6.644	0.016	0.010	0.013	0.014	0.018	0.019	0.022	0.019	0.015	0.013	0.012	0.010
105	2.332	1.471	0.599	0.705	0.822	0.900	0.960	0.976	0.941	0.821	0.767	0.593	0.590
106	2.357	1.413	0.567	0.668	0.776	0.842	0.921	0.944	0.907	0.813	0.722	0.583	0.569
107	2.386	1.382	0.566	0.637	0.768	0.817	0.883	0.921	0.886	0.799	0.714	0.586	0.559
108	2.439	1.306	0.500	0.620	0.732	0.778	0.833	0.851	0.838	0.747	0.678	0.591	0.509
109	2.581	1.107	0.431	0.533	0.606	0.682	0.731	0.748	0.716	0.634	0.587	0.511	0.417
110	2.940	0.675	0.241	0.305	0.359	0.396	0.439	0.445	0.426	0.380	0.352	0.291	0.256
111	3.435	0.234	0.073	0.094	0.118	0.131	0.140	0.155	0.149	0.128	0.109	0.099	0.084
112	3.918	0.014	0.011	0.012	0.013	0.014	0.016	0.017	0.016	0.015	0.014	0.012	0.011
113	1.234	0.767	0.305	0.381	0.451	0.488	0.527	0.541	0.514	0.456	0.440	0.364	0.296
114	1.321	0.781	0.302	0.370	0.444	0.465	0.509	0.521	0.493	0.449	0.423	0.337	0.291
115	1.329	0.751	0.311	0.369	0.431	0.467	0.501	0.511	0.488	0.441	0.396	0.331	0.281
116	1.375	0.719	0.287	0.350	0.414	0.459	0.496	0.501	0.490	0.424	0.379	0.319	0.253
117	1.405	0.604	0.229	0.297	0.351	0.373	0.411	0.418	0.402	0.361	0.340	0.288	0.211
118	1.657	0.377	0.158	0.188	0.226	0.237	0.271	0.275	0.255	0.229	0.207	0.163	0.142
119	1.927	0.100	0.041	0.053	0.068	0.073	0.087	0.089	0.075	0.071	0.065	0.049	0.040
120	2.213	0.010	0.004	0.006	0.007	0.010	0.011	0.012	0.010	0.008	0.006	0.004	0.003
121	0.591	0.338	0.109	0.139	0.167	0.185	0.210	0.212	0.200	0.179	0.162	0.104	0.103
122	0.603	0.330	0.095	0.127	0.161	0.169	0.197	0.202	0.195	0.172	0.152	0.121	0.097
123	0.603	0.318	0.092	0.119	0.153	0.177	0.193	0.199	0.194	0.167	0.144	0.100	0.091
124	0.615	0.299	0.086	0.111	0.143	0.159	0.182	0.188	0.181	0.152	0.136	0.100	0.086
125	0.646	0.253	0.067	0.095	0.125	0.137	0.153	0.158	0.147	0.125	0.108	0.090	0.053
126	0.793	0.178	0.072	0.089	0.103	0.112	0.124	0.132	0.124	0.110	0.096	0.075	0.069
127	0.836	0.047	0.018	0.023	0.032	0.033	0.041	0.042	0.040	0.033	0.032	0.022	0.018
128	1.018	0.001	0.001	0.002	0.003	0.004	0.004	0.005	0.004	0.003	0.003	0.002	0.001
129	5.031	3.097	1.282	1.541	1.819	1.982	2.071	2.097	2.029	1.886	1.707	1.413	1.071
130	4.992	3.046	1.166	1.437	1.646	1.826	2.002	2.041	2.017	1.832	1.686	1.474	1.135
131	5.085	2.980	1.136	1.475	1.627	1.766	1.955	2.013	1.982	1.831	1.698	1.480	1.382
132	5.245	2.781	1.094	1.321	1.510	1.670	1.863	1.892	1.871	1.726	1.647	1.418	1.156

Seq.	VP₁₁	VP₁₂	VP₁₃	VP₁₄	VP₁₅	VP_{CLb}	VP₁₆	VP₁₇	VP₁₈	VP₁₉	VP₂₀	VP_{avg.}	TP
89	0.169	0.173	0.214	0.240	0.260	0.262	0.243	0.210	0.195	0.149	0.140	0.201	0.430
90	0.163	0.171	0.211	0.230	0.253	0.256	0.248	0.209	0.183	0.165	0.161	0.197	0.446
91	0.164	0.167	0.207	0.217	0.245	0.248	0.243	0.206	0.182	0.161	0.153	0.192	0.451
92	0.153	0.162	0.198	0.215	0.237	0.238	0.226	0.205	0.173	0.153	0.147	0.184	0.471
93	0.130	0.141	0.177	0.191	0.204	0.208	0.199	0.172	0.169	0.140	0.134	0.161	0.525
94	0.080	0.090	0.110	0.118	0.128	0.129	0.122	0.107	0.093	0.088	0.074	0.098	0.695
95	0.033	0.037	0.044	0.047	0.051	0.053	0.050	0.044	0.038	0.035	0.031	0.040	0.836
96	0.003	0.004	0.005	0.005	0.006	0.007	0.006	0.005	0.004	0.004	0.003	0.004	1.054
97	1.456	1.499	1.804	1.917	2.065	2.080	2.067	1.831	1.751	1.566	1.382	1.696	3.214
98	1.414	1.466	1.675	1.823	1.981	1.995	1.978	1.820	1.631	1.469	1.372	1.620	3.340
99	1.352	1.373	1.672	1.805	1.905	1.922	1.916	1.662	1.573	1.474	1.204	1.571	3.469
100	1.263	1.319	1.572	1.704	1.823	1.842	1.807	1.719	1.534	1.358	1.188	1.498	3.633
101	1.078	1.093	1.316	1.407	1.518	1.525	1.486	1.412	1.296	1.110	0.986	1.248	4.229
102	0.645	0.660	0.779	0.853	0.927	0.931	0.903	0.864	0.735	0.636	0.614	0.750	5.107
103	0.185	0.198	0.240	0.268	0.285	0.289	0.283	0.253	0.240	0.181	0.177	0.226	5.990
104	0.014	0.015	0.016	0.017	0.018	0.019	0.018	0.017	0.016	0.015	0.014	0.015	6.629
105	0.652	0.704	0.819	0.890	0.949	0.976	0.931	0.845	0.829	0.717	0.649	0.779	1.553
106	0.648	0.633	0.770	0.855	0.917	0.935	0.883	0.810	0.791	0.641	0.621	0.742	1.615
107	0.625	0.639	0.758	0.833	0.901	0.917	0.880	0.802	0.748	0.630	0.619	0.728	1.658
108	0.570	0.596	0.699	0.771	0.837	0.858	0.823	0.743	0.691	0.591	0.561	0.681	1.758
109	0.474	0.497	0.566	0.658	0.729	0.738	0.728	0.678	0.615	0.542	0.491	0.587	1.994
110	0.285	0.305	0.374	0.406	0.440	0.451	0.424	0.387	0.362	0.311	0.271	0.348	2.592
111	0.084	0.090	0.114	0.134	0.147	0.156	0.142	0.123	0.117	0.092	0.086	0.111	3.324
112	0.012	0.014	0.016	0.017	0.018	0.019	0.017	0.016	0.014	0.012	0.011	0.014	3.904
113	0.337	0.355	0.436	0.463	0.510	0.517	0.507	0.455	0.402	0.305	0.296	0.411	0.823
114	0.331	0.352	0.421	0.456	0.507	0.515	0.500	0.439	0.389	0.303	0.293	0.400	0.921
115	0.315	0.326	0.341	0.463	0.504	0.512	0.492	0.424	0.385	0.301	0.291	0.389	0.940
116	0.326	0.336	0.414	0.452	0.495	0.501	0.476	0.416	0.376	0.293	0.284	0.383	0.992
117	0.277	0.284	0.341	0.374	0.420	0.425	0.417	0.375	0.341	0.291	0.272	0.330	1.075
118	0.171	0.174	0.203	0.233	0.266	0.271	0.261	0.229	0.202	0.169	0.155	0.205	1.452
119	0.047	0.052	0.066	0.072	0.084	0.086	0.086	0.067	0.053	0.049	0.044	0.061	1.866
120	0.006	0.007	0.008	0.011	0.012	0.013	0.011	0.009	0.008	0.007	0.005	0.007	2.206
121	0.119	0.123	0.164	0.190	0.210	0.212	0.193	0.160	0.145	0.099	0.090	0.150	0.441
122	0.113	0.121	0.161	0.180	0.203	0.206	0.198	0.159	0.133	0.115	0.111	0.147	0.456
123	0.114	0.117	0.157	0.167	0.195	0.198	0.193	0.156	0.132	0.111	0.103	0.142	0.461
124	0.103	0.112	0.148	0.165	0.187	0.188	0.176	0.155	0.123	0.103	0.097	0.133	0.482
125	0.080	0.091	0.127	0.141	0.154	0.158	0.149	0.122	0.119	0.090	0.084	0.111	0.535
126	0.080	0.090	0.110	0.118	0.128	0.129	0.122	0.107	0.093	0.088	0.074	0.098	0.695
127	0.023	0.027	0.034	0.037	0.041	0.043	0.040	0.034	0.028	0.025	0.021	0.030	0.806
128	0.002	0.003	0.004	0.004	0.005	0.006	0.005	0.004	0.003	0.003	0.002	0.003	1.015
129	1.505	1.790	1.950	2.025	2.098	2.121	2.101	2.028	1.974	1.854	1.594	1.773	3.258
130	1.416	1.444	1.732	1.934	2.060	2.060	2.043	1.842	1.702	1.645	1.422	1.661	3.331
131	1.396	1.546	1.708	1.907	2.002	2.005	1.924	1.757	1.634	1.612	1.389	1.652	3.433
132	1.322	1.475	1.606	1.805	1.872	1.896	1.817	1.665	1.536	1.521	1.322	1.552	3.693

Seq.	X_{w/o}	X_{end}	X_{damper}	Log(X_{damper})	V_{avg.}	Re	Pipe Factor
89	2.1447	2.145	0.0000		1792.71	240550.22	0.875
90	2.1447	2.256	0.0985	-1.006	1778.50	238642.73	0.882
91	2.1447	2.347	0.1882	-0.725	1754.14	235374.12	0.879
92	2.1447	2.564	0.4036	-0.394	1715.56	230197.75	0.879
93	2.1447	3.249	1.0813	0.034	1608.14	215783.56	0.881
94	2.1447	7.068	4.8764	0.688	1254.73	168361.73	0.868
95	2.1447	21.042	18.8084	1.274	797.83	107055.08	0.870
96	2.1447	262.550	260.2180	2.415	253.57	34024.38	0.786
97	1.8945	1.895	0.0000		4967.49	666547.65	0.902
98	1.8945	2.061	0.1536	-0.814	4854.99	651452.11	0.902
99	1.8945	2.209	0.2999	-0.523	4779.89	641375.29	0.902
100	1.8945	2.425	0.5140	-0.289	4668.06	626370.30	0.900
101	1.8945	3.390	1.4700	0.167	4259.98	571613.15	0.904
102	1.8945	6.805	4.8599	0.687	3304.04	443342.54	0.895
103	1.8945	26.505	24.5048	1.389	1813.16	243293.36	0.880
104	1.8945	441.066	438.9526	2.642	467.58	62740.86	0.857
105	1.9927	1.993	0.0000		3368.49	451990.72	0.894
106	1.9927	2.176	0.1685	-0.773	3287.08	441067.20	0.889
107	1.9927	2.277	0.2684	-0.571	3255.97	436892.66	0.890
108	1.9927	2.582	0.5694	-0.245	3148.97	422535.43	0.893
109	1.9927	3.397	1.3773	0.139	2923.68	392306.13	0.889
110	1.9927	7.455	5.4107	0.733	2250.14	301928.13	0.881
111	1.9927	29.811	27.7141	1.443	1274.12	170963.96	0.847
112	1.9927	279.553	277.3675	2.443	450.95	60508.99	0.881
113	2.0049	2.005	0.0000		2450.42	328802.03	0.881
114	2.0049	2.301	0.2841	-0.547	2418.93	324576.49	0.879
115	2.0049	2.414	0.3961	-0.402	2385.64	320109.50	0.872
116	2.0049	2.589	0.5699	-0.244	2366.80	317581.98	0.874
117	2.0049	3.259	1.2323	0.091	2196.32	294706.16	0.885
118	2.0049	7.081	5.0320	0.702	1731.46	232331.03	0.867
119	2.0049	30.476	28.3707	1.453	946.12	126951.74	0.836
120	2.0049	297.267	295.0711	2.470	329.37	44195.41	0.771
121	2.9402	2.940	0.0000		1480.17	198612.83	0.841
122	2.9402	3.103	0.1358	-0.867	1465.13	196594.06	0.849
123	2.9402	3.261	0.2917	-0.535	1437.76	192921.53	0.844
124	2.9402	3.618	0.6456	-0.190	1394.76	187151.58	0.842
125	2.9402	4.832	1.8506	0.267	1272.04	170684.97	0.837
126	2.9402	7.068	4.0809	0.611	1198.24	160781.93	0.868
127	2.9402	27.228	24.1861	1.384	657.72	88253.75	0.835
128	2.9402	340.691	337.5514	2.528	208.61	27991.74	0.737
129	1.8372	1.837	0.0000		5015.50	534229.31	0.917
130	1.8372	2.005	0.1557	-0.808	4854.82	517114.57	0.900
131	1.8372	2.078	0.2289	-0.640	4841.02	515644.87	0.907
132	1.8372	2.379	0.5271	-0.278	4692.31	499804.55	0.905

Seq.	Year	Month	Date	Time	T _{act}	P _{bar}	I	D	V _{P_{CLopen}}	Orient	Edge	I/D
133	2005	11	25	11.00	10	30.00	1.2	3.85	2.103	0	Con	0.312
134	2005	11	25	11.00	10	30.00	1.8	3.85	2.103	0	Con	0.468
135	2005	11	25	11.00	10	30.00	2.5	3.85	2.103	0	Con	0.649
136	2005	11	25	11.00	10	30.00	3.2	3.85	2.103	0	Con	0.831
137	2005	11	24	15.50	19	29.78	0	3.85	1.010	0	Con	0.000
138	2005	11	24	15.50	19	29.78	0.5	3.85	1.010	0	Con	0.130
139	2005	11	24	15.50	19	29.78	0.7	3.85	1.010	0	Con	0.182
140	2005	11	24	15.50	19	29.78	0.9	3.85	1.010	0	Con	0.234
141	2005	11	24	15.50	19	29.78	1.2	3.85	1.010	0	Con	0.312
142	2005	11	24	15.50	19	29.78	1.8	3.85	1.010	0	Con	0.468
143	2005	11	24	15.50	19	29.78	2.5	3.85	1.010	0	Con	0.649
144	2005	11	24	15.50	19	29.78	3.2	3.85	1.010	0	Con	0.831
145	2005	11	24	14.25	19	29.78	0	3.85	0.510	0	Con	0.000
146	2005	11	24	14.25	19	29.78	0.5	3.85	0.510	0	Con	0.130
147	2005	11	24	14.25	19	29.78	0.7	3.85	0.510	0	Con	0.182
148	2005	11	24	14.25	19	29.78	0.9	3.85	0.510	0	Con	0.234
149	2005	11	24	14.25	19	29.78	1.2	3.85	0.510	0	Con	0.312
150	2005	11	24	14.25	19	29.78	1.8	3.85	0.510	0	Con	0.468
151	2005	11	24	14.25	19	29.78	2.5	3.85	0.510	0	Con	0.649
152	2005	11	24	14.25	19	29.78	3.2	3.85	0.510	0	Con	0.831
153	2005	11	25	12.25	13	30.00	0	3.85	0.255	0	Con	0.000
154	2005	11	25	12.25	13	30.00	0.5	3.85	0.255	0	Con	0.130
155	2005	11	25	12.25	13	30.00	0.7	3.85	0.255	0	Con	0.182
156	2005	11	25	12.25	13	30.00	0.9	3.85	0.255	0	Con	0.234
157	2005	11	25	12.25	13	30.00	1.2	3.85	0.255	0	Con	0.312
158	2005	11	25	12.25	13	30.00	1.8	3.85	0.255	0	Con	0.468
159	2005	11	25	12.25	13	30.00	2.5	3.85	0.255	0	Con	0.649
160	2005	11	25	12.25	13	30.00	3.2	3.85	0.255	0	Con	0.831
161	2005	12	30	14.50	28	30.00	0	3.85	2.103	1	Con	0.000
162	2005	12	30	14.50	28	30.00	0.5	3.85	2.103	1	Con	0.130
163	2005	12	30	14.50	28	30.00	0.7	3.85	2.103	1	Con	0.182
164	2005	12	30	14.50	28	30.00	0.9	3.85	2.103	1	Con	0.234
165	2005	12	30	14.50	28	30.00	1.2	3.85	2.103	1	Con	0.312
166	2005	12	30	14.50	28	30.00	1.8	3.85	2.103	1	Con	0.468
167	2005	12	30	14.50	28	30.00	2.5	3.85	2.103	1	Con	0.649
168	2005	12	30	14.50	28	30.00	3.2	3.85	2.103	1	Con	0.831
169	2005	12	30	15.50	25	29.78	0	3.85	1.010	1	Con	0.000
170	2005	12	30	15.50	25	29.78	0.5	3.85	1.010	1	Con	0.130
171	2005	12	30	15.50	25	29.78	0.7	3.85	1.010	1	Con	0.182
172	2005	12	30	15.50	25	29.78	0.9	3.85	1.010	1	Con	0.234
173	2005	12	30	15.50	25	29.78	1.2	3.85	1.010	1	Con	0.312
174	2005	12	30	15.50	25	29.78	1.8	3.85	1.010	1	Con	0.468
175	2005	12	30	15.50	25	29.78	2.5	3.85	1.010	1	Con	0.649
176	2005	12	30	15.50	25	29.78	3.2	3.85	1.010	1	Con	0.831
177	2005	12	30	14.25	25	29.78	0	3.85	0.510	1	Con	0.000

Seq.	SP_{end}	SP_{Hood}	VP₁	VP₂	VP₃	VP₄	VP₅	VP_{CLa}	VP₆	VP₇	VP₈	VP₉	VP₁₀
133	5.212	2.428	0.931	1.152	1.375	1.479	1.603	1.648	1.624	1.487	1.329	1.139	0.855
134	5.560	1.408	0.548	0.613	0.809	0.866	0.965	0.983	0.939	0.863	0.773	0.662	0.524
135	5.860	0.357	0.130	0.167	0.200	0.244	0.260	0.261	0.252	0.235	0.215	0.166	0.134
136	6.674	0.066	0.022	0.023	0.038	0.040	0.043	0.049	0.045	0.039	0.038	0.035	0.022
137	2.243	1.376	0.675	0.805	0.841	0.934	0.959	1.007	0.978	0.902	0.826	0.726	0.684
138	2.270	1.346	0.616	0.722	0.797	0.847	0.907	0.940	0.919	0.811	0.764	0.624	0.631
139	2.292	1.301	0.602	0.735	0.798	0.846	0.905	0.910	0.898	0.803	0.746	0.604	0.608
140	2.345	1.221	0.575	0.685	0.742	0.811	0.858	0.870	0.848	0.761	0.704	0.566	0.561
141	2.498	1.058	0.492	0.623	0.680	0.696	0.748	0.762	0.737	0.661	0.593	0.481	0.482
142	2.782	0.718	0.329	0.402	0.435	0.468	0.500	0.513	0.486	0.443	0.397	0.330	0.334
143	3.261	0.299	0.115	0.152	0.176	0.197	0.211	0.221	0.210	0.185	0.165	0.138	0.100
144	3.644	0.034	0.020	0.026	0.026	0.030	0.031	0.033	0.029	0.026	0.021	0.020	0.019
145	1.104	0.591	0.342	0.379	0.407	0.456	0.462	0.503	0.477	0.467	0.444	0.368	0.338
146	1.122	0.566	0.310	0.348	0.368	0.377	0.398	0.425	0.416	0.411	0.372	0.341	0.300
147	1.165	0.531	0.292	0.341	0.354	0.365	0.386	0.411	0.411	0.391	0.366	0.333	0.297
148	1.220	0.475	0.279	0.291	0.343	0.404	0.409	0.415	0.410	0.382	0.351	0.295	0.287
149	1.266	0.427	0.227	0.285	0.326	0.331	0.346	0.359	0.341	0.319	0.303	0.277	0.223
150	1.459	0.249	0.149	0.169	0.194	0.203	0.208	0.225	0.212	0.201	0.190	0.173	0.155
151	1.745	0.054	0.028	0.031	0.038	0.042	0.045	0.047	0.046	0.044	0.041	0.038	0.029
152	1.864	0.008	0.006	0.008	0.009	0.009	0.010	0.013	0.009	0.008	0.007	0.006	0.005
153	0.618	0.287	0.118	0.142	0.193	0.211	0.231	0.264	0.229	0.209	0.190	0.153	0.125
154	0.616	0.299	0.112	0.125	0.190	0.195	0.216	0.235	0.217	0.199	0.177	0.140	0.113
155	0.595	0.283	0.104	0.119	0.180	0.189	0.198	0.215	0.192	0.188	0.173	0.121	0.101
156	0.609	0.269	0.091	0.101	0.167	0.177	0.185	0.206	0.179	0.175	0.162	0.101	0.099
157	0.696	0.225	0.090	0.098	0.148	0.168	0.181	0.193	0.167	0.160	0.153	0.097	0.083
158	0.788	0.143	0.061	0.075	0.087	0.094	0.112	0.124	0.109	0.093	0.080	0.077	0.047
159	1.001	0.008	0.024	0.032	0.035	0.042	0.049	0.050	0.040	0.035	0.029	0.020	0.025
160	1.008	0.002	0.006	0.007	0.009	0.011	0.013	0.014	0.008	0.005	0.004	0.003	0.002
161	4.981	3.047	1.252	1.511	1.789	1.952	2.041	2.067	1.999	1.856	1.677	1.383	1.041
162	4.942	2.996	1.136	1.407	1.616	1.796	1.972	2.011	1.987	1.802	1.656	1.444	1.105
163	5.035	2.930	1.106	1.445	1.597	1.736	1.925	1.983	1.952	1.801	1.668	1.450	1.352
164	5.195	2.731	1.064	1.291	1.480	1.640	1.833	1.862	1.841	1.696	1.617	1.388	1.126
165	5.162	2.378	0.901	1.122	1.345	1.449	1.573	1.618	1.594	1.457	1.299	1.109	0.825
166	5.510	1.358	0.518	0.583	0.779	0.836	0.935	0.953	0.909	0.833	0.743	0.632	0.494
167	5.810	0.307	0.100	0.137	0.170	0.214	0.230	0.231	0.222	0.205	0.185	0.136	0.104
168	6.624	0.016	0.019	0.020	0.035	0.037	0.040	0.046	0.042	0.036	0.035	0.032	0.019
169	2.213	1.346	0.635	0.765	0.801	0.894	0.919	0.967	0.938	0.862	0.786	0.686	0.644
170	2.240	1.316	0.576	0.682	0.757	0.807	0.867	0.900	0.879	0.771	0.724	0.584	0.591
171	2.262	1.271	0.562	0.695	0.758	0.806	0.865	0.870	0.858	0.763	0.706	0.564	0.568
172	2.315	1.191	0.535	0.645	0.702	0.771	0.818	0.830	0.808	0.721	0.664	0.526	0.521
173	2.468	1.028	0.452	0.583	0.640	0.656	0.708	0.722	0.697	0.621	0.553	0.441	0.442
174	2.752	0.688	0.289	0.362	0.395	0.428	0.460	0.473	0.446	0.403	0.357	0.290	0.294
175	3.231	0.269	0.075	0.112	0.136	0.157	0.171	0.181	0.170	0.145	0.125	0.098	0.060
176	3.614	0.014	0.016	0.022	0.022	0.026	0.027	0.029	0.025	0.022	0.017	0.016	0.015
177	1.084	0.571	0.332	0.369	0.397	0.446	0.452	0.493	0.467	0.457	0.434	0.358	0.328

Seq.	VP₁₁	VP₁₂	VP₁₃	VP₁₄	VP₁₅	VP_{CLb}	VP₁₆	VP₁₇	VP₁₈	VP₁₉	VP₂₀	VP_{avg.}	TP
133	1.139	1.219	1.445	1.585	1.601	1.647	1.560	1.458	1.385	1.170	0.765	1.302	3.910
134	0.673	0.702	0.833	0.885	0.959	0.966	0.939	0.838	0.748	0.596	0.559	0.758	4.802
135	0.161	0.176	0.219	0.243	0.261	0.263	0.253	0.222	0.203	0.162	0.120	0.198	5.662
136	0.027	0.031	0.036	0.043	0.048	0.047	0.043	0.040	0.035	0.028	0.026	0.035	6.639
137	0.664	0.746	0.843	0.889	0.982	1.004	0.973	0.844	0.776	0.742	0.703	0.821	1.422
138	0.639	0.688	0.852	0.871	0.947	0.960	0.914	0.835	0.753	0.729	0.651	0.772	1.498
139	0.642	0.681	0.798	0.842	0.897	0.906	0.875	0.794	0.709	0.703	0.641	0.753	1.539
140	0.614	0.635	0.650	0.818	0.842	0.866	0.831	0.723	0.661	0.658	0.608	0.704	1.641
141	0.504	0.574	0.664	0.715	0.751	0.762	0.724	0.672	0.668	0.614	0.517	0.626	1.872
142	0.343	0.387	0.461	0.482	0.502	0.510	0.497	0.473	0.431	0.430	0.368	0.423	2.359
143	0.139	0.153	0.187	0.199	0.216	0.219	0.206	0.177	0.171	0.167	0.136	0.168	3.093
144	0.019	0.023	0.027	0.031	0.033	0.034	0.031	0.030	0.026	0.019	0.015	0.025	3.619
145	0.307	0.392	0.403	0.436	0.486	0.509	0.492	0.445	0.410	0.342	0.331	0.407	0.697
146	0.306	0.333	0.391	0.437	0.471	0.484	0.467	0.432	0.388	0.341	0.313	0.374	0.748
147	0.301	0.341	0.382	0.401	0.412	0.419	0.410	0.399	0.371	0.340	0.307	0.359	0.806
148	0.295	0.329	0.350	0.373	0.380	0.416	0.391	0.384	0.346	0.321	0.267	0.343	0.877
149	0.231	0.288	0.322	0.347	0.355	0.368	0.349	0.329	0.311	0.282	0.235	0.300	0.966
150	0.155	0.181	0.201	0.209	0.219	0.224	0.210	0.204	0.195	0.186	0.150	0.188	1.271
151	0.031	0.036	0.046	0.049	0.051	0.052	0.047	0.044	0.041	0.039	0.029	0.039	1.706
152	0.004	0.007	0.008	0.009	0.011	0.013	0.010	0.009	0.007	0.006	0.005	0.008	1.856
153	0.130	0.153	0.214	0.223	0.249	0.260	0.241	0.234	0.224	0.168	0.110	0.185	0.433
154	0.124	0.136	0.211	0.215	0.246	0.258	0.238	0.227	0.207	0.149	0.104	0.174	0.442
155	0.115	0.129	0.200	0.202	0.227	0.247	0.234	0.213	0.191	0.141	0.103	0.163	0.432
156	0.102	0.111	0.187	0.188	0.214	0.243	0.219	0.186	0.181	0.132	0.090	0.149	0.460
157	0.102	0.109	0.169	0.180	0.211	0.222	0.195	0.172	0.165	0.115	0.082	0.139	0.557
158	0.073	0.086	0.108	0.110	0.120	0.130	0.118	0.114	0.111	0.075	0.053	0.089	0.699
159	0.036	0.043	0.045	0.049	0.049	0.052	0.038	0.035	0.031	0.024	0.023	0.035	0.966
160	0.007	0.008	0.008	0.010	0.012	0.016	0.011	0.009	0.008	0.007	0.006	0.007	1.001
161	1.475	1.760	1.920	1.995	2.068	2.091	2.071	1.998	1.944	1.824	1.564	1.743	3.238
162	1.386	1.414	1.702	1.904	2.030	2.030	2.013	1.812	1.672	1.615	1.392	1.631	3.311
163	1.366	1.516	1.678	1.877	1.972	1.975	1.894	1.727	1.604	1.582	1.359	1.622	3.413
164	1.292	1.445	1.576	1.775	1.842	1.866	1.787	1.635	1.506	1.491	1.292	1.522	3.673
165	1.109	1.189	1.415	1.555	1.571	1.617	1.530	1.428	1.355	1.140	0.735	1.271	3.891
166	0.643	0.672	0.803	0.855	0.929	0.936	0.909	0.808	0.718	0.566	0.529	0.727	4.783
167	0.131	0.146	0.189	0.213	0.231	0.233	0.223	0.192	0.173	0.132	0.090	0.168	5.642
168	0.024	0.028	0.033	0.040	0.045	0.044	0.040	0.037	0.032	0.025	0.023	0.032	6.592
169	0.624	0.706	0.803	0.849	0.942	0.964	0.933	0.804	0.736	0.702	0.663	0.781	1.432
170	0.599	0.648	0.812	0.831	0.907	0.920	0.874	0.795	0.713	0.689	0.611	0.732	1.508
171	0.602	0.641	0.758	0.802	0.857	0.866	0.835	0.754	0.669	0.663	0.601	0.713	1.549
172	0.574	0.595	0.610	0.778	0.802	0.826	0.791	0.683	0.621	0.618	0.568	0.664	1.651
173	0.464	0.534	0.624	0.675	0.711	0.722	0.684	0.632	0.628	0.574	0.477	0.586	1.882
174	0.303	0.347	0.421	0.442	0.462	0.470	0.457	0.433	0.391	0.390	0.328	0.383	2.369
175	0.099	0.113	0.147	0.159	0.176	0.179	0.166	0.137	0.131	0.127	0.096	0.128	3.103
176	0.015	0.019	0.023	0.027	0.029	0.030	0.027	0.026	0.022	0.015	0.011	0.021	3.593
177	0.297	0.382	0.393	0.426	0.476	0.499	0.482	0.435	0.400	0.332	0.321	0.397	0.687

Seq.	X_{w/o}	X_{end}	X_{damper}	Log(X_{damper})	V_{avg.}	Re	Pipe Factor
133	1.8372	3.004	1.1429	0.058	4297.32	457732.14	0.889
134	1.8372	6.337	4.4501	0.648	3278.75	349238.23	0.882
135	1.8372	28.523	26.5745	1.424	1678.04	178737.41	0.870
136	1.8372	191.722	189.6989	2.278	700.91	74657.75	0.849
137	1.7312	1.731	0.0000		3458.51	368385.95	0.904
138	1.7312	1.940	0.1954	-0.709	3353.46	357196.32	0.902
139	1.7312	2.044	0.2984	-0.525	3311.48	352724.02	0.911
140	1.7312	2.330	0.5814	-0.236	3202.38	341103.23	0.901
141	1.7312	2.988	1.2331	0.091	3020.47	321727.62	0.907
142	1.7312	5.580	3.8061	0.580	2481.54	264322.38	0.909
143	1.7312	18.367	16.5501	1.219	1566.01	166804.75	0.875
144	1.7312	145.780	143.8793	2.158	601.32	64050.22	0.861
145	1.7109	1.711	0.0000		2435.45	259413.21	0.897
146	1.7109	1.998	0.2715	-0.566	2334.80	248692.86	0.908
147	1.7109	2.246	0.5174	-0.286	2286.42	243539.61	0.930
148	1.7109	2.559	0.8282	-0.082	2234.51	238010.57	0.908
149	1.7109	3.223	1.4863	0.172	2089.46	222560.55	0.908
150	1.7109	6.780	5.0200	0.701	1652.71	176039.69	0.914
151	1.7109	43.250	41.4190	1.617	757.86	80724.50	0.893
152	1.7109	246.519	244.6185	2.388	331.18	35276.27	0.761
153	2.3495	2.350	0.0000		1623.00	172875.07	0.839
154	2.3495	2.542	0.1732	-0.761	1575.80	167847.25	0.840
155	2.3495	2.650	0.2786	-0.555	1525.50	162490.11	0.841
156	2.3495	3.083	0.7068	-0.151	1459.30	155438.28	0.816
157	2.3495	3.997	1.6173	0.209	1410.21	150209.72	0.820
158	2.3495	7.880	5.4796	0.739	1125.54	119887.49	0.836
159	2.3495	27.930	25.4858	1.406	702.84	74863.26	0.824
160	2.3495	135.258	132.7467	2.123	324.99	34616.04	0.703
161	1.8578	1.858	0.0000		5066.86	539700.31	0.916
162	1.8578	2.030	0.1593	-0.798	4901.71	522108.50	0.899
163	1.8578	2.105	0.2338	-0.631	4887.61	520607.40	0.905
164	1.8578	2.414	0.5398	-0.268	4734.60	504309.05	0.904
165	1.8578	3.060	1.1775	0.071	4327.49	460945.37	0.887
166	1.8578	6.574	4.6645	0.669	3273.47	348676.01	0.878
167	1.8578	33.590	31.6136	1.500	1572.92	167540.84	0.851
168	1.8578	208.743	206.6960	2.315	682.04	72648.13	0.838
169	1.8333	1.833	0.0000		3393.92	361505.97	0.899
170	1.8333	2.060	0.2112	-0.675	3285.37	349942.98	0.897
171	1.8333	2.174	0.3233	-0.490	3241.98	345321.68	0.906
172	1.8333	2.487	0.6329	-0.199	3129.01	333288.78	0.895
173	1.8333	3.211	1.3504	0.130	2940.08	313164.20	0.901
174	1.8333	6.193	4.3127	0.635	2375.27	253003.17	0.901
175	1.8333	24.281	22.3497	1.349	1372.85	146230.33	0.843
176	1.8333	173.007	170.9969	2.233	553.43	58949.28	0.839
177	1.7291	1.729	0.0000		2420.22	257791.63	0.895

Seq.	Year	Month	Date	Time	T _{act}	P _{bar}	I	D	V _{P_{CLopen}}	Orient	Edge	I/D
178	2005	12	30	14.25	25	29.78	0.5	3.85	0.510	1	Con	0.130
179	2005	12	30	14.25	25	29.78	0.7	3.85	0.510	1	Con	0.182
180	2005	12	30	14.25	25	29.78	0.9	3.85	0.510	1	Con	0.234
181	2005	12	30	14.25	25	29.78	1.2	3.85	0.510	1	Con	0.312
182	2005	12	30	14.25	25	29.78	1.8	3.85	0.510	1	Con	0.468
183	2005	12	30	14.25	25	29.78	2.5	3.85	0.510	1	Con	0.649
184	2005	12	30	14.25	25	29.78	3.2	3.85	0.510	1	Con	0.831
185	2005	11	25	14.00	18	30.00	0	3.85	0.255	1	Con	0.000
186	2005	11	25	14.00	18	30.00	0.5	3.85	0.255	1	Con	0.130
187	2005	11	25	14.00	18	30.00	0.7	3.85	0.255	1	Con	0.182
188	2005	11	25	14.00	18	30.00	0.9	3.85	0.255	1	Con	0.234
189	2005	11	25	14.00	18	30.00	1.2	3.85	0.255	1	Con	0.312
190	2005	11	25	14.00	18	30.00	1.8	3.85	0.255	1	Con	0.468
191	2005	11	25	14.00	18	30.00	2.5	3.85	0.255	1	Con	0.649
192	2005	11	25	14.00	18	30.00	3.2	3.85	0.255	1	Con	0.831
193	2005	12	10	14.00	27	29.80	0	3.85	2.103	0	Strt.	0.000
194	2005	12	10	14.00	27	29.80	0.5	3.85	2.103	0	Strt.	0.130
195	2005	12	10	14.00	27	29.80	0.7	3.85	2.103	0	Strt.	0.182
196	2005	12	10	14.00	27	29.80	0.9	3.85	2.103	0	Strt.	0.234
197	2005	12	10	14.00	27	29.80	1.2	3.85	2.103	0	Strt.	0.312
198	2005	12	10	14.00	27	29.80	1.8	3.85	2.103	0	Strt.	0.468
199	2005	12	10	14.00	27	29.80	2.5	3.85	2.103	0	Strt.	0.649
200	2005	12	10	14.00	27	29.80	3.2	3.85	2.103	0	Strt.	0.831
201	2005	12	10	15.25	26	29.80	0	3.85	1.010	0	Strt.	0.000
202	2005	12	10	15.25	26	29.80	0.5	3.85	1.010	0	Strt.	0.130
203	2005	12	10	15.25	26	29.80	0.7	3.85	1.010	0	Strt.	0.182
204	2005	12	10	15.25	26	29.80	0.9	3.85	1.010	0	Strt.	0.234
205	2005	12	10	15.25	26	29.80	1.2	3.85	1.010	0	Strt.	0.312
206	2005	12	10	15.25	26	29.80	1.8	3.85	1.010	0	Strt.	0.468
207	2005	12	10	15.25	26	29.80	2.5	3.85	1.010	0	Strt.	0.649
208	2005	12	10	15.25	26	29.80	3.2	3.85	1.010	0	Strt.	0.831
209	2005	12	10	17.00	26	29.78	0	3.85	0.510	0	Strt.	0.000
210	2005	12	10	17.00	26	29.78	0.5	3.85	0.510	0	Strt.	0.130
211	2005	12	10	17.00	26	29.78	0.7	3.85	0.510	0	Strt.	0.182
212	2005	12	10	17.00	26	29.78	0.9	3.85	0.510	0	Strt.	0.234
213	2005	12	10	17.00	26	29.78	1.2	3.85	0.510	0	Strt.	0.312
214	2005	12	10	17.00	26	29.78	1.8	3.85	0.510	0	Strt.	0.468
215	2005	12	10	17.00	26	29.78	2.5	3.85	0.510	0	Strt.	0.649
216	2005	12	10	17.00	26	29.78	3.2	3.85	0.510	0	Strt.	0.831
217	2005	12	10	18.50	24	29.78	0	3.85	0.255	0	Strt.	0.000
218	2005	12	10	18.50	24	29.78	0.5	3.85	0.255	0	Strt.	0.130
219	2005	12	10	18.50	24	29.78	0.7	3.85	0.255	0	Strt.	0.182
220	2005	12	10	18.50	24	29.78	0.9	3.85	0.255	0	Strt.	0.234
221	2005	12	10	18.50	24	29.78	1.2	3.85	0.255	0	Strt.	0.312
222	2005	12	10	18.50	24	29.78	1.8	3.85	0.255	0	Strt.	0.468

Seq.	SP_{end}	SP_{Hood}	VP₁	VP₂	VP₃	VP₄	VP₅	VP_{CLa}	VP₆	VP₇	VP₈	VP₉	VP₁₀
178	1.102	0.546	0.300	0.338	0.358	0.367	0.388	0.415	0.406	0.401	0.362	0.331	0.290
179	1.145	0.511	0.282	0.331	0.344	0.355	0.376	0.401	0.401	0.381	0.356	0.323	0.287
180	1.200	0.455	0.269	0.281	0.333	0.394	0.399	0.405	0.400	0.372	0.341	0.285	0.277
181	1.246	0.407	0.217	0.275	0.316	0.321	0.336	0.349	0.331	0.309	0.293	0.267	0.213
182	1.439	0.229	0.139	0.159	0.184	0.193	0.198	0.215	0.202	0.191	0.180	0.163	0.145
183	1.725	0.034	0.018	0.021	0.028	0.032	0.035	0.037	0.036	0.034	0.031	0.028	0.019
184	1.844	0.006	0.005	0.007	0.008	0.008	0.009	0.012	0.008	0.007	0.006	0.005	0.004
185	0.580	0.302	0.116	0.140	0.191	0.209	0.229	0.262	0.230	0.210	0.191	0.154	0.126
186	0.590	0.294	0.110	0.123	0.188	0.193	0.214	0.233	0.218	0.200	0.178	0.141	0.114
187	0.598	0.286	0.105	0.120	0.181	0.190	0.199	0.216	0.191	0.187	0.172	0.120	0.100
188	0.612	0.272	0.092	0.102	0.168	0.178	0.186	0.207	0.178	0.174	0.161	0.100	0.098
189	0.640	0.242	0.088	0.096	0.146	0.166	0.179	0.191	0.168	0.161	0.154	0.098	0.084
190	0.756	0.133	0.059	0.073	0.085	0.092	0.110	0.122	0.110	0.094	0.081	0.078	0.048
191	0.878	0.054	0.022	0.030	0.033	0.040	0.047	0.048	0.041	0.036	0.030	0.021	0.026
192	0.969	0.012	0.004	0.005	0.007	0.009	0.011	0.012	0.009	0.006	0.005	0.004	0.003
193	4.545	2.442	1.285	1.527	1.723	1.898	2.090	2.107	2.075	1.925	1.725	1.555	1.273
194	4.992	3.046	1.166	1.437	1.646	1.826	2.002	2.041	2.017	1.832	1.686	1.474	1.135
195	4.712	2.299	1.172	1.355	1.520	1.602	1.880	1.980	1.865	1.721	1.555	1.349	1.160
196	4.848	2.152	1.118	1.298	1.494	1.545	1.845	1.883	1.830	1.691	1.485	1.278	1.106
197	5.049	1.921	1.067	1.199	1.355	1.459	1.512	1.625	1.555	1.492	1.329	1.187	1.055
198	5.829	0.968	0.540	0.685	0.703	0.785	0.840	0.874	0.825	0.788	0.715	0.699	0.528
199	6.345	0.317	0.150	0.188	0.202	0.242	0.268	0.295	0.253	0.249	0.212	0.192	0.138
200	6.765	0.032	0.024	0.026	0.029	0.030	0.032	0.038	0.034	0.032	0.029	0.028	0.027
201	2.243	1.376	0.675	0.805	0.841	0.934	0.959	1.007	0.978	0.902	0.826	0.726	0.684
202	2.270	1.346	0.616	0.722	0.797	0.847	0.907	0.940	0.919	0.811	0.764	0.624	0.631
203	2.292	1.301	0.602	0.735	0.798	0.846	0.905	0.910	0.898	0.803	0.746	0.604	0.608
204	2.345	1.221	0.575	0.685	0.742	0.811	0.858	0.870	0.848	0.761	0.704	0.566	0.561
205	2.498	1.058	0.492	0.623	0.680	0.696	0.748	0.762	0.737	0.661	0.593	0.481	0.482
206	2.782	0.718	0.329	0.402	0.435	0.468	0.500	0.513	0.486	0.443	0.397	0.330	0.334
207	4.633	0.234	0.094	0.099	0.101	0.115	0.126	0.146	0.134	0.125	0.114	0.098	0.095
208	5.404	0.009	0.013	0.015	0.018	0.019	0.021	0.024	0.022	0.021	0.019	0.016	0.014
209	1.136	0.595	0.267	0.308	0.363	0.417	0.487	0.522	0.482	0.415	0.419	0.315	0.279
210	1.156	0.569	0.249	0.268	0.359	0.401	0.478	0.506	0.471	0.389	0.403	0.278	0.269
211	1.175	0.554	0.248	0.251	0.348	0.388	0.458	0.479	0.462	0.381	0.385	0.255	0.249
212	1.206	0.527	0.234	0.239	0.325	0.368	0.425	0.459	0.432	0.349	0.350	0.259	0.242
213	1.267	0.475	0.220	0.222	0.317	0.329	0.387	0.401	0.393	0.301	0.308	0.249	0.227
214	1.488	0.254	0.138	0.169	0.172	0.185	0.194	0.224	0.191	0.199	0.206	0.159	0.149
215	1.722	0.084	0.048	0.059	0.072	0.079	0.082	0.091	0.078	0.070	0.071	0.058	0.046
216	1.903	0.012	0.009	0.010	0.012	0.012	0.013	0.015	0.014	0.011	0.011	0.010	0.009
217	0.577	0.299	0.115	0.139	0.190	0.208	0.228	0.261	0.231	0.211	0.192	0.155	0.127
218	0.587	0.291	0.109	0.122	0.187	0.192	0.213	0.232	0.219	0.201	0.179	0.142	0.115
219	0.595	0.283	0.104	0.119	0.180	0.189	0.198	0.215	0.192	0.188	0.173	0.121	0.101
220	0.609	0.269	0.091	0.101	0.167	0.177	0.185	0.206	0.179	0.175	0.162	0.101	0.099
221	0.637	0.239	0.087	0.095	0.145	0.165	0.178	0.190	0.169	0.162	0.155	0.099	0.085
222	0.753	0.130	0.058	0.072	0.084	0.091	0.109	0.121	0.111	0.095	0.082	0.079	0.049

Seq.	VP₁₁	VP₁₂	VP₁₃	VP₁₄	VP₁₅	VP_{CLb}	VP₁₆	VP₁₇	VP₁₈	VP₁₉	VP₂₀	VP_{avg.}	TP
178	0.296	0.323	0.381	0.427	0.461	0.474	0.457	0.422	0.378	0.331	0.303	0.364	0.738
179	0.291	0.331	0.372	0.391	0.402	0.409	0.400	0.389	0.361	0.330	0.297	0.349	0.796
180	0.285	0.319	0.340	0.363	0.370	0.406	0.381	0.374	0.336	0.311	0.257	0.333	0.867
181	0.221	0.278	0.312	0.337	0.345	0.358	0.339	0.319	0.301	0.272	0.225	0.290	0.956
182	0.145	0.171	0.191	0.199	0.209	0.214	0.200	0.194	0.185	0.176	0.140	0.178	1.261
183	0.021	0.026	0.036	0.039	0.041	0.042	0.037	0.034	0.031	0.029	0.019	0.029	1.696
184	0.003	0.006	0.007	0.008	0.010	0.012	0.009	0.008	0.006	0.005	0.004	0.007	1.837
185	0.129	0.152	0.213	0.222	0.248	0.259	0.243	0.236	0.226	0.170	0.112	0.184	0.395
186	0.123	0.135	0.210	0.214	0.245	0.257	0.240	0.229	0.209	0.151	0.106	0.174	0.416
187	0.118	0.132	0.203	0.205	0.230	0.250	0.232	0.211	0.189	0.139	0.101	0.163	0.435
188	0.105	0.114	0.190	0.191	0.217	0.246	0.217	0.184	0.179	0.130	0.088	0.149	0.462
189	0.101	0.108	0.168	0.179	0.210	0.221	0.197	0.174	0.167	0.117	0.084	0.139	0.501
190	0.072	0.085	0.107	0.109	0.119	0.129	0.120	0.116	0.113	0.077	0.055	0.089	0.667
191	0.035	0.042	0.044	0.048	0.048	0.051	0.040	0.037	0.033	0.026	0.025	0.035	0.843
192	0.006	0.007	0.007	0.009	0.011	0.015	0.008	0.007	0.004	0.002	0.001	0.006	0.963
193	1.301	1.532	1.733	1.908	2.009	2.109	2.045	2.025	1.749	1.405	1.291	1.692	2.853
194	1.416	1.444	1.732	1.934	2.060	2.060	2.043	1.842	1.702	1.645	1.422	1.661	3.331
195	1.188	1.355	1.541	1.611	1.815	2.013	1.945	1.920	1.555	1.273	1.178	1.517	3.195
196	1.134	1.298	1.504	1.534	1.739	1.921	1.792	1.788	1.492	1.204	1.129	1.454	3.394
197	1.083	1.201	1.355	1.449	1.560	1.670	1.645	1.610	1.335	1.063	1.073	1.322	3.727
198	0.556	0.672	0.713	0.785	0.830	0.874	0.845	0.821	0.726	0.566	0.546	0.704	5.125
199	0.171	0.189	0.212	0.242	0.261	0.280	0.272	0.248	0.223	0.175	0.165	0.211	6.134
200	0.029	0.030	0.031	0.032	0.034	0.035	0.034	0.031	0.030	0.029	0.028	0.030	6.735
201	0.664	0.746	0.843	0.889	0.982	1.004	0.973	0.844	0.776	0.742	0.703	0.821	1.422
202	0.639	0.688	0.852	0.871	0.947	0.960	0.914	0.835	0.753	0.729	0.651	0.772	1.498
203	0.642	0.681	0.798	0.842	0.897	0.906	0.875	0.794	0.709	0.703	0.641	0.753	1.539
204	0.614	0.635	0.650	0.818	0.842	0.866	0.831	0.723	0.661	0.658	0.608	0.704	1.641
205	0.504	0.574	0.664	0.715	0.751	0.762	0.724	0.672	0.668	0.614	0.517	0.626	1.872
206	0.343	0.387	0.461	0.482	0.502	0.510	0.497	0.473	0.431	0.430	0.368	0.423	2.359
207	0.106	0.119	0.114	0.126	0.131	0.156	0.145	0.129	0.119	0.111	0.106	0.115	4.518
208	0.016	0.018	0.019	0.020	0.021	0.023	0.022	0.019	0.018	0.017	0.016	0.018	5.386
209	0.259	0.309	0.427	0.478	0.491	0.522	0.499	0.494	0.471	0.315	0.253	0.382	0.754
210	0.271	0.290	0.421	0.469	0.475	0.506	0.487	0.482	0.457	0.301	0.242	0.367	0.789
211	0.220	0.281	0.398	0.458	0.461	0.502	0.472	0.456	0.414	0.292	0.212	0.348	0.827
212	0.211	0.250	0.377	0.452	0.455	0.466	0.449	0.428	0.382	0.255	0.206	0.329	0.877
213	0.200	0.229	0.337	0.362	0.391	0.423	0.401	0.392	0.338	0.241	0.201	0.298	0.969
214	0.140	0.153	0.187	0.224	0.229	0.236	0.221	0.218	0.198	0.152	0.129	0.179	1.309
215	0.046	0.057	0.061	0.069	0.072	0.078	0.073	0.068	0.060	0.055	0.048	0.063	1.659
216	0.006	0.007	0.008	0.009	0.010	0.011	0.010	0.009	0.008	0.007	0.007	0.009	1.894
217	0.126	0.149	0.210	0.219	0.245	0.256	0.245	0.238	0.228	0.172	0.114	0.184	0.393
218	0.120	0.132	0.207	0.211	0.242	0.254	0.242	0.231	0.211	0.153	0.108	0.174	0.413
219	0.115	0.129	0.200	0.202	0.227	0.247	0.234	0.213	0.191	0.141	0.103	0.163	0.432
220	0.102	0.111	0.187	0.188	0.214	0.243	0.219	0.186	0.181	0.132	0.090	0.149	0.460
221	0.098	0.105	0.165	0.176	0.207	0.218	0.199	0.176	0.169	0.119	0.086	0.139	0.498
222	0.069	0.082	0.104	0.106	0.116	0.126	0.122	0.118	0.115	0.079	0.057	0.089	0.664

Seq.	X_{w/o}	X_{end}	X_{damper}	Log(X_{damper})	V_{avg.}	Re	Pipe Factor
178	1.7291	2.026	0.2797	-0.553	2317.63	246863.95	0.906
179	1.7291	2.282	0.5338	-0.273	2268.32	241611.38	0.928
180	1.7291	2.606	0.8558	-0.068	2215.27	235960.99	0.906
181	1.7291	3.301	1.5440	0.189	2066.93	220160.58	0.905
182	1.7291	7.107	5.3265	0.726	1617.91	172332.48	0.910
183	1.7291	57.836	55.9734	1.748	657.55	70039.32	0.862
184	1.7291	282.246	280.3205	2.448	309.85	33003.98	0.737
185	2.1433	2.143	0.0000		1631.49	173779.41	0.842
186	2.1433	2.392	0.2297	-0.639	1584.04	168725.35	0.843
187	2.1433	2.663	0.4973	-0.303	1534.67	163466.74	0.838
188	2.1433	3.096	0.9259	-0.033	1468.19	156385.68	0.813
189	2.1433	3.594	1.4207	0.153	1417.66	151002.58	0.823
190	2.1433	7.518	5.3233	0.726	1131.52	120524.85	0.841
191	2.1433	24.316	22.0775	1.344	707.34	75342.51	0.837
192	2.1433	163.341	161.0256	2.207	291.65	31065.57	0.662
193	1.8833	1.687	-0.1965		5205.14	554429.10	0.896
194	1.8833	2.005	0.1096	-0.960	5158.51	549461.85	0.900
195	1.8833	2.106	0.2069	-0.684	4928.97	525012.26	0.872
196	1.8833	2.334	0.4319	-0.365	4826.30	514076.87	0.874
197	1.8833	2.820	0.9134	-0.039	4601.24	490104.54	0.896
198	1.8833	7.278	5.3414	0.728	3358.31	357712.68	0.898
199	1.8833	29.118	27.1263	1.433	1836.90	195658.30	0.856
200	1.8833	225.309	223.2345	2.349	691.94	73702.22	0.905
201	1.7312	1.731	0.0000		3482.52	370943.40	0.904
202	1.7312	1.940	0.1954	-0.709	3376.74	359676.09	0.902
203	1.7312	2.044	0.2984	-0.525	3334.46	355172.74	0.911
204	1.7312	2.330	0.5814	-0.236	3224.61	343471.28	0.901
205	1.7312	2.988	1.2331	0.091	3041.44	323961.16	0.907
206	1.7312	5.580	3.8061	0.580	2498.76	266157.39	0.909
207	1.7312	39.312	37.4777	1.574	1302.78	138766.21	0.873
208	1.7312	297.428	295.5147	2.471	517.12	55081.63	0.878
209	1.9729	1.973	0.0000		2376.29	253112.61	0.856
210	1.9729	2.147	0.1577	-0.802	2329.92	248173.04	0.852
211	1.9729	2.374	0.3824	-0.417	2268.48	241629.20	0.843
212	1.9729	2.671	0.6765	-0.170	2203.31	234686.59	0.843
213	1.9729	3.252	1.2521	0.098	2098.54	223527.38	0.851
214	1.9729	7.296	5.2723	0.722	1628.05	173412.36	0.883
215	1.9729	26.288	24.2163	1.384	965.67	102858.99	0.865
216	1.9729	199.594	197.4405	2.295	374.42	39881.83	0.857
217	2.1320	2.132	0.0000		1646.58	175386.35	0.844
218	2.1320	2.380	0.2292	-0.640	1598.64	170280.23	0.846
219	2.1320	2.650	0.4961	-0.304	1548.83	164974.69	0.841
220	2.1320	3.083	0.9243	-0.034	1481.61	157815.03	0.816
221	2.1320	3.581	1.4190	0.152	1430.55	152375.94	0.826
222	2.1320	7.507	5.3238	0.726	1141.32	121568.38	0.847

Seq.	Year	Month	Date	Time	T_{act}	P_{bar}	I	D	VP_{CLopen}	Orient	Edge	I/D
223	2005	12	10	18.50	24	29.78	2.5	3.85	0.255	0	Strt.	0.649
224	2005	12	10	18.50	24	29.78	3.2	3.85	0.255	0	Strt.	0.831
225	2005	12	31	11.00	27	29.80	0	3.85	2.103	1	Strt.	0.000
226	2005	12	31	11.00	27	29.80	0.5	3.85	2.103	1	Strt.	0.130
227	2005	12	31	11.00	27	29.80	0.7	3.85	2.103	1	Strt.	0.182
228	2005	12	31	11.00	27	29.80	0.9	3.85	2.103	1	Strt.	0.234
229	2005	12	31	11.00	27	29.80	1.2	3.85	2.103	1	Strt.	0.312
230	2005	12	31	11.00	27	29.80	1.8	3.85	2.103	1	Strt.	0.468
231	2005	12	31	11.00	27	29.80	2.5	3.85	2.103	1	Strt.	0.649
232	2005	12	31	11.00	27	29.80	3.2	3.85	2.103	1	Strt.	0.831
233	2005	12	31	13.00	26	29.80	0	3.85	1.010	1	Strt.	0.000
234	2005	12	31	13.00	26	29.80	0.5	3.85	1.010	1	Strt.	0.130
235	2005	12	31	13.00	26	29.80	0.7	3.85	1.010	1	Strt.	0.182
236	2005	12	31	13.00	26	29.80	0.9	3.85	1.010	1	Strt.	0.234
237	2005	12	31	13.00	26	29.80	1.2	3.85	1.010	1	Strt.	0.312
238	2005	12	31	13.00	26	29.80	1.8	3.85	1.010	1	Strt.	0.468
239	2005	12	31	13.00	26	29.80	2.5	3.85	1.010	1	Strt.	0.649
240	2005	12	31	13.00	26	29.80	3.2	3.85	1.010	1	Strt.	0.831
241	2005	12	31	16.00	26	29.78	0	3.85	0.510	1	Strt.	0.000
242	2005	12	31	16.00	26	29.78	0.5	3.85	0.510	1	Strt.	0.130
243	2005	12	31	16.00	26	29.78	0.7	3.85	0.510	1	Strt.	0.182
244	2005	12	31	16.00	26	29.78	0.9	3.85	0.510	1	Strt.	0.234
245	2005	12	31	16.00	26	29.78	1.2	3.85	0.510	1	Strt.	0.312
246	2005	12	31	16.00	26	29.78	1.8	3.85	0.510	1	Strt.	0.468
247	2005	12	31	16.00	26	29.78	2.5	3.85	0.510	1	Strt.	0.649
248	2005	12	31	16.00	26	29.78	3.2	3.85	0.510	1	Strt.	0.831
249	2005	12	31	18.50	24	29.78	0	3.85	0.255	1	Strt.	0.000
250	2005	12	31	18.50	24	29.78	0.5	3.85	0.255	1	Strt.	0.130
251	2005	12	31	18.50	24	29.78	0.7	3.85	0.255	1	Strt.	0.182
252	2005	12	31	18.50	24	29.78	0.9	3.85	0.255	1	Strt.	0.234
253	2005	12	31	18.50	24	29.78	1.2	3.85	0.255	1	Strt.	0.312
254	2005	12	31	18.50	24	29.78	1.8	3.85	0.255	1	Strt.	0.468
255	2005	12	31	18.50	24	29.78	2.5	3.85	0.255	1	Strt.	0.649
256	2005	12	31	18.50	24	29.78	3.2	3.85	0.255	1	Strt.	0.831

Seq.	SP_{end}	SP_{Hood}	VP₁	VP₂	VP₃	VP₄	VP₅	VP_{CLa}	VP₆	VP₇	VP₈	VP₉	VP₁₀
223	0.875	0.051	0.021	0.029	0.032	0.039	0.046	0.047	0.042	0.037	0.031	0.022	0.027
224	0.966	0.009	0.003	0.004	0.006	0.008	0.010	0.011	0.010	0.007	0.006	0.005	0.004
225	4.485	2.382	1.245	1.487	1.683	1.858	2.050	2.067	2.035	1.885	1.685	1.515	1.233
226	4.932	2.986	1.126	1.397	1.606	1.786	1.962	2.001	1.977	1.792	1.646	1.434	1.095
227	4.652	2.239	1.132	1.315	1.480	1.562	1.840	1.940	1.825	1.681	1.515	1.309	1.120
228	4.788	2.092	1.078	1.258	1.454	1.505	1.805	1.843	1.790	1.651	1.445	1.238	1.066
229	4.989	1.861	1.027	1.159	1.315	1.419	1.472	1.585	1.515	1.452	1.289	1.147	1.015
230	5.769	0.908	0.500	0.645	0.663	0.745	0.800	0.834	0.785	0.748	0.675	0.659	0.488
231	6.285	0.257	0.110	0.148	0.162	0.202	0.228	0.255	0.213	0.209	0.172	0.152	0.098
232	6.705	0.026	0.020	0.022	0.025	0.026	0.028	0.034	0.030	0.028	0.025	0.024	0.023
233	2.203	1.336	0.625	0.755	0.791	0.884	0.909	0.957	0.928	0.852	0.776	0.676	0.634
234	2.230	1.306	0.566	0.672	0.747	0.797	0.857	0.890	0.869	0.761	0.714	0.574	0.581
235	2.252	1.261	0.552	0.685	0.748	0.796	0.855	0.860	0.848	0.753	0.696	0.554	0.558
236	2.305	1.181	0.525	0.635	0.692	0.761	0.808	0.820	0.798	0.711	0.654	0.516	0.511
237	2.458	1.018	0.442	0.573	0.630	0.646	0.698	0.712	0.687	0.611	0.543	0.431	0.432
238	2.742	0.678	0.279	0.352	0.385	0.418	0.450	0.463	0.436	0.393	0.347	0.280	0.284
239	4.593	0.194	0.044	0.049	0.051	0.065	0.076	0.096	0.084	0.075	0.064	0.048	0.045
240	5.364	0.005	0.008	0.010	0.013	0.014	0.016	0.019	0.017	0.016	0.014	0.011	0.009
241	1.116	0.575	0.237	0.278	0.333	0.387	0.457	0.492	0.452	0.385	0.389	0.285	0.249
242	1.136	0.549	0.219	0.238	0.329	0.371	0.448	0.476	0.441	0.359	0.373	0.248	0.239
243	1.155	0.534	0.218	0.221	0.318	0.358	0.428	0.449	0.432	0.351	0.355	0.225	0.219
244	1.186	0.507	0.204	0.209	0.295	0.338	0.395	0.429	0.402	0.319	0.320	0.229	0.212
245	1.247	0.455	0.190	0.192	0.287	0.299	0.357	0.371	0.363	0.271	0.278	0.219	0.197
246	1.468	0.234	0.108	0.139	0.142	0.155	0.164	0.194	0.161	0.169	0.176	0.129	0.119
247	1.702	0.064	0.018	0.029	0.042	0.049	0.052	0.061	0.048	0.040	0.041	0.028	0.016
248	1.883	0.010	0.006	0.007	0.009	0.009	0.010	0.012	0.011	0.008	0.008	0.007	0.006
249	0.547	0.269	0.095	0.119	0.170	0.188	0.208	0.241	0.211	0.191	0.172	0.135	0.107
250	0.557	0.261	0.089	0.102	0.167	0.172	0.193	0.212	0.199	0.181	0.159	0.122	0.095
251	0.565	0.253	0.084	0.099	0.160	0.169	0.178	0.195	0.172	0.168	0.153	0.101	0.081
252	0.579	0.239	0.071	0.081	0.147	0.157	0.165	0.186	0.159	0.155	0.142	0.081	0.079
253	0.607	0.209	0.067	0.075	0.125	0.145	0.158	0.170	0.149	0.142	0.135	0.079	0.065
254	0.723	0.100	0.038	0.052	0.064	0.071	0.089	0.101	0.091	0.075	0.062	0.059	0.029
255	0.845	0.021	0.001	0.009	0.012	0.019	0.026	0.027	0.022	0.017	0.011	0.002	0.007
256	0.936	0.006	0.001	0.002	0.004	0.006	0.008	0.009	0.008	0.005	0.004	0.003	0.002

Seq.	VP₁₁	VP₁₂	VP₁₃	VP₁₄	VP₁₅	VP_{CLb}	VP₁₆	VP₁₇	VP₁₈	VP₁₉	VP₂₀	VP_{avg.}	TP
223	0.032	0.039	0.041	0.045	0.045	0.048	0.042	0.039	0.035	0.028	0.027	0.035	0.840
224	0.003	0.004	0.004	0.006	0.008	0.012	0.010	0.009	0.006	0.004	0.003	0.006	0.960
225	1.261	1.492	1.693	1.868	1.969	2.069	2.005	1.985	1.709	1.365	1.251	1.651	2.834
226	1.376	1.404	1.692	1.894	2.020	2.020	2.003	1.802	1.662	1.605	1.382	1.621	3.311
227	1.148	1.315	1.501	1.571	1.775	1.973	1.905	1.880	1.515	1.233	1.138	1.477	3.175
228	1.094	1.258	1.464	1.494	1.699	1.881	1.752	1.748	1.452	1.164	1.089	1.414	3.374
229	1.043	1.161	1.315	1.409	1.520	1.630	1.605	1.570	1.295	1.023	1.033	1.282	3.707
230	0.516	0.632	0.673	0.745	0.790	0.834	0.805	0.781	0.686	0.526	0.506	0.664	5.105
231	0.131	0.149	0.172	0.202	0.221	0.240	0.232	0.208	0.183	0.135	0.125	0.170	6.115
232	0.025	0.026	0.027	0.028	0.030	0.031	0.030	0.027	0.026	0.025	0.024	0.026	6.679
233	0.614	0.696	0.793	0.839	0.932	0.954	0.923	0.794	0.726	0.692	0.653	0.771	1.432
234	0.589	0.638	0.802	0.821	0.897	0.910	0.864	0.785	0.703	0.679	0.601	0.722	1.508
235	0.592	0.631	0.748	0.792	0.847	0.856	0.825	0.744	0.659	0.653	0.591	0.703	1.549
236	0.564	0.585	0.600	0.768	0.792	0.816	0.781	0.673	0.611	0.608	0.558	0.654	1.651
237	0.454	0.524	0.614	0.665	0.701	0.712	0.674	0.622	0.618	0.564	0.467	0.576	1.882
238	0.293	0.337	0.411	0.432	0.452	0.460	0.447	0.423	0.381	0.380	0.318	0.373	2.369
239	0.056	0.069	0.064	0.076	0.081	0.106	0.095	0.079	0.069	0.061	0.056	0.065	4.528
240	0.011	0.013	0.014	0.015	0.016	0.018	0.017	0.014	0.013	0.012	0.011	0.013	5.351
241	0.229	0.279	0.397	0.448	0.461	0.492	0.469	0.464	0.441	0.285	0.223	0.352	0.764
242	0.241	0.260	0.391	0.439	0.445	0.476	0.457	0.452	0.427	0.271	0.212	0.337	0.799
243	0.190	0.251	0.368	0.428	0.431	0.472	0.442	0.426	0.384	0.262	0.182	0.318	0.837
244	0.181	0.220	0.347	0.422	0.425	0.436	0.419	0.398	0.352	0.225	0.176	0.298	0.888
245	0.170	0.199	0.307	0.332	0.361	0.393	0.371	0.362	0.308	0.211	0.171	0.268	0.979
246	0.110	0.123	0.157	0.194	0.199	0.206	0.191	0.188	0.168	0.122	0.099	0.149	1.319
247	0.016	0.027	0.031	0.039	0.042	0.048	0.043	0.038	0.030	0.025	0.018	0.033	1.669
248	0.003	0.004	0.005	0.006	0.007	0.008	0.007	0.006	0.005	0.004	0.004	0.006	1.877
249	0.106	0.129	0.190	0.199	0.225	0.236	0.225	0.218	0.208	0.152	0.094	0.164	0.383
250	0.100	0.112	0.187	0.191	0.222	0.234	0.222	0.211	0.191	0.133	0.088	0.153	0.404
251	0.095	0.109	0.180	0.182	0.207	0.227	0.214	0.193	0.171	0.121	0.083	0.143	0.422
252	0.082	0.091	0.167	0.168	0.194	0.223	0.199	0.166	0.161	0.112	0.070	0.129	0.450
253	0.078	0.085	0.145	0.156	0.187	0.198	0.179	0.156	0.149	0.099	0.066	0.119	0.488
254	0.049	0.062	0.084	0.086	0.096	0.106	0.102	0.098	0.095	0.059	0.037	0.068	0.655
255	0.012	0.019	0.021	0.025	0.025	0.028	0.022	0.019	0.015	0.008	0.007	0.014	0.831
256	0.001	0.002	0.002	0.004	0.006	0.010	0.008	0.007	0.004	0.002	0.001	0.004	0.932

Seq.	X_{w/o}	X_{end}	X_{damper}	Log(X_{damper})	V_{avg.}	Re	Pipe Factor
223	2.1320	24.349	22.1217	1.345	712.74	75917.87	0.852
224	2.1320	166.571	164.2667	2.216	291.27	31024.72	0.708
225	1.7161	1.716	0.0000		4943.26	526534.66	0.894
226	1.7161	2.042	0.3134	-0.504	4897.89	521701.54	0.898
227	1.7161	2.151	0.4170	-0.380	4674.39	497895.99	0.869
228	1.7161	2.386	0.6504	-0.187	4574.33	487237.92	0.871
229	1.7161	2.893	1.1522	0.062	4354.92	463867.66	0.893
230	1.7161	7.690	5.9176	0.772	3134.38	333860.37	0.892
231	1.7161	35.930	34.0959	1.533	1586.95	169035.45	0.829
232	1.7161	258.044	256.1307	2.408	618.89	65921.60	0.893
233	1.8572	1.857	0.0000		3374.37	359423.07	0.898
234	1.8572	2.089	0.2154	-0.667	3264.99	347772.11	0.896
235	1.8572	2.205	0.3298	-0.482	3221.27	343115.71	0.905
236	1.8572	2.525	0.6466	-0.189	3107.38	330984.70	0.894
237	1.8572	3.267	1.3819	0.140	2916.74	310679.00	0.900
238	1.8572	6.361	4.4550	0.649	2345.44	249826.18	0.898
239	1.8572	70.095	68.1094	1.833	976.75	104039.29	0.800
240	1.8572	409.380	407.3274	2.610	439.35	46797.24	0.841
241	2.1737	2.174	0.0000		2279.57	242809.40	0.845
242	2.1737	2.373	0.1785	-0.748	2231.01	237637.10	0.841
243	2.1737	2.637	0.4395	-0.357	2166.42	230757.78	0.831
244	2.1737	2.981	0.7812	-0.107	2098.09	223479.82	0.830
245	2.1737	3.661	1.4560	0.163	1988.27	211781.67	0.837
246	2.1737	8.846	6.6128	0.820	1484.33	158104.80	0.864
247	2.1737	51.203	48.9013	1.689	694.11	73934.09	0.775
248	2.1737	291.777	289.4065	2.462	308.29	32837.62	0.806
249	2.3386	2.339	0.0000		1552.81	165398.70	0.829
250	2.3386	2.636	0.2718	-0.566	1501.59	159942.58	0.829
251	2.3386	2.964	0.5964	-0.224	1448.38	154275.61	0.823
252	2.3386	3.502	1.1295	0.053	1375.80	146544.59	0.794
253	2.3386	4.122	1.7455	0.242	1320.67	140672.09	0.803
254	2.3386	9.624	7.2215	0.859	1000.76	106596.68	0.811
255	2.3386	60.906	58.4311	1.767	448.20	47739.94	0.705
256	2.3386	257.338	254.8079	2.406	230.91	24595.91	0.618